January 2013

Accelerated Fuzzy Clustering

Jonathon Karl Parker
University of South Florida, jkparker@mail.usf.edu

Accelerated Fuzzy Clustering

by

Jonathon Karl Parker

A dissertation submitted in partial fulfillment
of the requirements for the degree of
Doctor of Philosophy
Department of Computer Science and Engineering
College of Engineering
University of South Florida

Major Professor: Lawrence Hall, Ph.D.
Dmitry Goldgof, Ph.D.
Sudeep Sarkar, Ph.D.
Bo Zeng, Ph.D.
Joni Downs, Ph.D.

Date of Approval:
November 4, 2013

Keywords: fuzzy c-means, scalable, statistical sampling, stopping criterion, representative object

Dedication

for my son, James

Acknowledgments

"you don't forget, because you always remember"- Lawrence "Yogi" Berra [1]

This dissertation would not have been possible without the support and encouragement from my wife, Ann.

I acknowledge and thank my major professor, Dr. Lawrence Hall, for his patience and mentorship over the years. I would also like to acknowledge my committee members, Dr. Dmitry Goldgof, Dr. Sudeep Sarkar, Dr. Bo Zeng, and Dr. Joni Downs, for their attention to detail and advice. Faculty members of the University of South Florida deserve special mention. I deeply appreciate the knowledge and patience of Dr. Rahul Tripathi, the insight and optimism of Dr. Abraham Kandel, the wisdom and kindness of Dr. Rafael Perez, the hard-earned praise of Dr. Nagarajan Ranganathan, and the fruitful collaboration with Dr. Joni Downs. I would also like to thank Dr. Carlos Otero for our engaging, but brief time working together.

I also wish to thank Dr. Kurt Kramer for his infinite patience and plankton data, Dr. Tim Havens for his assistance, and Dr. James Bezdek for his encouragement and praise.

Table of Contents

List of Tables

List of Figures

Abstract

Clustering algorithms are a primary tool in data analysis, facilitating the discovery of groups and structure in unlabeled data. They are used in a wide variety of industries and applications. Despite their ubiquity, clustering algorithms have a flaw: they take an unacceptable amount of time to run as the number of data objects increases. The need to compensate for this flaw has led to the development of a large number of techniques intended to accelerate their performance. This need grows greater every day, as collections of unlabeled data grow larger and larger.

How does one increase the speed of a clustering algorithm as the number of data objects increases and at the same time preserve the quality of the results? This question was studied using the Fuzzy c-means clustering algorithm as a baseline. Its performance was compared to the performance of four of its accelerated variants. Four key design principles of accelerated clustering algorithms were identified. Further study and exploration of these principles led to four new and unique contributions to the field of accelerated fuzzy clustering. The first was the identification of a statistical technique that can estimate the minimum amount of data needed to ensure a multinomial, proportional sample. This technique was adapted to work with accelerated clustering algorithms. The second was the development of a stopping criterion for incremental algorithms that minimizes the amount of data required, while maximizing quality. The third and fourth techniques were new ways of combining representative data objects. Five new accelerated algorithms were created to demonstrate the value of these contributions.

One additional discovery made during the research was that the key design principles most often improve performance when applied in tandem. This discovery was applied during the creation of the new accelerated algorithms. Experiments show that the new algorithms improve speedup with minimal quality loss, are demonstrably better than related methods and occasionally are an improvement in both speedup and quality over the base algorithm.

Chapter 1: Introduction

"You've got to be careful if you don't know where you're going, 'cause you might not get there." - Lawrence "Yogi" Berra [2]

1.1 Cluster Analysis

Cluster analysis is an exploratory technique used to discover groups and structure in a set of data objects [3] [4]. A data object can represent any *object* of interest, but there is one caveat: It must be possible to measure the similarity (or dissimilarity) of one object to another. Each data object will have one or more features associated with it. For example, a dataset of athletes might record: age, height, and weight as some of its features.

A clustering algorithm accepts as input a dataset and produces as output a set of cluster assignments for all data objects in the dataset. A set of assignments to clusters is also referred to as a partition of the data. But what is a cluster? Intuition tells you that a cluster is a group of data objects, which are more similar to each other than to other objects in the dataset [3] [4]. There are many different types of clustering algorithms. One taxonomy used classifies clustering algorithms as hierarchical or partitional; though each class of algorithm has subclassifications [3]. Under the partitional classification, there is a subclass that seeks to minimize an objective functional value [5]. Another subclassification consists of those that are density-based.

Three of the most common clustering algorithms of the hierarchical, objective function minimization, and density-based types are discussed in detail in Section 2.1.

Cluster analysis is used to explore data in a wide variety of disciplines [5]. A non exhaustive list includes grouping web-based news articles [6], image processing [7], literature-based discovery

[8], marketing [9], medical research [10] [11], military intelligence [12], oil exploration [13], and psychology [14].

A human being has little difficulty finding groups of data objects, especially when a small number of data objects is plotted in two dimensions (two features). Figure 1.1 displays such a two dimensional plot of thirty data objects. Three clusters are shown, helpfully displayed as red circles, green rectangles, and blue diamonds. People will have little difficulty detecting the three clusters, even if the data objects are displayed in the same shape and color.

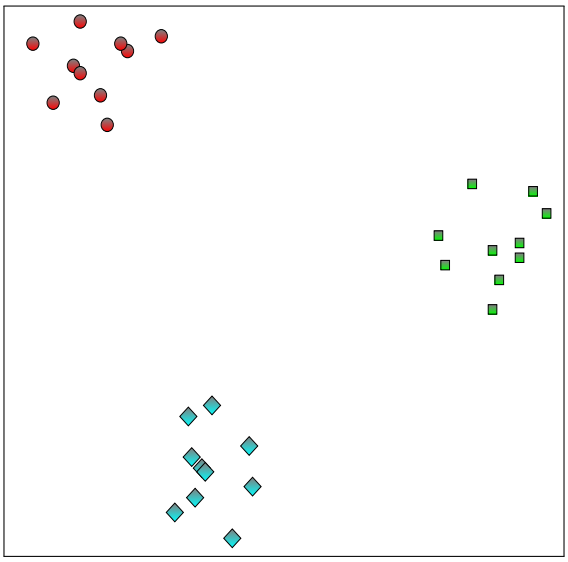

Figure 1.1: A Simple Clustering Scenario

Figure 1.2 displays a slightly different two dimensional plot. Most would also decide there are three clusters in this plot. There would be ambiguity, however, as to which clusters the two blue diamond data objects belong.

One assumes intuitively that a data object can only belong to one cluster. The existence of the blue-colored data objects challenges this intuition. Can a data object be in more than one cluster simultaneously? Can a data object be assigned to no cluster at all?

The answer to both questions is yes. A clustering algorithm that assigns data objects to a single cluster is called a *hard* clustering algorithm. The most basic, hard clustering algorithms are discussed in Section 2.1. A *fuzzy* clustering algorithm allows a data object to have simultaneous

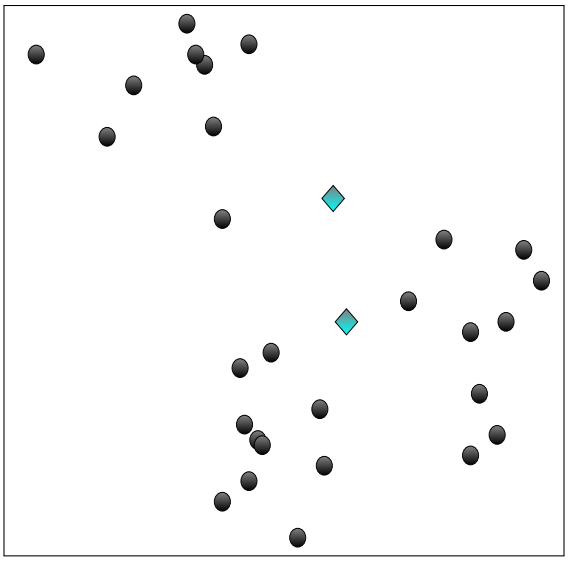

Figure 1.2: A Fuzzy Clustering Scenario

membership in multiple clusters. Fuzzy set theory and fuzzy clustering algorithms are discussed in Section 2.2. A clustering algorithm that does not necessarily assign every data object to a cluster is described in Section 2.1.3.

Fuzzy clustering algorithms have some advantages over hard clustering algorithms. The principle advantages are that a data object can belong to multiple clusters and the degree to which it belongs to these clusters is calculable. This provides more options to the data analyst. One application is image processing, where the boundary between two regions can be vague. Another possible application is clustering a Geographic Information Systems (GIS) dataset of land parcels. If the underlying groups and structure pertain to land usage, one may discover parcels used for multiple purposes.

1.2 Handling Big Data

Unfortunately, cluster analysis is not an exercise as simple as viewing Figure 1.1 or 1.2. Datasets typically have a large number of data objects and three or more dimensions, making plotting of objects and visual assignment of them to clusters infeasible. Therefore, non-trivial datasets are clustered using computer-based algorithms.

Electronic datasets have been growing in size for decades. Huber discussed in 1994 a classification system for dataset sizes, which ended with the term "monster" to describe a dataset having 10^{12} data objects [15]. Such a system proved unsuitable for Havens, who extends Huber's classification with the Very Large (VL) dataset, which has $> 10^{12}$ data objects [16].

The larger volumes of data available today are typically called "Big Data" [17]. The definitions for Big Data are generally subjective.

Madden offers such a subjective definition for Big Data. He describes Big Data as data "too big, too fast, or too hard for existing tools to process" [18]. So the conception of Big Data is relative to one's power to deal with it. Jacobs defines Big Data in this context by its effects, namely as "data whose size forces us to look beyond the tried and true methods that are prevalent at the time" [19].

Ratner states that Big Data is in the mind of the data analyst; how much data is needed for it to be "Big" is subjective. He then goes on to describe necessary qualities of data to be considered "Big." One quality comes from the field of classical statistics, where the sample size is so large that the "asymptotic properties of the method kick in for valid results" [20].

In summary, a Big Data dataset is cumbersome because of its size, but valuable because of the information it potentially contains.

Clustering algorithms are only one of many analytic tools that can be applied to Big Data. The runtime for a typical clustering algorithm will scale linearly to quadratically, with respect to the number of data objects. The larger the dataset, the longer the algorithm will take to produce a partition. Processing the entire dataset with typical clustering algorithms can be infeasible for real-world applications, taking more time than a required decision about the data allows.

Techniques are therefore needed to accelerate the clustering algorithms. A related challenge is to preserve the quality of the clustering algorithm's results while accelerating its operation simultaneously. The quality should be equivalent to clustering all the data with a classical algorithm. These areas are the subject of this dissertation.

I used large datasets for experimentation, but not truly "Big Data." An implied task is to report the differences in runtime and quality of the accelerated clustering algorithms when compared to basic algorithms. If the datasets were so large as to be Big Data, the runtime of the basic algorithms

on the full datasets would preclude receiving results in a timely fashion. Thus, I infer from the runtime complexity of the algorithms and the results of smaller scale experiments, the expected performance on Big Data.

1.3 Contributions

I investigated the key algorithm design principles that accelerate fuzzy clustering algorithms while preserving quality. Quality is defined as closely approximating well known fuzzy clustering algorithms. My investigation identified four main ideas to apply to the development of accelerated fuzzy clustering algorithms on Big Data:

1. Use of a statistically significant sample of the dataset reduces runtime while preserving quality.
2. An algorithm designed to cluster the data incrementally can produce a high-quality result when stopped before all data has been processed. This is especially true when the data is presented in random order.
3. The use of representative objects, either weighted or un-weighted, can overcome difficulties of scale, if properly utilized.
4. For a particular class of clustering algorithms, providing a "starting point" close to the optimal solution reduces runtime and can improve quality.

None of these ideas are original. All are sound, previously-used tools for the construction of accelerated clustering algorithms. The contributions made in this dissertation are unique, fully developed, implemented strategies to employ these ideas to accelerate fuzzy clustering. The specific contributions of this dissertation are as follows:

- Identification of a statistical method never before used with accelerated fuzzy clustering algorithms. This method estimates the minimum sample size required to represent each cluster proportionally. I modified the statistical formula to make it compatible with clustering algorithms.

- Creation of an early stopping criterion for incremental or "single pass" algorithms. This criterion determines the point at which processing additional data will have little added benefit. This allows the clustering algorithm to terminate early, providing a greater speedup with little loss in quality.

- Different methods of combining representative objects were explored using fuzzy clustering algorithms which produce partitions by minimizing an objective function. I discovered that the best method used information from the intermediate results to improve quality and speedup.

- I developed a new method to combine representative objects in the context of density-based fuzzy clustering algorithms.

- I created five original algorithms that apply these contributions and the four main ideas listed above.

1.4 Organization

In Chapter 2, I provide detailed background on relevant clustering algorithms, accelerated variants, and metrics used to assess performance. In Chapter 3, I describe the data used for experiments.

In Chapter 4, a series of exploratory experiments are documented. Observations made from the experimental results were condensed into the four main ideas identified above.

In Chapters 5, 6, and 7 these ideas are developed into the specific contributions made to the field of Computer Science. To demonstrate the value of these contributions, five original algorithms we created implemented these contributions. Experimentation and discussion are included.

Chapter 8 summarizes my work and concludes the dissertation.

Chapter 2: Background

"It's déjà vu all over again." - Lawrence "Yogi" Berra [2]

2.1 Basic Clustering Algorithms

Many clustering algorithms have been developed over the last five decades [5]. Only a relatively small number of algorithms out of the number available could be chosen to be the focus of my dissertation. One can categorize the choices by considering different types of clustering algorithms. A taxonomy of clustering algorithms was described by Jain [3]. One distinction made in his taxonomy is whether the clustering algorithm is hierarchical or partitional. A hierarchical algorithm produces a nested grouping of partitions; at each level of the hierarchy there is a different number of clusters. A partitional algorithm produces a single partition with a fixed number of clusters.[1]

One can distinguish partitional algorithms as to whether the basis for partition is minimizing an objective function or density-based [3] [5]. In a density-based algorithm, clusters are defined as regions of high density, separated by regions of low density [24, 5].

Three of the most basic clustering algorithms of these types are described below. Each basic algorithm selected is the original or best-known representative of its type: hierarchical (Single Linkage), objective function minimizing (Hard c-means), and density-based (DBSCAN).

2.1.1 Single Linkage (SL)

Of the three basic algorithms, Single Linkage is the oldest. The first work that suggests Single Linkage, initially published in French and Polish in 1951, was rediscovered in 1957 and published in English [25].

[1] Some of the material in this chapter has been previously published by me [21] [22] [23], and is re-used under terms of the copyright © 2010, 2012 and 2013 IEEE.

Single Linkage, also referred to as "Single Link" or "Nearest Neighbor," is a hierarchical, agglomerative clustering algorithm. It employs a dissimilarity coefficient, $\rho(x_i, x_j)$, that defines the degree to which two data objects in dataset X are dissimilar [26]. For numeric data, $\rho(x_i, x_j)$ is often a distance metric, such as the Euclidean distance.

At the beginning of the algorithm, each data object in the dataset ($x_i \in X$) is considered to be its own cluster. The algorithm merges into a single cluster the two clusters (which initially are data objects) that are least dissimilar. Single Linkage repeats the merging of the least dissimilar clusters until all n data objects in X have been assigned to a single cluster.

A formal description, adapted from [27], is presented as Algorithm 1. For efficiency, implementations of the algorithm usually store the dissimilarities in a dissimilarity matrix.

The algorithm returns a list of merges, M. The decision to merge two clusters is based on the dissimilarity coefficient. Thus, given a dataset, a dissimilarity coefficient, and rules for tie-breaking, Single Linkage is deterministic in that it will always return the same list of merges [27].

Single Linkage begins with n clusters. With each merge, the number of clusters is reduced by 1. If the cluster assignments prior to each merge are listed, a numeric hierarchy of height $n - 1$ is created. A dendrogram is the most common way to display a hierarchy.

This process is shown in Figure 2.1. Figure 2.1(a) shows a simple dataset consisting of 12 data objects. Merges are indicated by line segments connecting two data objects. Each line segment is annotated with a number to show the order of the merges. Note that data objects a and b are connected with a line segment annotated with a '1'. This is the first merge. Likewise, the '2' between objects f and g indicates the second merge. All $n - 1$ merges are shown in Figure 2.1(a).

Figure 2.1(b) shows the dendrogram that displays the hierarchical structure created by Single Linkage. The y axis shows the order of the merges connecting data objects. The number assigned to the merge is also called a *splitting level* [25].

A human would typically consider the dataset shown in Figure 2.1(a) as having three clusters. If Single Linkage were halted after splitting level 9, the merges labeled '10' and '11' would not be made and three clusters would remain. The red line in Figure 2.1(b) shows the effect on the dendrogram.

Algorithm 1: Single Linkage

1: **Input:** X, $\rho(x_i, x_j)$
2: **for** $i = 1$ to n **do**
3: $L[i] = i$ (each initial cluster is labeled with the index of its data object)
4: **for** $j = 1$ to i **do**
5: $D(x_i, x_j) = D(x_j, x_i) = \rho(x_i, x_j)$
6: **end for**
7: **end for**
8: **for** $k = 1$ to $n - 1$ **do**
9: $(a, b) = argmin_{(a,b):D(a,b)\neq -1} D(a, b)$
10: $M.append(a, b)$
11: $D(a, b) = D(b, a) = -1$
12: **for** $j = 1$ to n **do**
13: **if** $L[j] = b$ **then**
14: $L[b] = a$ (cluster b is now part of cluster a)
15: **end if**
16: $D(a, x_j) = D(b, x_j) = min(D(a, x_j), D(b, x_j))$
17: **end for**
18: **end for**
19: **return** M

where:
X is a dataset consisting of n data objects.
$\rho(x_i, x_j)$ is the dissimilarity coefficient.
x_i is the i^{th} data object in X.
D is the dissimilarity matrix and $D(x_i, x_j)$ is the dissimilarity between x_i and x_j.
$D(a, b) = -1$ indicates objects a and b are in the same cluster.
L is an array holding the current set of cluster labels.
M is an ordered list holding the pairs of merges.

If the dataset is small, examining a dendrogram visually can reveal the number of clusters. When the dataset is larger, some method is needed in order to split the hierarchy represented by the dendrogram. Three of the many methods for splitting the dendrogram are described by Manning [27].

The first method splits the dendrogram at a user-defined value of dissimilarity. Note that the dissimilarity between objects increases monotonically as they are merged by Algorithm 1. Thus, if a particular value of dissimilarity were exceeded, all subsequent merges would be of this value or greater. The second method calculates the difference between the successive dissimilarities during

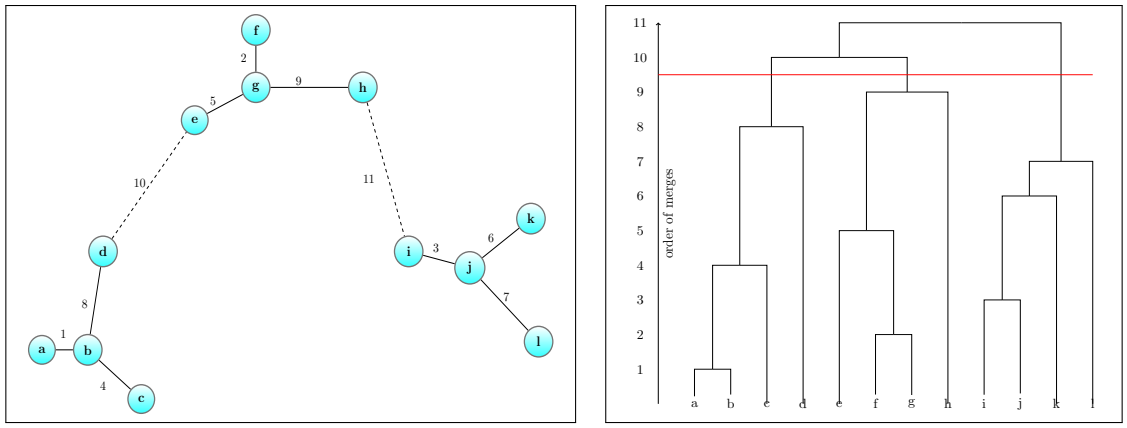

(a) Clustering a Small Dataset (b) Resulting Dendrogram

Figure 2.1: Clustering with Single Linkage

Numbers indicate the order of the merges. Dotted links are merges that would not be made if three clusters are desired.

the merge process. The splitting level at which this difference is greatest is used. The third method splits the dendrogram in order to produce a predefined number of clusters.

A criticism of the Single Linkage algorithm is that clearly distinct clusters (from an observer's perspective) can be prematurely merged together due to a single pair of nearby objects or a noisy dataset. This phenomenon is called "chaining" [28] [25]. It has been pointed out that chaining is not a flaw, but rather a feature of hierarchical clustering which may be desirable given a particular dataset and application [26].

Figure 2.2 shows the effect of ill-placed noise objects on a simple dataset. Data objects 'f' and 'g' are noise and unfortunately placed between two natural clusters represented by data objects a-e and h-l respectively. Figure 2.2(a) shows the order of merges. The first two merges have a dissimilarity of δ; all subsequent merges have a dissimilarity of $\delta + \epsilon$. Contrast the resulting dendrogram (Figure 2.2(b)) with the previous example (Figure 2.1(b)). In this dendrogram, the structure of the data is more difficult to discern.

There are many variants of Single Linkage, some of which are designed to avoid the chaining effect [27] [28] [26]. Of these, the best known are Complete Linkage and Average Linkage. Complete Linkage merges clusters based on the most dissimilar data objects in each cluster, as opposed to the

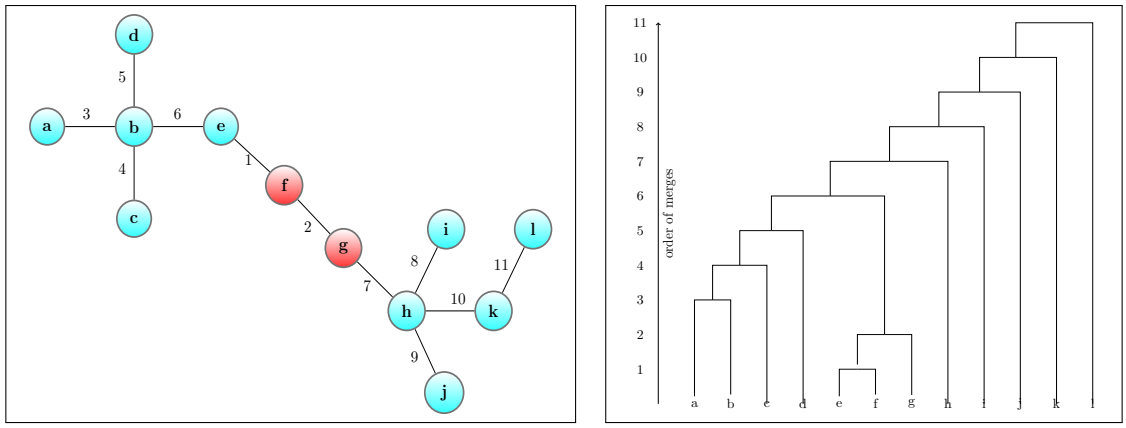

(a) Dataset with Noise Points (b) Resulting Dendrogram

Figure 2.2: Single Linkage Chaining

Numbers indicate the order of the merges. The red-colored data objects are noise.

least dissimilar [27]. Average Linkage merges clusters based on the average dissimilarity between data objects in each cluster [28].

Algorithms in the Single Linkage family have many scientific applications, including bioinformatics [29] and document clustering [27].

2.1.1.1 Runtime Complexity

A literal implementation of Single Linkage has a time complexity of $O(n^3)$, where n is the number of data objects [25] [27]. In line 9 of Algorithm 1, the dissimilarity matrix D is searched exhaustively for the pair of clusters that have the minimum dissimilarity. D has a size of $O(n^2)$, and line 9 is executed $O(n)$ times, resulting in a runtime complexity of $O(n^3)$.

Sibson developed an improved implementation of Single Linkage with a runtime complexity of $O(n^2)$ [25]. A similar implementation appears in [27]. Improved implementations exist for the variants of Single Linkage with runtime complexities of $O(n^2 log(n))$ [27]; the need to recalculate the dissimilarities at each merge stymies the development of an $O(n^2)$ algorithm.

2.1.2 Hard c-means (HCM)

The hard c-means (HCM) algorithm, attributed to MacQueen [30], was independently discovered multiple times [31] [28]. This algorithm, though typically called k-means clustering, is referred

to here as hard c-means in order to conform with the conventions of the fuzzy clustering literature [32].

HCM is a distance-based, partitioning algorithm [3]. It clusters a dataset in which each data object consists of a vector of s features. The HCM algorithm seeks to reduce the sum of squared error, represented by the square of the Euclidean distance between each data object and its closest respective cluster center [3] [28] [33]. The value of the sum of the squared error for a partition is:

$$J = \sum_{j=1}^{c} \sum_{i, x_i \in c_j}^{n} ||x_i - c_j||^2 \tag{2.1}$$

where:

J is the sum of the squared error.

X is a dataset where $n = |X|$, and x_i is the i^{th} data object.

C is the set of cluster centers where $c = |C|$, and c_j is the j^{th} cluster center.

The partition produced by HCM is defined by:

$$X_j = \{x_i : ||x_i - c_j||^2 \leq ||x_i - c_k||^2 \, , 1 \leq i \leq n, \; 1 \leq k \leq c\} \tag{2.2}$$

where:

n, x_i, and c_j are defined as above, and

X_j is the subset of data objects from X belonging to the j^{th} cluster.

In cases where a data object is equidistant from two or more cluster centers, the object must be arbitrarily assigned to one of the clusters. The simplest solution to implement is to assign the object to the cluster center with the lowest index.

The cluster center, c_j, is represented by an s-dimensional vector. Given the entire set of data objects $X_j \subset X$ belonging to cluster j, the cluster center can be calculated by:

$$c_j = \frac{1}{|X_j|} \sum_{x_i \in X_j} x_i \tag{2.3}$$

Finding the set of cluster centers that minimizes J is an NP-hard problem [34]. The HCM algorithm's strategy for minimizing Equation 2.1, is to alternate between Equations (2.2) and (2.3). An algorithm that uses a pair of equations in this way is said to use Alternating Optimization (AO) [35]. An initial set of cluster centers, C, is required for Equation 2.2. A termination criterion is also required for HCM.

While there are several initialization strategies [3], the most common strategy is to randomly select a set of c data objects to provide the initial positions of the cluster centers [33]. HCM terminates when Equation (2.2) results in no data object changing its currently assigned cluster. Alternatively, HCM can be implemented to terminate if the difference between successive values for J does not exceed a user-defined value. A more formal description is as follows [3] [33]:

Algorithm 2: Hard c-means

1: **Input:** X, c
2: Choose c data objects from X to provide initial cluster centers for C
3: Assign each data object to the nearest cluster center using Equation 2.2
4: **while** At least one cluster assignment changes for $x_i \in X$ **do**
5: Update all $c_j \in C$ using Equation 2.3
6: Assign each data object to the nearest cluster center using Equation 2.2
7: **end while**
8: **return** C

One must consider some limitations when using HCM to cluster data. The first is that the HCM algorithm requires an initial set of cluster centers, which implies that the number of clusters is known [3]. The second is that the HCM algorithm is non-deterministic if this initial set of clusters is chosen randomly [27]. The final set of cluster centers returned by HCM is highly dependent on the initial set of clusters provided [3]. The third limitation is that all clusters will be hyperspherically shaped, since each data object is assigned to the nearest cluster center.

Figure 2.3 shows how HCM clusters a simple dataset. In the subfigures, circles represent the data objects (X), squares represent the cluster centers (C), and data objects are assigned to cluster centers with the same color. Subfigure 2.3(a) shows the initial cluster center positions and cluster

assignments. The squares representing the cluster centers are slightly offset to show the data objects beneath. Subfigures 2.3(b), 2.3(c), and 2.3(d) show three successive iterations of the cluster center positions and cluster assignments on line 6 of Algorithm 2. In the final subfigure, the data objects will not change their currently assigned cluster and HCM will terminate.

The series of images demonstrating k-means were produced from an interactive online resource [36].

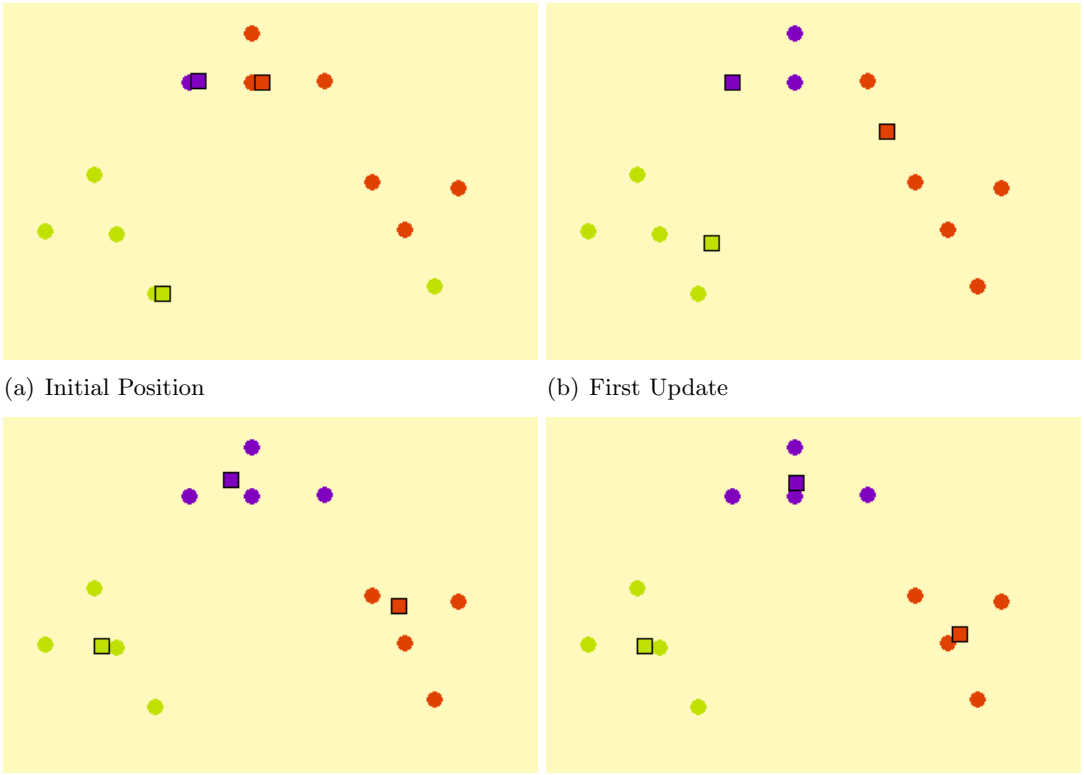

(a) Initial Position (b) First Update

(c) Second Update (d) Final Update

Figure 2.3: Clustering with Hard c-means

2.1.2.1 Runtime Complexity

The HCM algorithm has a time complexity of $O(nisc)$, where n is the number of data objects, i the number of iterations, s the number of features, and c the number of clusters [33]. This can be verified by examining Algorithm 2 and Equations 2.2 and 2.3.

Equation 2.2 is calculated on line 3 of Algorithm 2. This equation requires a comparison of the squared distance of every data object to every cluster. The distance calculation requires $O(s)$ time, and the distance is calculated $O(nc)$ times, for an overall time complexity of $O(nsc)$.

Equation 2.3 is calculated on line 5 of Algorithm 2. This equation finds the average position of the data objects assigned to each respective cluster. This can be implemented in $O(ns)$ time. On line 6, Equation 2.2 is calculated again.

Lines 5 and 6 of Algorithm 2 are executed once per iteration, i, until HCM terminates. The total time complexity (T) is therefore:

$$\begin{aligned} T &= O(nsc) + i \times (O(ns) + O(nsc)) \\ &= O(nsc) + O(nis) + O(nisc) \\ &= O(nisc) \end{aligned}$$

2.1.3 Density Based Spatial Clustering of Applications with Noise (DBSCAN)

DBSCAN is a density-based clustering algorithm, first published in 1996 [24]. Its similarity to the earlier Jarvis-Patrick algorithm [37] and Parzen window density estimation [38] was noted by Jain [5].

Conceptually, DBSCAN works as follows. An s-dimension space is defined by the features of the data objects in a dataset (X). DBSCAN partitions this space into two types of regions, dense regions considered part of a cluster and sparse regions not considered part of a cluster. Data objects in the former region are assigned to a cluster, whereas any data objects in the latter region are considered to be noise. Data objects in a contiguous region of "dense" space are assigned to the same cluster.

DBSCAN then overcomes the limitations of the distance-based HCM algorithm described in Section 2.1.2, namely that the: (1) number of clusters must be known in advance, (2) clusters are hyperspherical, and (3) all data objects must belong to a cluster [21].

The local density at each data object is assessed using two parameters, ε (distance) and $MinPts$ (a lower bound on the minimum number of points, i.e., data objects). A single data object is considered a "core point" if it is located within ε distance of at least $MinPts$ data objects. All data objects within ε distance of a core point are considered members of its cluster [21].

Clusters are created from multiple core points located within ε distance from each other. Other non-core data objects within ε distance of a core point are assigned to that core point's cluster. These non-core data objects are called "border points." As a result, large, irregularly shaped clusters can be found. As mentioned above, data objects not assigned to a cluster are considered noise [21].

The original presentation of DBSCAN, presented below as Algorithm 3, formally defines a number of terms to clarify how the algorithm works [24]:

1. ε Neighborhood ($N_\varepsilon(x_i)$): The set of data objects within distance ε of data object x_i.
2. Core Point: A data object, x_i, where $|N_\varepsilon(x_i)| \geq MinPts$.
3. Border Point: A data object, x_i, where $|N_\varepsilon(x_i)| < MinPts$, $x_i \in N_\varepsilon(x_j)$ and x_j is a core point.
4. Directly density-reachable: Data object, x_i, is directly density-reachable from x_j if $x_i \in N_\varepsilon(x_j)$ and x_j is a core point.
5. Density-reachable: Data object, x_i, is density-reachable from x_j if there is a chain of directly density-reachable core points between them.
6. Density-connected: Two data objects, x_i and x_j, are density-connected if both are density-reachable to some data object x_k.

When a core point, x_i, not assigned to a cluster is identified on line 12, the algorithm discovers all data objects directly density-reachable from x_i. Subsequently, a recursive call of the Function ExpandCluster on line 17 allows DBSCAN to find all objects density-reachable from the original core point. Line 16 ensures the same cluster assignments both for border points and core points.

Algorithm 3: DBSCAN

1: **Input:** X, ε, $MinPts$
2: Assign each data object in X a cluster ID number = 0 ($x_i.id = 0$)
3: $ClustId = 1$
4: **for** $i = 1$ to n **do**
5: **if** $x_i.id = 0$ **then**
6: ExpandCluster(x_i)
7: **end if**
8: **end for**

9: **Function** ExpandCluster(x_i)
10: **if** $|N_\varepsilon(x_i)| < MinPts$ **then** {x_i is not a core point}
11: **return**
12: **else** {x_i is a core point}
13: $x_i.id = ClustId$
14: $\mathbf{C} = N_\varepsilon(x_i)$
15: **for all** $x_j \in \mathbf{C}$ **do** {x_j is a member of x_i's cluster}
16: $x_j.id = ClustId$
17: ExpandCluster(x_j)
18: **end for**
19: $ClustId = ClustId + 1$
20: **return**
21: **end if**

---

where:
X is a dataset consisting of n data objects.
ε is a distance.
$MinPts$ is an integer.
x_i is the i^{th} data object in X.
$\mathbf{C}$ is a set of data objects.
A ClusterID = 0 signifies the data object is NOISE.

DBSCAN requires two parameters, ε and $MinPts$, which define the threshold density for a cluster. These values can be set empirically. Ester provides a method to set them that works well in low dimensions [24].

2.1.3.1 Runtime Complexity

A naive implementation of DBSCAN has a runtime complexity of $O(n^2)$. Discovery of all data objects in $N_\varepsilon(x_i)$ requires calculating the distance between x_i and $\forall\, x_j \in X$. This step, which

occurs on line 10 of Algorithm 3, has a time complexity $O(n)$ and is executed $O(n)$ times (line 4 of Algorithm 3).

If the dataset were sorted into a structure such as an R* tree [39], the discovery of all data objects in $N_\varepsilon(x_i)$ would have an average runtime complexity of $O(log(n))$. If this precondition is met, DBSCAN has a runtime complexity of $O(n\,log(n))$

2.2 Algorithms Based on Fuzzy Sets

2.2.1 Fuzzy Sets and Logic

The clustering algorithms discussed in Section 2.1 are based on classical set theory. These algorithms produce a crisp partition that assigned data objects to a single cluster. A crisp partition can be expressed as a binary membership matrix, U, where $u_{ik} \in \{0, 1\}$ refers to the membership value of the k^{th} data object, x_k, in the i^{th} cluster.

In contrast, fuzzy set theory allows an object to have varying grades of membership in a set [40]. When fuzzy sets are used in a clustering algorithm, a data object can have a grade of membership in multiple clusters [21]. A fuzzy clustering algorithm produces a fuzzy partition which can also be expressed by a membership matrix, U. The grade of membership of a data object k in cluster i is u_{ik}. This is subject to the following constraints [41] [22]:

$$u_{ik} \in [0, 1], 1 \leq i \leq c, 1 \leq k \leq n \tag{2.4}$$

$$\sum_{i=1}^{c} u_{ik} = 1, 1 \leq k \leq n \tag{2.5}$$

$$\sum_{k=1}^{n} u_{ik} > 0, 1 \leq i \leq c \tag{2.6}$$

where n is the number of data objects and c is the number of clusters.

Fuzzy approaches have been successfully integrated in many clustering algorithms [32] [42] [43] [44] [45]. Three such applications are discussed in this section.

2.2.2 Fuzzy c-means (FCM)

The Fuzzy c-means (FCM) algorithm, developed by Bezdek [41], is based on earlier work by Ruspini and Dunn [28] [5]. As the name suggests, it is a fuzzy variant of HCM.

FCM produces a set of c cluster centers by approximately minimizing the objective function that calculates the within-group sum of squared distances from each data object to each cluster center. FCM alternates between calculating optimal cluster centers, given the membership values of each data object, and calculating membership values, given the cluster centers [22]. If data objects are defined as feature vectors, x_k in R^s, the objective function (J_m) is expressed as [23]:

$$J_m(U, V) = \sum_{i=1}^{c} \sum_{k=1}^{n} u_{ik}^m D_{ik}(x_k, v_i) \tag{2.7}$$

The functions for determining optimal membership values and optimal cluster centers are derived from Equation 2.7 using Lagrange multipliers [41]:

$$u_{ik} = \frac{D_{ik}(x_k, v_i)^{\frac{1}{1-m}}}{\sum_{j=1}^{c} D_{jk}(x_k, v_j)^{\frac{1}{1-m}}} \tag{2.8}$$

$$v_i = \frac{\sum_{j=1}^{n} (u_{ij})^m x_j}{\sum_{j=1}^{n} (u_{ij})^m} \tag{2.9}$$

where:

X is a dataset where $n = |X|$, and x_i is the i^{th} data object.

$m > 1$ controls how fuzzy the clusters are.

c is the number of clusters.

U is the membership matrix; u_{ik} refers to the membership value of the k^{th} data element (x_k) for the i^{th} cluster.

V is the set of cluster centers; v_i is the i^{th} cluster center.

$D_{ik}(x_k, v_i)$ is the squared distance between the k^{th} data object and i^{th} cluster center; any inner product induced distance metric can be used (e.g. Euclidean).

There are implementation options. The U or V matrices may be initialized with any valid set of values. Typically, the u_{ik} are initialized with a set of values adhering to (2.4) to (2.6) or each v_i is set to equal the position of a randomly selected data object in X. The FCM algorithm terminates when the difference between successive membership matrices or sets of cluster centers does not exceed a given parameter ϵ [22]. Algorithm 4 describes the implementation used in this research.

Algorithm 4: Fuzzy c-means

```
1: Input: X, c, m, ε
2: Choose c data objects from X to provide initial positions for V
3: Assign initial cluster membership values using Equation 2.8.
4: maxChange = 1 + ε
5: while maxChange > ε do
6:    U_prev = U
7:    Update all v_i ∈ V using Equation 2.9.
8:    Reassign cluster memberships to each data object using Equation 2.8.
9:    maxChange = calcMaxChange(U, U_prev)
10: end while
11: return U, V
```

The function $calcMaxChange(U, U_{prev})$ returns the maximum difference in cluster membership (u_{ik}) across two iterations.

2.2.2.1 Runtime Complexity

A literal implementation of the FCM algorithm has an expected runtime complexity of $O(nisc^2)$ [46], where n is the number of data objects, c the number of clusters, s the dimension of the data, and i the number of iterations. An optimization proposed by Kolen and Hutcheson [47] reduces the runtime to $O(nisc)$. The remainder of this work uses Kolen's optimization. For details, see [47] and Section A.2.3.

2.2.3 Fuzzy c-medoids (FCMdd)

The HCM and FCM algorithms assume that the data objects are represented by numeric feature vectors. Both algorithms produce cluster centers located in R^s, the feature space of the dataset.

Not all datasets, however, consist of data objects represented by feature vectors. Relational data objects, as opposed to numeric (i.e., object) data, do not have a representation in R^s [48]. For relational data, a measure for similarity or dissimilarity between a pair of data objects can be defined. A dissimilarity coefficient, $\rho(x_i, x_j)$, as described in Section 2.1.1, is typically used.

Single Linkage and DBSCAN do not produce cluster centers in R^s. They therefore can produce clusters from either numeric or relational data. Single Linkage requires no modification to do so. DBSCAN requires that "distance" be replaced with ρ and that the parameter ϵ be appropriately set.

HCM and FCM require modification to accept relational data. Conceptually, HCM and FCM both seek to minimize an objective function based on the total squared error of a partition of the data. When using relational data, minimization of such an objective function is still possible.

Hathaway modified Equation 2.7 to accommodate relational data [48]. This modification substituted a mean cluster membership vector for cluster centers. Versions include Relational Hard c-means (RHCM), Relational Fuzzy c-means (RFCM), and Non-Euclidean RFCM (NERF) [48] [49].

One can also select representative data objects from the dataset as cluster centers. When discussing clustering algorithms, such representative objects are referred to as medoids. In the field of Operations Research, variations of this problem are known as the facility location problem and k-median problem [50] [28].

Crisp set versions of a "Hard c-medoid" algorithm include Partitioning Around Medoids (PAM), and Clustering Large Applications (CLARA) [51] [28]. Its fuzzy set version is Fuzzy c-medoids (FCMdd) [44]. Krishnapuram originally developed the FCMdd algorithm to cluster textual data [52] [44].

FCMdd minimizes the objective function J_m.

$$J_m(V, X) = \sum_{i=1}^{n} \sum_{j=1}^{c} u_{ij}^m \rho(x_i, v_j) \tag{2.10}$$

where:

X is a dataset where $n = |X|$, and x_i is the i^{th} data object.

$m > 1$ is the "fuzzifier."

c is the number of clusters.

U is the membership matrix; u_{ij} refers to the membership value of the i^{th} data element (x_i) for the j^{th} cluster.

V is the set of cluster centers; v_j is the j^{th} cluster center.

$\rho(x_i, v_j)$ is the dissimilarity between the i^{th} data object and j^{th} cluster center.

The same membership function used for FCM can be used for FCMdd if the squared distance is replaced with the dissimilarity. Although other membership functions can be used [44], I implemented Equation 2.11 for the work described here.

$$u_{ij} = \frac{\rho(x_i, v_j)^{\frac{1}{1-m}}}{\sum_{k=1}^{c} \rho(x_i, v_k)^{\frac{1}{1-m}}} \tag{2.11}$$

Like FCM, FCMdd is provided an initial set of medoids, V. Note that unlike FCM, the medoids are always data objects, x_i. It then alternates between calculating the membership matrix, U (based on the values in V), and calculating new medoids, V (based on the values in U), until a termination criterion is met.

Unfortunately, no equation is provided for the optimization of the medoids. FCMdd is not a true alternating optimization algorithm, and a Lagrangian "hill-climbing" formula cannot be used as with FCM [41] [44].

Selection of the optimal c medoids that reduce the value of J_m for the current values in U would require testing $\binom{n}{c}$ combinations. Clearly, this is intractable, so a heuristic proposed by Fu [53] is used. The heuristic keeps all but one $v_j \in V$ fixed, and it evaluates the remaining $n - c$ data objects in $x_i \in X$. If there are any x_i, if substituted for v_j in Equation 2.10, that would result in a lower value for J_m, the x_i that would minimize J_m replaces v_j in V. Each $v_j \in V$ is considered per iteration.

FCMdd's initialization and termination criterion remain to be discussed. Initialization of FCMdd requires the selection of c medoids to populate V. The most obvious technique is to select c data objects randomly. Empirically, Krishnapuram noted that FCMdd often would become stuck in local extrema if this technique was used [44].

An alternative technique is to randomly select a single data object, x_i, to insert into V. Then, the data object, $x_j \in X$, with the greatest dissimilarity from x_i should be selected and placed into V. For the remaining $c-2$ medoids, each successive data object, $x_k \in X$, with the greatest sum of dissimilarity to all objects currently in V will be selected. This technique, described in [52] as "Initialization III," experimentally produces higher-quality partitions than those produced by random selection. Initialization III was used in research.

Similarly to HCM, the FCMdd algorithm terminates when V remains unchanged between updates to U. FCMdd also terminates if it reaches a maximum number of iterations (MAX_ITER). In the implementation for research, MAX_ITER was hard-coded to equal 100. It was noted in [54] that the algorithm can get stuck in a cycle where the medoids in V alternate between two assignments until MAX_ITER is reached. This condition was tested for also. If V, in iteration i, had the same assignments as V, in iteration $i+2$, the algorithm terminated. A single test is sufficient, because the update process is deterministic for a given dataset and starting set of medoids.

The formal description of FCMdd as listed in Algorithm 5 is slightly modified from its original publication [44].

2.2.3.1 Runtime Complexity

Krishnapuram reported the runtime complexity of FCMdd as $O(n^2)$ [52]. If the number of iterations, i, and the number of clusters, c, are considered, the runtime complexity will be higher. An in-depth analysis of runtime complexity follows. One assumption made in the analysis is that the dissimilarity between two data objects can be calculated in constant time.

On line 2 of Algorithm 5, the initial set of medoids is selected. This initialization technique has a runtime complexity of $O(nc^2)$ [52]. The **while** statement on line 5 is executed i times. Within the **while** statement, the membership matrix is updated on line 7. This step has a runtime complexity

Algorithm 5: Fuzzy c-medoids

1: **Input:** X, c, m
2: Select c data objects from X to provide an initial set of medoids V.
3: Set $V_{old} = NULL$
4: Set $ITER = 0$
5: **while** ($V_{old} \neq V$ and $ITER < MAX\_ITER$) **do**
6: $V_{old} = V$
7: Update membership matrix U using Equation 2.11
8: **for** $j = 1$ to c **do**
9: $p = \text{argmin}_{(1 \leq k \leq n)} \sum_{i=1}^{n} u_{ij}^{m} \rho(x_k, x_i)$
10: $v_j = x_p$
11: **end for**
12: $ITER = ITER + 1$
13: **end while**
14: **return** C

of $O(nc)$. Also within the **while** statement, on line 9, an estimate is calculated of the impact of changing v_i. This step has a runtime complexity of $O(n^2)$, is within the **for** loop on line 8, and is executed c times. The total runtime complexity (T) is therefore:

$$\begin{aligned} T &= O(nc^2) + i \times (O(nc) + c \times O(n^2)) \\ &= O(nc^2) + O(nci) + O(n^2ci) \\ &= O(n^2ci) \end{aligned}$$

2.2.4 Fuzzy Neighborhood DBSCAN (FN-DBSCAN)

Nasibov and Ulutagay modified the DBSCAN algorithm to integrate fuzzy set theory [45]. Fuzzy Neighborhood Density-Based Spatial Clustering of Applications with Noise (FN-DBSCAN) employs a fuzzy neighborhood function rather than a crisp set definition to assess density [55]. FN-DBSCAN repairs one of DBSCAN's flaws [21]. Since DBSCAN uses a crisp definition for density, a data object, x_p, at nearly ε distance from a group of data objects, is assigned the same density as a data object, x_q, in close proximity to a similar group of data objects (Figure 2.4).

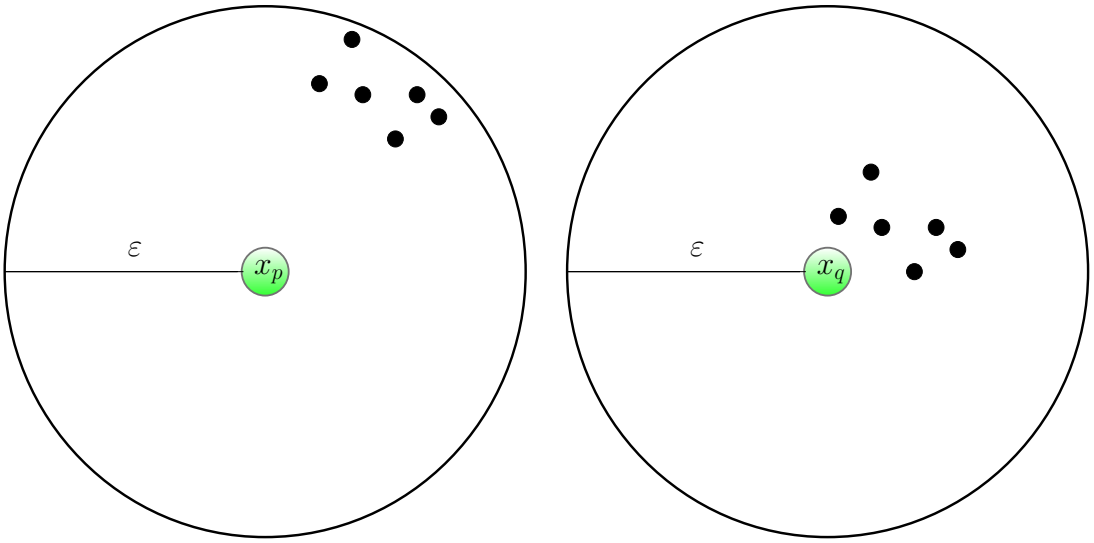

(a) x_p is in a sparse region (b) x_q is in a dense region

Figure 2.4: Data Objects x_p and x_q Have Same Density in DBSCAN, but Have Different Densities in FN-DBSCAN

FN-DBSCAN corrects the density calculation by using a fuzzy membership function, where the density at a data object is the sum of the values of the fuzzy membership functions of all data objects within distance ε. Otherwise, the algorithm is identical to DBSCAN. Many fuzzy neighborhood membership functions have been developed; Nasibov and Ulutagay discussed the use of linear, trapezoidal, and exponential fuzzy neighborhood functions [56] [45].

The linear fuzzy neighborhood function, the most straightforward, is defined as [45]:

$$\mu(x_i, x_j) = \begin{cases} 1 - (\rho(x_i, x_j)/\varepsilon), & \text{if } \rho(x_i, x_j) \leq \varepsilon \\ 0, & \text{otherwise} \end{cases} \tag{2.12}$$

where $\rho(x_i, x_j)$ is the distance between data objects x_i and x_j.

Figure 2.5 shows how the value of the fuzzy neighborhood function varies with distance. The figure assumes that the data is scaled so that the maximum dissimilarity is equal to one.

A choice of fuzzy neighborhood function must be supplied to FN-DBSCAN as a parameter. Because the focus of my dissertation is to reduce the runtime of fuzzy clustering algorithms, the choice of the fuzzy neighborhood function is not an important factor as long as the choice is the same

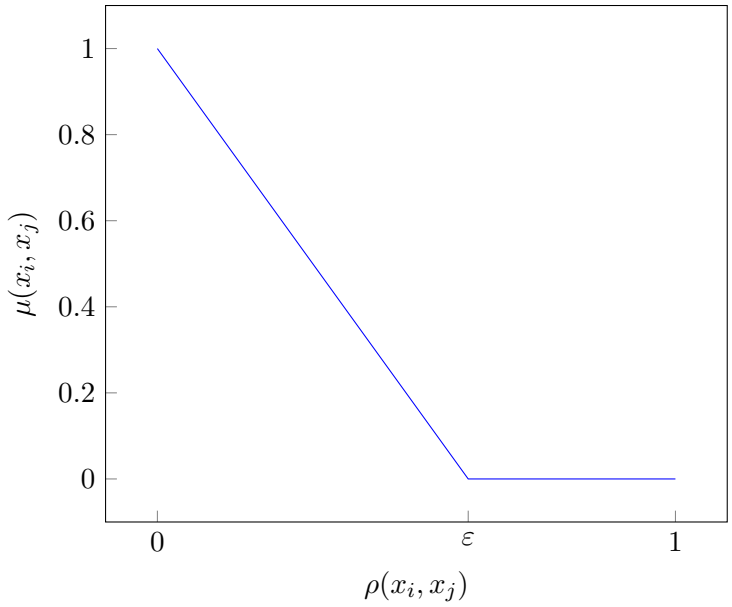

Figure 2.5: Linear Neighborhood Function Used in FN-DBSCAN

for all experiments. Therefore, the simplest fuzzy neighborhood function, the linear neighborhood function, was used.

Like DBSCAN, FN-DBSCAN requires two additional parameters: distance, ε, and minimum cardinality, $MinCard$. The term "minimum cardinality," used instead of "minimum number of points," accurately reflects how FN-DBSCAN uses the sum of the fuzzy neighborhood function values for each data object to calculate the density. If, for a data object, the fuzzy set cardinality, $FSCard$, is greater than $MinCard$, that data object is a core point [45] [55].

$$FSCard(x_i) = \sum_{j=1}^{n} \mu(x_i, x_j) \tag{2.13}$$

Except for this change, the FN-DBSCAN algorithm is identical to DBSCAN [21]. The runtime complexity is also identical.

2.3 Accelerated Clustering Algorithms

2.3.1 Significant Work Related to Acceleration

The focus of my dissertation is to reduce the runtime of fuzzy clustering algorithms while keeping quality loss to a minimum. As clustering algorithm research has has intense focus for five decades, there has been and continues to be much interest in accelerating clustering algorithms. This section describes significant work relevant to the methods used and experiments described in this dissertation. Accelerated algorithms, used for experiments in the research or related to this work, are described in the sections below.

A literal implementation of the FCM algorithm, as described in Section 2.2.2.1, has an expected runtime complexity of $O(nisc^2)$, where n is the number of data objects, c the number of clusters, s the number the data features, and i the number of iterations. As previously mentioned, it is possible to reduce the runtime to $O(nisc)$ with the optimization proposed by Kolen and Hutcheson [47].

Given a dataset with c natural clusters, an FCM variant can be accelerated further by reducing n, s, or i. There are techniques for reducing the number of features, s, but many of these techniques preprocess the data rather than being integrated into the algorithm itself [57] [58]. An alternative technique, subspace clustering, looks for clusters using a subset of the available features [59] [60]. Each cluster found can use a different subset of the available features. This line of research, however, was not pursued. My dissertation focused on techniques that reduce the amount of data used, n, and the number of iterations, i.

Algorithms such as FCM, designed to minimize an objective function value, have shorter runtimes if their initial cluster centers are close to the final solution. The shorter runtime is due to a reduction in iterations before termination. Bradley and Fayyad [61] investigated the effects of an improved starting position for HCM. A better start position reduced the runtime, but their study was focused on quality, not speed.

Processing a small data sample to obtain an improved initial starting point for FCM has been investigated. Cheng describes an iterative process to develop a "good" starting point [62]. This

method, Multistage Random Sampling FCM (mrFCM), consists of two parts. The first part progressively samples the dataset, improving the starting clusters until a termination criterion is met. Then mrFCM uses these starting clusters to initialize FCM on the full dataset.

Similarly, Altman uses FCM to obtain a set of cluster centers from a small sample of data objects. These cluster centers are used to initialize the membership matrix, U, before clustering the full dataset with FCM [63].

In Partition Simplification FCM (psFCM), Hung and Yang [64] partition the data using a k-d tree to obtain a simplified dataset, which in turn is used as a subsample to estimate the position of the cluster centers. The resulting estimate is used to initialize FCM on the full dataset.

The Single Pass FCM (SPFCM) algorithm, discussed in Section 2.3.2, incrementally clusters the data and passes on the cluster centers from each increment as an initialization for the next [46]. Online FCM (OFCM), discussed in Section 2.3.3, follows a similar strategy [65].

Provost presented an overview of the progressive sampling technique in the context of induction (a.k.a. classification) algorithms [66]. Progressive sampling uses an initial subsample to form a classifier, which is tested on labeled data. The subsample progressively increases in size arithmetically or geometrically, creating a new classifier each time it grows. When the accuracy of the classifier ceases to improve significantly when compared to the previous sample, the addition of data is terminated.

Progressive sampling techniques have been applied to clustering problems. These techniques accelerate a clustering algorithm by reducing the number of data objects, n, that are clustered.

Domingos and Hulten [67] used Hoeffding bounds in a progressive sampling technique both to estimate the initial sample size and to estimate the sufficiency of the sample size at any point in the progression. The technique, developed for HCM, assumes that each data object has membership in only one cluster. It calculates the worst-case bounds, and the sample sizes are typically large.

Pal and Bezdek [68] and Wang et al. [69] used progressive sampling to select a subsample representative of the dataset. They used a divergence test to assess whether the subsample matched the distribution of the dataset. If the test failed, progressively larger subsamples were taken until

the test passed. Finally a clustering algorithm was run on the chosen subsample. This technique, extensible Fast FCM (eFFCM), is discussed in detail in Section 2.3.4.

A very simple way to reduce n is to select a sample of the dataset and to apply the clustering algorithm to the sample. Havens et al. [16] use this technique in the random sampling plus extension FCM (rseFCM) algorithm, which is discussed further in Section 2.3.5

2.3.1.1 Relational Clustering

Fewer techniques exist for accelerating relational clustering algorithms.

Clustering Large Applications (CLARA) accelerates the PAM algorithm by repetitively sampling the dataset [28]. Each sample is clustered using PAM, and the clustering solution is extended to the entire dataset. The clustering solution with the lowest (best) objective function is returned. The sample size and number of samples taken are user-determined.

An optimization to FCMdd is Linearized Fuzzy C-Medoids (LFCMdd). This accelerated variant, as the name suggests, reduces the runtime complexity to be linear with respect the number of data objects, i.e., $O(nci)$. LFCMdd considers only the data objects with the highest membership values as candidates to update the current set of cluster centers [44].

Labroche directly adapted SPFCM and OFCM to use FCMdd as the base algorithm [54]. These accelerated algorithms, History Based Online Fuzzy C-Medoids (HOFCMD) and Online Fuzzy C-Medoids (OFCMD), are otherwise identical to SPFCM and OFCM respectively.

Bezdek (et al.) created an accelerated, relational version of eFFCM called extended non-Euclidean relational fuzzy c-means (eNERF) [70]. The eFFCM algorithm, described in detail in Section 2.3.4, depends on the existence of features from which to select a sample of the data. These features, of course, do not exist in relational data. To solve this problem, eNERF considers relations between data objects rather than features, and then selects a subset of relations that are dissimilar to each other. The eNERF algorithm otherwise uses a strategy similar to that of eFFCM.

2.3.2 Single Pass Fuzzy c-means (SPFCM)

Prodip Hore developed SPFCM as part of his dissertation research [71]. The SPFCM algorithm breaks the dataset into equally sized "partial data accesses" (PDA). A user-provided parameter, "fractional PDA" ($fPDA \leq 0.5$), defines the PDA size as $fPDA \times n$ where n equals the total number of data objects. SPFCM incrementally processes the entire dataset one PDA at a time. Each PDA is processed by a weighted version of FCM, aptly named Weighted FCM (WFCM). In the WFCM algorithm, each data object, x_i, has an associated weight, w_i. The objective function and cluster center calculation from Section 2.2.2 are modified as follows [46] [11]:

$$J_{mw}(U,V) = \sum_{i=1}^{c}\sum_{k=1}^{n} u_{ik}^{m} w_k D_{ik}(x_k, v_i) \tag{2.14}$$

$$v_i = \frac{\sum_{j=1}^{n} w_j (u_{ij})^m x_j}{\sum_{j=1}^{n} w_j (u_{ij})^m} \tag{2.15}$$

where w_i is a non-zero weight for a data object.

Data objects are initially given a weight of 1. After the cluster centers, $v_i \in V$, are calculated from the first PDA, the cluster centers are assigned weights using the following Equation [11]:

$$w_i' = \sum_{j=1}^{n} (u_{ij}) w_j, 1 \leq i \leq c \tag{2.16}$$

SPFCM uses weighted cluster centers as representative objects. These weighted cluster centers represent the partition information from the first PDA. The c cluster centers are added as additional data examples to the second PDA, which is then clustered by WFCM. The positions of the cluster centers calculated from the first PDA are used as the initial values for V in the second PDA. This process is repeated until all PDAs have been clustered. SPFCM returns as a final solution the set of cluster centers from the last PDA.

The SPFCM algorithm assumes that the data objects in the dataset have been randomly ordered. Datasets with some sort of inherent order in the data, typical in images, can result in PDAs

significantly different with respect to the overall distribution. The implementation used in this research randomizes the data prior to processing.

2.3.2.1 Runtime Complexity

The runtime complexity of FCM is $O(nisc)$ (Section 2.2.2.1). Note that the runtime complexity is linear with respect to n, the number of data objects. The SPFCM algorithm also processes the entire dataset, albeit incrementally, so a cursory analysis of the runtime complexity would also yield $O(nisc)$.

Hore reports that SPFCM had a shorter runtime than FCM on the datasets he tested [46]. Hore identified the cause: after the first PDA had been clustered, the derived cluster centers were used to initialize V in the subsequent PDA. Initial cluster centers closer to the optimal cluster centers allow the algorithms in the HCM family to terminate with fewer iterations [61].

Reviewing complexity analysis in a similar manner as [46] [71], the following notation is used:
n is the size of the dataset.
p is the PDA value as a fraction (fPDA).
$d = \frac{1}{p}$ is the number of partial data accesses required.
i_j: is the number of iterations in the j^{th} PDA.

$$\begin{array}{ll} T_j = O(pni_jsc) & \text{runtime complexity for the } j^{th} \text{ PDA} \\ \hat{i} = p\sum_{j=1}^{d} i_j & \text{average number of iterations per PDA} \\ T = O(\sum_{j=1}^{d} pni_jsc) & \text{total runtime complexity for SPFCM} \\ T = O(n\hat{i}sc) & \text{substituting } \hat{i} \text{ into expression for } T \end{array} \tag{2.17}$$

The runtime complexity of SPFCM is $O(n\hat{i}sc)$. When SPFCM clusters a dataset it has a shorter runtime compared with FCM because typically, $\hat{i} < i$.

2.3.3 Online Fuzzy c-means (OFCM)

Prodip Hore also developed OFCM as part of his dissertation research [71]. OFCM breaks the dataset into PDAs and clusters each PDA, in the same manner as SPFCM. The OFCM algorithm

produces a set of cluster centers from each PDA and, using Equation 2.16, calculates their weights. These weighted cluster centers represent the partition information in each PDA.

The OFCM and SPFCM algorithms, though similar, have one major difference [11]. Unlike SPFCM, OFCM saves each set of weighted cluster centers, instead of adding them to the subsequent PDA. After all PDAs have been clustered, the saved sets of weighted cluster centers from each PDA are combined into one dataset. Then, WFCM clusters this combined dataset. OFCM returns as a final solution the set of cluster centers from the combined dataset.

An advantage of OFCM is that the processing of a dataset can be separated over distance or time. In these cases, the initial set of cluster centers is chosen locally by random selection. Alternatively, cluster centers from a previous PDA can be used as initial cluster centers. While the latter strategy matches the original implementation of the algorithm [65], a PDA not representative of the entire dataset will provide a poor initial set of starting clusters. OFCM does not assume that the dataset is in random order. In this dissertation, except where explicitly noted, the datasets clustered by OFCM were not randomized.

The runtime complexity analysis of OFCM is fundamentally the same as the analysis in Section 2.3.2.1.

2.3.4 Extensible Fast Fuzzy c-means (eFFCM)

The eFFCM algorithm clusters a statistically significant *sample*, $\hat{X}$, as opposed to the full dataset, X. Statistical significance is tested for by comparing the distribution of the sample with the distribution of X using the Chi-square (χ^2) statistic or Kullback-Leibler divergence. It is formally presented as Algorithm 6.

If the initial sample fails testing, additional data is progressively added to the sample and the new sample is tested. This procedure is repeated until a sample has passed the statistical test [68] [72]. The size of each additional subsample is constant; therefore the sampling procedure uses progression with an arithmetic schedule [66]. The final statistically significant sample, $\hat{X}$, is then clustered by FCM to obtain a set of cluster centers.

Algorithm 6: Extensible Fast Fuzzy c-means

1: **Input:** X, c, m, ϵ, $fPDA$, $\delta fPDA$, α
2: $n = |X|$
3: $\hat{n} = fPDA \times n$
4: Randomly select $\hat{n}$ data objects from X into sample set $\hat{X}$
5: **while** $test(\hat{X}, X, \alpha)$ is **false do**
6: $\quad \hat{a} = \delta fPDA \times n$
7: $\quad$ Randomly select $\hat{a}$ data objects from X.
8: $\quad$ Add the $\hat{a}$ selected data objects to $\hat{X}$.
9: **end while**
10: V = FCM($\hat{X}$, c, m, ϵ)
11: Extend V to X to calculate U.
12: **return** U, V

where:
X is a dataset.
c is the number of clusters.
$m > 1$ is the "fuzzifier."
ϵ is a parameter for FCM's termination criterion.
$fPDA$ is the fractional size of the initial sample, $\hat{n} = fPDA \times |X|$.
$\delta fPDA$ is the fractional size of the progressive sample.
$test$ is a statistical test.
α is the desired level of significance for the statistical test.

Extension of the set of cluster centers, V (produced from $\hat{X}$), to the full dataset produces a partition of X. Equation 2.8 and V are used to calculate the membership of $x_i \in X$ in $v_j \in V$.

The use of the statistical tests implies that the distribution of the dataset is known. For most datasets, the distribution must be calculated or estimated before running the algorithm. A successful implementation requires decisions concerning the method used to model the distribution, the statistical test to use, the initial sample size, the rate of arithmetic progression, and the termination criterion [73].

2.3.4.1 Runtime Complexity

The runtime complexity of eFFCM is the same as that of FCM (Section 2.2.2.1). The eFFCM algorithm typically has a shorter runtime, because the number of data objects clustered, $\hat{n}$, will

typically be less than n, the number of data objects in the full dataset. This makes eFFCM's runtime $O(\hat{n}isc)$.

Selection of the sample and extension of the solution to the full dataset are separate steps. Their runtime complexities must be added to those of eFFCM. It takes $O(n)$ time to model the distribution and to obtain random samples. Extending the solution using Equation 2.8 has a time complexity of $O(nsc)$. This makes the total runtime $O(\hat{n}isc) + O(nsc) + O(n)$.

If one assumes that $\hat{n}i \geq n$, the runtime complexity for eFFCM remains $O(\hat{n}isc)$. Experimental results, discussed in Section 4.4, show that this is a reasonable assumption. As a practical concern, the sampling and extension do add significant overhead to an implementation of the algorithm.

2.3.5 Random Sampling Plus Extension Fuzzy c-means (rseFCM)

This algorithm uses FCM to cluster a random sample, $\hat{X}$, of the dataset, X. The size of $\hat{X}$ is a user-defined parameter [16]. Using Equation 2.8, a complete partition of X is produced by extending the set of cluster centers produced from $\hat{X}$ to the full dataset.

If $\hat{n} = |\hat{X}|$ is substituted for n, the runtime complexity of rseFCM will be the same as that of FCM (Section 2.2.2.1). Randomly selecting $\hat{X}$ takes $O(n)$ time. Thus, the total runtime is $O(\hat{n}isc)$.

2.3.6 Density Based Distributed Clustering (DBDC)

Density Based Distributed Clustering (DBDC) is a distributed, scalable version of DBSCAN that can provide a speedup over DBSCAN [74] [21]. The DBDC algorithm assumes the existence of multiple sites with local datasets. The goal of the algorithm is to cluster the union of all the local datasets. Conceptually, this has the same structure as any accelerated algorithm that breaks a large dataset into smaller subsets.

DBDC uses DBSCAN to cluster the local datasets at each site. Each local clustering solution is represented by a set of data objects, the "specific core points," and a set of distances, the "specific ε-ranges." The set of specific core points is a subset of the core points defined by DBSCAN such that none of the specific core points are within ε distance of each other. Each specific core point is assigned a specific ε-range to define the extent of the search space volume it represents.

Each local set of specific core points and specific ε-ranges are combined to create a global dataset. DBSCAN clusters this global dataset, with $MinPts$ set to 2. The rationale for $MinPts$'s setting is that the global dataset only consists of core points. Thus, two core points define a larger cluster if their distance apart is ε or less.

The user sets the ε parameter. The authors of the algorithm suggested using the largest specific ε-range for ε, but they admit that this setting might not work for all datasets. The value for ε would need to exceed the specific ε-range for datasets in which the specific core points for a cluster only exist in one local model. Otherwise, these specific core points for this cluster would be greater than ε apart in the global dataset and would not define a cluster.

2.3.7 Scalable DBDC (SDBDC)

The Scalable DBDC (SDBDC) algorithm was designed to repair flaws in DBDC [75]. In addition to the difficulty in setting epsilon (described above), DBDC ignores "noise" at each local site that could potentially define a cluster when combined globally.

SDBDC makes the same assumptions as DBDC but uses a different criterion to select representative data objects at each local site. DBSCAN clusters the data objects at each local site. Fuzzy logic is not explicitly mentioned in [75], but a linear fuzzy membership function does calculate the sum of the membership functions within ε distance of each data object. This sum is referred to as a "representation quality."

The representation qualities for each data object are listed in descending order. The data object with the highest representation quality is selected as a representative object and removed from the list. The representation quality is recalculated for each data object remaining in the list, and the list is resorted. This process repeats until enough representative data objects have been selected. Januzac (et al.) designed SDBDC to allow the user to determine an acceptable trade-off between speedup and quality of results. Thus, the actual number of representative objects from each local site is user-configured.

Additional data is recorded for each representative data object: the number of data objects "covered" by each representative object and the distance to the farthest data object it "covers." These are called the "covering number" and the "covering radius."

The representative data objects from each local site are combined globally, and a modified version of DBSCAN clusters the data. The global algorithm is more complex, since it considers the "covering number" as a weight and modifies the ε parameter with the "covering radius" separately for each representative data object.

2.4 Evaluation Metrics

This section presents the evaluation metrics used in this dissertation and related works.

The term, "quality", is frequently used when evaluating experimental results. Quality, properly defined, refers to "the degree of excellence which a thing possesses" [76]. In this dissertation, quality is only used to describe the results (cluster centers, partition, etc.) obtained from the clustering algorithm. The degree to which the accelerated algorithm succeeds at its task is referred to as speedup, never quality.

Quality can only be measured by some objective function. The FCM family of algorithms seeks to reduce an objective function. We compare the final objective function values of two algorithms using the $DQ\,R_m\%$ metric which is described below.

It is possible for two algorithms to have identical objective function values, but result in different partitions. So, the second way to evaluate the final partition was to compare the degree to which the partitions produced by two algorithms differ. Assuming the reference algorithm produces an ideal partition, what is being measured is the degree to which the competing algorithm is faithful to the reference. These types of metrics are referred to in this dissertation as "fidelity" metrics. The term, "fidelity", is used to differentiate a metric from $DQ\,R_m$. In this research, $CC\%$, $DFV\%$, and ARI are recorded as fidelity metrics and described below.

2.4.1 Relative Speedup (SU)

Because the goal of the dissertation is to develop new methods that reduce the runtime of clustering algorithms, a metric is necessary to compare competing algorithms. The *SU* metric calculates the ratio between the runtimes of two algorithms. If t_1 is the runtime of candidate algorithm 1 and t_2 the runtime of the reference algorithm, the speedup of algorithm 1 relative to algorithm 2, SU_{12}, is:

$$SU_{12} = \frac{t_2}{t_1} \tag{2.18}$$

For example, if algorithm 1 has a runtime of 150ms and algorithm 2 a runtime of 750ms, the speedup equals 5. Algorithm 1 is five times as fast as algorithm 2.

2.4.2 Difference in Quality of Objective Function

Many clustering algorithms are designed to minimize the value of a squared error function, also called the *objective function*. Minimization of this value is the goal of the HCM algorithm and its variants, so comparisons using the objective function, J_m, have been employed as a means of comparing the quality of results of different algorithmic variants [46] [77].

If J_{m1} is the objective function value for algorithm 1, and J_{m2} the objective function value for (the reference) algorithm 2, then the percentage difference in quality of algorithm 1 relative to that of algorithm 2 is:

$$DQ\, J_m\% = \left(\frac{J_{m1} - J_{m2}}{J_{m2}} \right) \times 100 \tag{2.19}$$

The accelerated algorithms based on FCM (SPFCM, OFCM, eFFCM, rseFCM) use different strategies to sample the dataset. Values of J_m produced by these accelerated algorithms potentially use different-sized samples and are thereby not comparable. Calculation of $DQJ_m\%$ would require extension of the clustering solutions to the full dataset in order to obtain membership values (Equation 2.8) so that J_m can be calculated for each algorithm.

Fortunately, the objective function J_m (2.7) is mathematically equivalent to a reformulated optimization criterion (R_m) [78] [77]:

$$R_m(V) = \sum_{k=1}^{n} \left(\sum_{i=1}^{c} D_{ik}(x_k, v_i)^{\frac{1}{(1-m)}} \right)^{(1-m)} \tag{2.20}$$

The R_m calculation is more convenient than J_m because it requires only the original dataset and the cluster centers. The percentage difference in quality between algorithm 1 and 2 is calculated as follows [46]:

$$DQ\, R_m\% = \left(\frac{R_{m1} - R_{m2}}{R_{m2}} \right) \times 100 \tag{2.21}$$

where R_{m1} is the reformulated optimization criterion for algorithm 1, and R_{m2} for (the reference) algorithm 2.

2.4.3 Cluster Change Percentage

Clustering algorithms in the HCM family require an initial starting point, typically a starting set of cluster centers, V_{init}. When V_{init} is randomly selected over multiple trials, the algorithm often produces different partitions for every trial. Two trials of a clustering algorithm may have similar values for J_m but radically different partitions. It is theoretically possible, though unlikely, for two different partitions to have identical J_m values. So, other metrics are needed that do not have this problem.

The cluster change percentage, $CC\%$, is a complimentary method of comparing the fidelity of clustering algorithms. The assigned cluster for each data object in the dataset is compared between two partitions. An indicator variable, δ_i, is set to 0 if the cluster assignments are the same in both partitions, and it is set to 1 if they are different. In the case of fuzzy clustering, the cluster assignments are "hardened" by assigning each data object to the cluster in which its membership value, u_{ij}, is highest. For a pair of partitions, A and B, the $CC\%$ is [77]:

$$CC\%(A, B) = \frac{\sum_{i=1}^{n} \delta_i}{n} \times 100 \tag{2.22}$$

This metric requires a method to identify corresponding clusters in partitions A and B. In my research, the Hungarian Method was used [79].

A small amount of cluster change indicates that the two partitions are very close. When one partition is from the reference algorithm, a small $CC\%$ value signifies that the candidate algorithm has created a highly similar partition to the original algorithm.

When comparing two or more experiments, each involving multiple trials of clustering algorithms, the use of $CC\%$ is straightforward, as long as the data objects have been defined as feature vectors in R^s. For an algorithm, the averages for the values in V over all experiments can be used to define the partition. Equation 2.22 can then be used to calculate the $CC\%$ between any pair of algorithms. The fact that the cluster centers have representation in R^s also allows examination of how the positions of cluster centers in V vary, indicating the consistency of the clustering method (see Section 2.4.4).

When the algorithms and data are relational, the cluster centers do not have representation in R^s, and the use of Equation 2.22 is not so straightforward. For instance, if there were 30 trials per experiment, there would be 30 sets of medoids. It is not possible to average the medoids as if they were cluster centers and to use the procedure described above.

Within multiple trials of an experiment using a relational algorithm, it is possible to compute the $CC\%$ between any pair of trials. For an experiment consisting of t trials, the average $CC\%$ can be calculated over every pair of trials. This I define as the $intra\,CC\%$:

$$intra\,CC\% = \frac{1}{\binom{t}{2}} \sum_{i=1}^{t} \sum_{j=i+1}^{t} CC\%(T_i, T_j) \tag{2.23}$$

where T_i is the partition from the i^{th} trial.

The $CC\%$ can also be calculated between the trials of two experiments with different clustering algorithms. This I define as the $inter\,CC\%$:

$$inter\,CC\% = \frac{1}{t^2} \sum_{i=1}^{t} \sum_{j=1}^{t} CC\%(T_i, T_j) \tag{2.24}$$

where the i subscript indicates trials from one algorithm and the j subscript indicates trials from the other. Equation 2.24 assumes that both experiments have the same number of trials.

2.4.4 Difference in Fidelity of Partitions

As noted in Section 2.4.3, algorithms that randomly select an initial set of cluster centers, V_{init}, could, over many trials, produce a different partition every trial.

Difference in fidelity of partitions (DFV) compares the variation of the cluster centers (V) produced by a candidate algorithm to that of a reference algorithm [77]. DFV can be used to assess the variation that a single algorithm experiences over multiple trials, or it can be used to compare two different algorithms. DFV is calculated as a percentage:

$$DFV\% = \left(\frac{\sum_{i=1}^{t} \sum_{j=1}^{c} ||V'_{ij} - Vavg_j||}{t \times \sum_{j=1}^{c} ||Vavg_j||} \right) \times 100 \tag{2.25}$$

where:

t: is the number of trials.

V'_{ij}: is the j^{th} cluster center from the i^{th} trial of the candidate algorithm.

$Vavg_j$: is the average position the j^{th} cluster center produced by the reference algorithm.

$||\cdot||$: is the length of the vector $(\cdot)$.

The DFV metric provides an indication of a candidate algorithm's stability, compared either to itself or to a reference algorithm. It requires a method to identify corresponding cluster centers across trials. In my research, the Hungarian Method was used [79].

2.4.5 Adjusted Rand Index (ARI)

The Rand Index evaluates the similarity between two partitions [80]. Given two partitions, A and B, the Rand Index returns a value in the range of 0 to 1; 0 when the partitions are in complete disagreement, and 1 when the partitions are in complete agreement.

The cluster assignments of every possible pair of data objects ($x_i, x_j \in X$) are used[2] to calculate the Rand Index (RI) [81]:

$$RI = \frac{a+d}{a+b+c+d} \tag{2.26}$$

where:

a - the number of pairs of data objects with the same cluster assignments in both partitions A and B.

b - the number of pairs of data objects with the same cluster assignments in partition A but different cluster assignments in partition B.

c - the number of pairs of data objects with different cluster assignments in partition A with the same cluster assignments in partition B.

d - the number of pairs of data objects with the different cluster assignments in both partitions A and B.

A difficulty with RI is that it does not take chance into account. If the data objects in both partitions were assigned clusters randomly, then a number of pairs would coincide purely by chance. A modified form, the Adjusted Rand Index (ARI), corrects this problem [82]:

$$ARI = \frac{RI - E[RI]}{1 - E[RI]} \tag{2.27}$$

where $E[RI]$ is the expected value of RI if data objects in the partitions are distributed randomly.

ARI returns a value of 1 when the partitions are in complete agreement, 0 when the partitions return the value expected by chance, and a negative value when the partitions are in greater disagreement than would be expected by chance.

The Rand Index and ARI can be used to compare the partition of an accelerated (candidate) algorithm to that of the reference algorithm. The Rand Index and ARI also assume that the

[2]Given $n = |X|$, the number of pairs equals $\binom{n}{2}$. RI calculation has a time complexity of $O(n^2)$ and can be impractical for very large datasets.

clustering is discrete, i.e., hard [80] [82]. For fuzzy clustering, the partitions must be hardened by assigning each data object to the cluster in which it has the highest membership value [16].

2.4.6 Accuracy

When the actual class labels are available for a test dataset, calculating the percentage accuracy of a clustering solution is an obvious metric, but somewhat misleading because clustering algorithms do not optimize accuracy. Each cluster label is associated with a class label and any data object whose cluster label does not match its associated class is considered inaccurate. Prior to the calculation, clusters must be aligned to the class labels. In my research, the Hungarian method was used [79].

2.4.7 Some Statistics

2.4.7.1 Welch's t-test

This test for significance compares the means of two populations when the numbers of samples in each population are small and the sample variances cannot be assumed to be equal [83]. The t statistic and the associated degrees of freedom are calculated as follows [84]:

$$t = \frac{\bar{X}_1 - \bar{X}_2}{\sqrt{\frac{s_1^2}{n_1} + \frac{s_2^2}{n_2}}} \tag{2.28}$$

$$\nu = \frac{\left(\frac{s_1^2}{n_1} + \frac{s_2^2}{n_2}\right)^2}{\frac{s_1^4}{n_1^2(n_1-1)} + \frac{s_2^4}{n_2^2(n_2-1)}} \tag{2.29}$$

where:

$\bar{X}_i$: is the i^{th} sample mean

s_i: is the i^{th} sample standard deviation

n_i: is the i^{th} sample size

ν : are the degrees of freedom

2.4.7.2 Z-test

Mean values and sample standard deviations were calculated for many of the metrics in the experiments. The z statistic can then be calculated to test for statistical significance in the difference between mean values produced by two different algorithms [84].

$$z = \frac{(\overline{X_1}) - (\overline{X_2})}{\sqrt{(\sigma_1^2/n_1) + (\sigma_2^2/n_2)}} \tag{2.30}$$

where:

X_1 and X_2 are mean values from algorithms 1 and 2 respectively.

σ_1^2 and σ_2^2 are samples variances from algorithms 1 and 2 respectively.

n_1 and n_2 are the metric populations from algorithms 1 and 2 respectively.

The most common test I used was an estimation of whether two mean values were different, i.e., a two-tailed test. Using the null hypothesis, H_0, that there is no difference between means, and the alternative hypothesis, H_1, that $X_1 \neq X_2$, if z exceeds the value for the specified confidence level, H_0 must be rejected. Typically, the 95% confidence level is used, in which $z = 1.96$, and a calculated value $z > 1.96$ or $z < -1.96$ means there is a significant difference.

Chapter 3: Datasets

"I don't know what the best type is, but I know none is bad." - Lawrence "Yogi" Berra [2]

3.1 About the Datasets

Seventeen original datasets were used in experiments. Eleven datasets were obtained from real-world data sources, the other six were artificially constructed. An additional six datasets were derived from subsets of real world datasets, bringing the total number of datasets used to twenty three.[3]

The datasets are described in detail in the sections below. Table 3.1 lists the number of data objects, features and classes for all datasets.

3.2 MRI Datasets

Three datasets used in experiments, MRI016, MRI017, and MRI018, are magnetic resonance images (MRI) of a normal human brain. Each dataset has approximately four million data objects. The images were pre-processed to remove non-brain tissue (bone, fat, skin, etc.) and air. The three data features in these datasets are the intensities of the T1-weighted, T2-weighted, and proton density-weighted sequences. The values are integers ranging from 0 to 1951. These images were clustered into the three classes: cerebro-spinal fluid (CSF), gray matter (GM), and white matter (WM) [11].

Four additional datasets (MRI016R, MRI017R, MRI017R-2, and MRI018R) were derived from the MRI datasets for experiments with relational clustering. See Section 6.2 for details.

[3]Some of the material in this chapter has been previously published by me [21] [22] [23], and is re-used under terms of the copyright © 2010, 2012 and 2013 IEEE.

Table 3.1: Datasets

Dataset	data objects (n)	features (s)	classes (c)
Breast Cancer	699	10	2
D3C6-1	12,000	3	6
D3C6-2	12,000	3	6
D4C5	16,000	4	5
D6C5	1,000,000	6	5
D7C10	12,000	7	10
D10C7	1,000,000	10	7
Heart-Statlog	270	13	2
Iris	150	4	3
Landsat	6,435	36	6
Letters AY	1575	16	2
MRI016	3,882,771	3	3
MRI017	3,898,407	3	3
MRI018	4,293,292	3	3
MRI016R	12,000	3	3
MRI017R	12,000	3	3
MRI017R-2	20,000	3	3
MRI018R	12,000	3	3
Pendigits	10,992	16	10
Pendigits015	3341	16	3
PLK01	203,278	21	20
PLK02	16,000	21	4
Vote	435	16	2

3.3 Plankton Datasets

The plankton dataset, PLK01, was derived from a set of plankton images collected by the Shadow Imaging Particle Profiler and Evaluation Recorder (SIPPER) imaging system [85]. The images of plankton in this dataset were collected during three cruises in the Gulf of Mexico (2002, 2008, and 2010) and two in the Western Pacific (2007 and 2008) [86] [87]. At the University of South Florida's College of Marine Science, experts classified these images into a type of marine object, typically a class of plankton.

The data features are primarily calculated from the images. Examples of features include moment invariants, filled area, convex area, intensity, and transparency. The ocean depth at which the sample was collected is also a data feature. The mean and standard deviation were calculated

for each feature. The values for each feature were fitted to a standard normal distribution, so that the mean feature value would equal zero and the feature value would equal the number of standard deviations the value is above or below the mean [87].

Initially, there were a total of 482,719 data objects, with 88 features, representing 168 classes of marine object. The number of data objects in the classes ranged from a single example (elongate phytoplankton: chaetoceros) to 99,414 (noise: air bubble). Attempts cluster the entire dataset with $c = 168$ did not provide stable results. The data objects belonging to noise, detritus, and other small, non-homogeneous classes were removed, and the remaining data objects were placed in random order. Using the WEKA data mining tool [88], feature selection was performed with Consistency Subset Evaluation and Linear Forward Selection [89]. These efforts left 203,278 data objects and 21 features. Analysis of the cleaned dataset showed 20 predominant classes.

A second dataset, PLK02, was created out of PLK01. A total of 16,000 data objects was randomly selected from PLK01. Each selected data object was in one of four classes: crustacean ostracod, elongate chaetognath, elongate strands, and protist. An equal number of data objects (4,000) was selected from each class.

The full plankton dataset (PLK01) is very challenging to cluster using the FCM family of algorithms. One of the reasons is its imbalanced data distribution by class [90]. The FCM algorithm and other algorithms that reduce a squared error term perform best when the distribution by class is roughly equal [91]. The PLK02 dataset, with an equal number of data objects in each class, represents a lesser challenge.

3.4 UCI Datasets

The University of California, Irvine (UCI) Machine Learning Repository is a resource well-known to data scientists [92]. As of 2013, it holds over 240 pre-processed datasets for experimentation and testing of machine learning algorithms. Several datasets from this repository were used in experiments.

3.4.1 Breast Cancer (Wisconsin)

The Wisconsin Breast Cancer dataset consists of test results for 699 clinical cases [93]. Each of the 10 features is the value of a diagnostic measure, scaled between 1 and 10. The class values, which were not used in the research, indicate if the test results indicated a malignant or benign tumor.

3.4.2 Heart-Statlog

The Heart-Statlog dataset consists of information from 270 clinical cases [94]. Each of the 13 features is the value of a diagnostic measure. The class values, which were not used in the research, indicate the presence or absence of heart disease.

3.4.3 Iris

The Iris dataset consists of field measurements of 150 iris flowers. Each of the four features are the length or width of some part of the flower. The class values are the three different species of iris measured [95].

3.4.4 Landsat

The Landsat dataset is imagery from the National Aeronautics and Space Administration's (NASA) Landsat Multispectral Scanner (MSS). Each of the 6,435 data objects is derived from a 3×3 pixel area of imagery of the Earth's surface. The 36 features are the intensities of light in four spectral bands for each of the nine pixels. The values are integers ranging from 0 to 255. The dataset was clustered into six classes, corresponding to six different land cover types [96].

3.4.5 Letters

The Letters dataset consists of data from 20,000 images, each of which is one of the 26 capital letters in the English language. Each image is unique; the original image was a letter in 1 of 20 fonts which was randomly distorted. The image data features are each converted to an integer ranging from 0 to 15 [97].

A subset dataset was created from letters that just consists of the letters 'A' and 'Y'. This dataset consists of 1,575 data objects.

3.4.6 Pendigits

Pendigits is a collection of 10,992 handwritten numerals collected from 44 different writers. The handwritten numerals were plotted on an $x \times y$ coordinate grid. The 16 features are 8 (x, y) coordinates from the handwritten numeral. The coordinates were spatially resampled to be separated by an equal arc-length. The values are integers ranging from 0 to 100. The dataset was clustered into ten classes, corresponding to numerals from 0 to 9 [98].

A subset dataset of Pendigits was created using just the digits 0, 1 and 5. It was appropriately named Pendigits015 and consists of 3,341 data objects.

3.4.7 Vote

The Vote dataset holds the 1984 United States Congressional voting records. Each record contains the votes of 435 Congressmen for 16 important votes that year [99]. 'Yes' votes were converted to equal '1' and 'No' votes converted to equal '0'. The class values, which were not used in the research, are the political party of each Congressman.

3.5 Artificial

A total of six artificial datasets were created for experiments. A simple program was written to generate artificial datasets. The program input consists of the locations of c cluster centers in R^s as well as the desired variance and number of data objects for each cluster center. Each data object deviates from its cluster center in each dimension by a random amount determined by a gaussian distribution using the provided variance. The generated examples were then output in random order. Each artificial dataset was provided its own unique random seed, to ensure that the dataset generation program did not produce the same series of pseudo-random numbers.

The names of the datasets are designed to reflect the number of features (dimensions) and number of clusters. For example, dataset D4C5 has 4 features and 5 clusters. Its configuration data was as follows:

Table 3.2: Configuration Data for D4C5

Item	Cluster	Value(s)
Number Attributes		4
Number Clusters		5
Cluster Center	1	0,0,0,0
Cluster Center	2	0.5,0.866,0,0
Cluster Center	3	1,0,0,0
Cluster Center	4	0.5,0.289,0.816,0
Cluster Center	5	0.5,0.289,0.204,0.791
Variance	1-5	0.08
Data Objects	1-5	3200

The artificial datasets were designed to moderately challenge FCM and its variants. Notes on some of the artificial datasets are below.

3.5.1 D3C6 Series

The original D3C6 dataset (D3C6-1) was designed for use with FCMdd. It, however, proved extremely challenging. The variance was set so high relative to the scale of the data objects that a significant number of data objects overlapped clusters. FCMdd did a poorer job of determining the structure of the data than it did on real world datasets! So a second dataset, D3C6-2, with the same number of clusters and features was created. D3C6-2 has the same relative positions of the cluster centers, but the variance is set so there is much less overlap.

The poor performance obtained from D3C6-1 turned out to be very revealing about how FCMdd clustered data. The results from both datasets are presented in Section 6.2.3.

3.5.2 D4C5

The clusters in this dataset are all equidistant from each other. The distance between any two clusters is of unit length.

Chapter 4: A Simple Experiment

" You can observe a lot by watching." - Lawrence "Yogi" Berra [2]

4.1 Introduction

FCM forms the basis for many accelerated algorithms [62] [64] [68] [100] [46] [65] [16]. Some of these algorithms were discussed in Chapter 2. It is difficult to select the best accelerated algorithm for a particular application, despite a careful review of the published literature. This is so because the research in published works was performed on disparate hardware, operating systems, and code bases. Speedup and quality metrics used in published works are not uniform.[4]

A series of experiments was conducted using FCM and four accelerated variants (SPFCM, OFCM, eFFCM, rseFCM) [22]. Analysis of the results compared the speedup and quality of the accelerated variants to FCM and to each other. The goals of the experimentation were to gain insight into why different accelerated algorithms obtain different levels of performance and to explore ways to improve this class of algorithm.

4.2 Experimental Procedures

Experiments were conducted using five datasets: MRI016, MRI017, MRI18, Pendigits, and Landsat[5]. Details on the datasets are in Chapter 3. Details on the software implementation of the algorithms are in Appendix A.2.

For each experiment runtime and quality metric values were recorded. As noted in Section 2.1.2, this class of algorithms produces non-deterministic results when random initialization is

[4]Some of the material in this chapter has been previously published by me [22] and is re-used under terms of the copyright © 2012 IEEE.

[5]Results for an initial set of experiments were published in [22]. The results presented here used an updated codebase that implemented Kolen's optimization (Section A.2.3) and improved precision.

used. Initialization for all algorithms was performed by randomly selecting c data objects in X to be the initial values of V. Each experiment consisted of 30 trials to ensure a statistically significant sample. While the initialization for each trial of an experiment was different, the same set of 30 initializations was used for each algorithm in the experiments. The average values over 30 trials were recorded for the runtime and quality metrics.

The algorithms have several tunable parameters. Common parameters (m, ϵ) and algorithm-specific parameters (α, δPDA) were fixed for all experiments. Only two parameters were varied. The fractional partial data access, $fPDA$, was varied to show its effects on speedup and quality. An additional set of experiments was performed using SPFCM and OFCM to investigate the effects of randomizing the dataset prior to clustering. When the flag parameter, *Randomize*, was set to '1', the order of the data objects was randomized. These parameters are summarized in Table 4.1.

Table 4.1: Experiment Parameter Settings

Parameter	Value
m	2.0
ϵ	0.001
α	0.200
δPDA	0.02
$fPDA$	0.05, 0.10 or 0.20
Randomize	0 or 1

The $fPDA$ parameter is used in every accelerated algorithm to determine a sample size, $\hat{n} = fPDA \times |X|$. In the SPFCM and OFCM algorithms, $\hat{n}$ defines the size of the PDA. In the eFFCM algorithm, $\hat{n}$ is the initial sample size. In the rseFCM algorithm, $\hat{n}$ is the sole sample size.

The implementation of the eFFCM algorithm uses the χ^2 statistic. (See Appendix A for details.) A significance level, α, for the χ^2 statistic had to be chosen. Initial trials showed that high values for α, such as 0.95 or 0.90, would often require over 50% of the data before the goodness of fit test passed. Since this seemed an unduly large penalty on the runtime of the algorithm, a rather relaxed value of 0.20 was chosen for α. In choosing a value for α, there is a tradeoff between speed and selecting a diverse sample. We attempted to increase the speedup at a potential quality cost compared to FCM.

For each experiment the results from all algorithms on the same dataset with identical parameter settings were recorded. Regarding each algorithm, runtime, the number of iterations to termination, the cluster center positions, and R_m were recorded.

4.3 Results

The metrics collected were used to calculate relative speedup (SU), $DQ\,R_m\%$, $DFV\%$, and $CC\%$ between the five algorithms for the five datasets. This created a large volume of data; Table 4.2 shows results for just one dataset (MRI016), one $fPDA$ (0.05), and one metric (SU).

Table 4.3 shows, with respect to FCM, each algorithm's speedup and quality for each PDA, over all the MRI datasets. The average of results for the MRI datasets are reported, because there was little difference between them. The Pendigits and Landsat datasets (Tables 4.4 and 4.5) had more differences between them.

The speedups of each accelerated algorithm vs. FCM ranged from below 1 to over 10. The quality and fidelity metrics of each accelerated algorithm deviated from FCM by 0% to 11%.

Table 4.2: Speedup Comparison for MRI016, $fPDA = 0.05$

Algorithm	vs. FCM	vs. SPFCM	vs. OFCM	vs. eFFCM	vs. rseFCM
FCM	1.0000	0.2479	0.6161	0.4966	0.1434
SPFCM	4.0343	1.0000	2.4854	2.0034	0.5786
OFCM	1.6232	0.4024	1.0000	0.8061	0.2328
eFFCM	2.0137	0.4992	1.2406	1.0000	0.2888
rseFCM	6.9721	1.7282	4.2953	3.4623	1.0000

4.4 Discussion

The results show real differences in the speedup and quality of FCM's accelerated variants.

The quality measures of all accelerated variants represent a degradation from FCM. On the MRI datasets, for all $fPDA$s and quality metrics, there is only a little deviation from the reference algorithm, FCM (Table 4.3). Compared to the other datasets, the MRI datasets have a larger number of data objects ($> 3 \times 10^7$), and lower numbers of data features (3) and clusters (3).

Table 4.3: Average Performance vs. FCM on MRI Datasets

$fPDA$	Algorithm	Speedup	$DQ\,R_m\%$	$DFV\%$	$CC\%$
0.05	SPFCM	3.511	0.000%	0.045%	0.042%
0.05	OFCM	1.459	0.079%	0.512%	0.515%
0.05	eFFCM	1.872	0.001%	0.051%	0.053%
0.05	rseFCM	6.291	0.005%	0.148%	0.109%
0.10	SPFCM	3.037	0.000%	0.038%	0.038%
0.10	OFCM	1.408	0.087%	0.583%	0.654%
0.10	eFFCM	1.969	0.001%	0.052%	0.052%
0.10	rseFCM	4.767	0.003%	0.112%	0.087%
0.20	SPFCM	2.417	0.000%	0.029%	0.031%
0.20	OFCM	1.321	0.115%	0.776%	0.792%
0.20	eFFCM	1.925	0.001%	0.050%	0.054%
0.20	rseFCM	3.005	0.001%	0.069%	0.069%

Table 4.4: Average Performance vs. FCM on Pendigits Dataset

$fPDA$	Algorithm	Speedup	$DQ\,R_m\%$	$DFV\%$	$CC\%$
0.05	SPFCM	5.121	0.653%	6.675%	7.032%
0.05	OFCM	1.352	0.149%	2.897%	7.760%
0.05	eFFCM	2.766	0.209%	3.572%	3.030%
0.05	rseFCM	10.599	1.331%	9.089%	7.487%
0.10	SPFCM	3.809	0.308%	5.084%	4.512%
0.10	OFCM	1.724	0.138%	2.655%	5.959%
0.10	eFFCM	2.981	0.228%	3.891%	2.702%
0.10	rseFCM	6.161	0.705%	7.033%	5.977%
0.20	SPFCM	2.771	0.283%	4.070%	10.116%
0.20	OFCM	1.169	0.113%	2.211%	2.802%
0.20	eFFCM	2.600	0.374%	4.854%	4.376%
0.20	rseFCM	3.635	0.421%	5.094%	4.522%

Table 4.5: Average Performance vs. FCM on Landsat Dataset

$fPDA$	Algorithm	Speedup	$DQ\,R_m\%$	$DFV\%$	$CC\%$
0.05	SPFCM	1.914	0.469%	1.310%	1.321%
0.05	OFCM	1.045	0.635%	1.200%	5.206%
0.05	eFFCM	1.309	0.163%	0.550%	0.389%
0.05	rseFCM	3.353	2.009%	2.241%	1.601%
0.10	SPFCM	1.703	0.513%	1.025%	1.134%
0.10	OFCM	1.030	0.918%	2.201%	10.956%
0.10	eFFCM	1.320	0.190%	0.594%	0.280%
0.10	rseFCM	2.745	0.779%	1.314%	0.653%
0.20	SPFCM	1.534	0.097%	0.505%	0.326%
0.20	OFCM	0.907	0.777%	1.740%	9.029%
0.20	eFFCM	1.315	0.205%	0.611%	0.202%
0.20	rseFCM	2.151	0.337%	0.831%	0.357%

The Pendigits and Landsat results show that $DQ\,R_m\%$ deviates from FCM by 0.1% to 2.0% (Tables 4.4 and 4.5). On average, this is a much higher deviation than in the MRI datasets. The $DFV\%$ and $CC\%$ metrics from the Pendigits and Landsat results are, on average, much higher than corresponding values in the MRI datasets. Occasionally, corresponding values are two orders of magnitude higher! The Pendigits and Landsat datasets both have fewer objects and a greater number of features than the MRI datasets.

Overall, the gains in speed are modest; the greatest speedup is around 10 times. In general, speedup was inversely proportional to the total sample size (eFFCM and rseFCM) or the $fPDA$ (SPFCM and OFCM). Analyses of the speedup and effects on quality for each accelerated variant are given in the subsections below.

4.4.1 rseFCM's Speedup

This accelerated variant of FCM reduces runtime by reducing the size of the dataset. The FCM runtime complexity is linear with respect to n, so a reduction in n would have a corresponding reduction in runtime. The rseFCM algorithm should therefore have a speedup inversely proportional to $fPDA$, but this does not take into account the time needed for random selection of data from

disk. The runtime reported in this dissertation does include this time, plus other overhead, which decreases the speedup.

Table 4.6 shows the runtimes, overhead, and speedup for rseFCM on all datasets averaged over 30 trials. The absolute overhead time for random data selection is roughly constant for a given dataset, so it has an impact inversely proportional to the $fPDA$. The procedure used for random selection of data could have been more efficient. The last column of Table 4.6 shows the speedup if there had been no overhead from random selection of data. This can be considered an upper bound on speed for the datasets tested.

See Appendix A.2 for details on how the data was randomly selected.

Table 4.6: rseFCM Speedup vs. FCM with Overhead

Dataset	$fPDA$	rseFCM time (msec)	rseFCM overhead (msec)	Pct. over-head	FCM time (msec)	Speedup	Speedup less overhead
MRI016	0.05	7701	4765	61.88%	53692	6.97	18.29
MRI017	0.05	7354	4968	67.56%	41643	5.66	17.45
MRI018	0.05	7659	5290	69.07%	47785	6.24	20.17
Pendigits	0.05	172	97	56.40%	1823	10.60	24.31
Landsat	0.05	153	126	82.35%	513	3.35	19.00
MRI016	0.10	10218	4808	47.05%	53352	5.22	9.86
MRI017	0.10	9767	4969	50.88%	42194	4.32	8.79
MRI018	0.10	10165	5343	52.56%	48366	4.76	10.03
Pendigits	0.10	298	101	33.89%	1836	6.16	9.32
Landsat	0.10	188	129	68.62%	516	2.74	8.75
MRI016	0.20	16806	5075	30.20%	53673	3.19	4.58
MRI017	0.20	14620	5009	34.26%	42005	2.87	4.37
MRI018	0.20	16470	5617	34.10%	48565	2.95	4.47
Pendigits	0.20	510	106	20.78%	1854	3.64	4.59
Landsat	0.20	239	137	57.32%	514	2.15	5.04

4.4.2 eFFCM's Speedup

The eFFCM algorithm (Tables 4.3, 4.4, and 4.5) always provides faster results than FCM, and the quality difference across all measures never exceeds 5%. On the low dimensionality MRI datasets, the quality difference never exceeds 1%.

The closest alternative to eFFCM is rseFCM. The eFFCM algorithm decreases the runtime in the same manner as rseFCM; the random sample size, n, is smaller than the full dataset. Both algorithms use a random sample of the dataset, but they differ in that eFFCM requires a statistical test before accepting a sample. Table 4.7 lists paired results for the averages of all experiments for each dataset.

Table 4.7: Averaged Results for eFFCM and rseFCM

Dataset	Algorithm	Time (msec)	Pct. over-head	Pct. Data used	Speedup	$DQ\,R_m\%$	$DFV\%$	$CC\%$
MRI	eFFCM	24966	33.76%	33.3%	1.92	0.001%	0.051%	0.053%
MRI	rseFCM	11196	49.73%	11.7%	4.69	0.003%	0.110%	0.088%
Pendigits	eFFCM	663	29.48%	25.3%	2.78	0.270%	4.106%	3.369%
Pendigits	rseFCM	327	37.02%	11.7%	6.80	0.819%	7.072%	5.995%
Landsat	eFFCM	391	66.10%	29.8%	1.31	0.186%	0.585%	0.290%
Landsat	rseFCM	193	69.43%	11.7%	2.75	1.041%	1.462%	0.870%

Judging from $DQ\,R_m\%$, eFFCM's results are consistently of higher quality than rseFCM's. The eFFCM algorithm's lower values for $CC\%$ and $DFV\%$, compared to rseFCM's, reinforce this observation. This is especially clear in the case of the high dimensionality Landsat and Pendigits datasets. However, rseFCM results show a significantly higher speedup than eFFCM.

Compared with rseFCM, eFFCM takes a "double hit" in overhead from the sample selection process and from the increased sample size. Assuming that all other factors (parameters and randomization) are equal, the sample selection process for eFFCM will take longer than rseFCM because of the need to test for significance and, if the initial sample fails the χ^2 test, the possibility of resampling. When the total data used by eFFCM exceeds the size of the PDA used by rseFCM, the runtime will increase proportionally. Therefore, on average, the runtime of eFFCM will be longer than that of rseFCM. Table 4.7 clearly demonstrates the difference in runtimes. For example, eFFCM consistently uses more data than rseFCM and has a consistently smaller speedup.

The difference in quality between eFFCM and rseFCM is greatest when the dataset has a large number of features, justifying the need for statistical testing. When there are fewer features, as in

the case of the MRI datasets, rseFCM has quality nearly equal to eFFCM's, but it has a greater speedup.

4.4.3 SPFCM's Speedup

The SPFCM algorithm provides a reliable speedup with little or no loss in quality over all datasets. The SPFCM results are shown in Table 4.8.

The speedup ranges from roughly 1.5 to 5.1, but this takes into account the time needed to place the data in random order, disk I/O, and other overhead. In some applications, the data is naturally in random order or has been pre-randomized. If the speedup calculation is adjusted to make this assumption, the speedup ranges from 3.2 to 8.8. The percentage of the runtime taken by overhead from randomization of the dataset is listed in the column labeled 'Pct. overhead' in Table 4.8. The difference in speedup is shown in the columns 'Speedup' and 'Adj. Speedup'.

The speedup was inversely proportional with respect to the $fPDA$ across all datasets. This was predicted from the analysis of the runtime complexity. SPFCM's runtime is linear with respect to the number of data objects in each PDA. The speedup occurred because the weighted cluster centers passed to the next PDA were a better estimate of the final cluster centers compared with random initialization. Thus, fewer iterations were required until termination. When $fPDA$ was large, there were fewer PDAs and fewer opportunities to reduce the number of iterations. Details on the runtime complexity are in Section 2.3.2.1.

Based on $DQ\,R_m\%$, the FCM and SPFCM provide the same quality on the MRI datasets. The corresponding cluster change percentages are very low, ranging from 0.010% to 0.067%. The Landsat and Pendigits datasets have small degradations in R_m of less than 1%. Their cluster change percentages, however, are much higher than those of the MRI datasets, ranging from 0.3% to 10.1%.

The poorer fidelity, as measured by $CC\%$, in these datasets is not surprising. They both have more attributes and clusters than the MRI datasets, and therefore more boundary areas between clusters in higher-dimensional space. So a small perturbation in cluster center position has the

potential to alter the membership of a higher percentage of data objects compared with the MRI datasets.

Table 4.8: SPFCM Performance

Dataset	$fPDA$	Time (msec)	Pct. overhead	Speedup	Adj. Speedup	$DQ\,R_m\%$	$CC\%$
MRI016	0.05	13309	43.69%	4.03	7.16	0.000%	0.010%
MRI016	0.10	15967	36.51%	3.34	5.26	0.000%	0.012%
MRI016	0.20	20153	29.14%	2.66	3.76	0.000%	0.018%
MRI017	0.05	13071	45.52%	3.19	5.85	0.000%	0.049%
MRI017	0.10	14976	39.08%	2.82	4.62	0.000%	0.047%
MRI017	0.20	18865	31.18%	2.23	3.24	0.000%	0.036%
MRI018	0.05	14430	44.80%	3.31	6.00	0.001%	0.067%
MRI018	0.10	16377	39.78%	2.95	4.90	0.000%	0.055%
MRI018	0.20	20568	31.79%	2.36	3.46	0.000%	0.040%
Pendigits	0.05	356	41.57%	5.12	8.76	0.653%	7.032%
Pendigits	0.10	482	31.12%	3.81	5.53	0.308%	4.512%
Pendigits	0.20	669	22.42%	2.77	3.57	0.283%	10.116%
Landsat	0.05	268	72.39%	1.91	6.93	0.469%	1.321%
Landsat	0.10	303	63.70%	1.70	4.69	0.513%	1.134%
Landsat	0.20	335	57.31%	1.53	3.59	0.097%	0.326%

4.4.4 OFCM's Speedup

The OFCM algorithm produces a negligible speedup over FCM. The OFCM results are shown in Table 4.9. In the last experiment listed in Table 4.9, note that OFCM was actually slower than FCM. At the time of this particular research, an attempt to cross reference results showed that published papers on OFCM [71] [65] [11] did not compare OFCM's speed to FCM's. A subsequent paper by Havens [16] reported results similar to these.

OFCM is very similar to SPFCM. The primary differences are that the input data for OFCM is not assumed to be in random order, and that weighted clusters from the previous PDA are not added to the subsequent PDA.

These differences are related to the purpose of OFCM, which is to handle large amounts of streaming data [71]. It is assumed that the data is processed as it comes, and that weighted cluster centers derived from processing each chunk are saved to be combined with additional cluster centers

later on. Because of the intended purpose, the datasets were not randomized before processing by OFCM.

The quality of results with respect to $DQ\,R_m\%$ was inconsistent over the datasets tested. For example, OFCM had an average $DQ\,R_m\%$ value on Landsat over 5 times of that on Pendigits. The fidelity of results with respect to $DFV\%$ and $CC\%$ was also inconsistent across datasets, with no strict correlation between fidelity and quality.

A visual inspection of the original Pendigits dataset, containing the class definitions, showed that the data was somewhat randomly distributed with respect to classes. This was not the case for the other datasets. In the case of MRI images, the image data was read in order. The three types of brain tissue that constitute clusters are not randomly distributed in a normal human brain, which increased the likelihood that each PDA processed by OFCM was a non-representative sample of the whole dataset.

Table 4.9: OFCM Performance

Dataset	$fPDA$	Speedup	$DQ\,R_m\%$	$DFV\%$	$CC\%$
MRI016	0.05	1.62	0.016%	0.218%	0.187%
MRI016	0.10	1.54	0.027%	0.353%	0.351%
MRI016	0.20	1.36	0.097%	0.863%	0.904%
MRI017	0.05	1.25	0.085%	0.578%	0.581%
MRI017	0.10	1.30	0.079%	0.620%	0.631%
MRI017	0.20	1.23	0.077%	0.643%	0.250%
MRI018	0.05	1.51	0.138%	0.738%	0.779%
MRI018	0.10	1.39	0.155%	0.778%	0.981%
MRI018	0.20	1.37	0.170%	0.823%	1.221%
Pendigits	0.05	1.35	0.149%	2.897%	7.760%
Pendigits	0.10	1.72	0.138%	2.655%	5.959%
Pendigits	0.20	1.17	0.113%	2.211%	2.802%
Landsat	0.05	1.04	0.635%	1.200%	5.206%
Landsat	0.10	1.03	0.918%	2.201%	10.956%
Landsat	0.20	0.91	0.777%	1.740%	9.029%

These non-representative samples were a factor in OFCM's performance with respect to speedup and quality. When a PDA is not representative of the whole dataset, there will be two main effects: (1) the PDA might terminate more slowly due to the splitting of homogeneous clusters, and (2)

the PDA will pass on to the next PDA a set of cluster center initializations not representative of the ideal cluster centers.

In the original experimental plan, SPFCM used randomized data, and OFCM did not. In order to test the effect of randomized data, additional experiments of 30 trials each were performed with SPFCM and OFCM. The first set of experiments compared SPFCM and OFCM on non-randomized datasets with identical cluster initialization. The second set of experiments compared the algorithms on pre-randomized datasets. The only overhead to the algorithms was a small amount of disk I/O. The number of iterations of the core WFCM algorithm for each trial was recorded.

Table 4.10: Average Performance of OFCM vs. SPFCM

Dataset	Random	Algorithm	Time (msec)	Iter. per PDA ($\hat{i}$)	Speedup vs. FCM	$DQ\,R_m$%
MRI	no	OFCM	34371	13.41	1.40	0.094%
MRI	no	SPFCM	17591	6.11	2.83	4.608%
MRI	yes	OFCM	14632	5.32	3.23	0.000%
MRI	yes	SPFCM	11757	3.92	4.18	0.000%
Pendigits	no	OFCM	1332	51.49	1.42	0.133%
Pendigits	no	SPFCM	428	13.26	5.36	0.395%
Pendigits	yes	OFCM	1123	43.73	1.60	-0.155%
Pendigits	yes	SPFCM	421	13.15	4.93	0.062%
Landsat	no	OFCM	520	39.30	0.99	0.776%
Landsat	no	SPFCM	187	8.49	2.82	10.859%
Landsat	yes	OFCM	432	30.33	1.24	0.010%
Landsat	yes	SPFCM	196	9.16	2.80	0.820%

Table 4.10 lists the results of these experiments, averaged across each dataset. The average iterations per PDA and speedup vs. FCM are listed. The results show that randomized data consistently reduces the number of iterations for OFCM, which directly correlates to a faster runtime. Also, SPFCM consistently uses a smaller number of iterations to terminate, compared to an identically configured set of OFCM trials.

When identically configured and applied to the same dataset, these algorithms have only two differences: (1) SPFCM includes the weighted cluster centers from the previous PDA while OFCM saves them to disk, and (2) OFCM runs WFCM on weighted cluster centers after all data has been processed.

Let us first consider difference (2). An examination of the trial diagnostic logs showed that the final step of OFCM (in which the weighted data objects are clustered) only added between 2 and 7 iterations. For the datasets used in experiments, the number of weighted data objects clustered in this step is only between 15 and 200. This final step of OFCM adds only a negligible amount of time.

This leaves difference (1). OFCM uses the positions of the previous c cluster centers as initial values for V, but SPFCM uses both the positions for V and the c weighted data objects. Examination of Equation (2.15) shows how the weights associated with the data objects influence the values in V. OFCM's PDAs lack both the data objects and their weights, so it takes longer to terminate with the initialized values. This was verified by reviewing the experiments' diagnostic logs. Despite identical initialization, OFCM required more iterations to terminate per PDA. In the course of the investigation, it was also discovered that the number of iterations required for SPFCM to terminate dropped to a very low level, very quickly. We note that the weights increase for each new PDA. This has significant implications that are discussed in Section 5.3.

Table 4.10 also lists the $DQ\,R_m\%$ for each experiment. For all experiments, OFCM has a lower value for $DQ\,R_m\%$ than SPFCM does under identical conditions.[6] Earlier remarks on the experimental results state that OFCM has quality inferior to SPFCM's on the MRI and Landsat datasets, but these remarks compared OFCM clustering non-randomized datasets.

SPFCM's speedup is superior to OFCM's for the same reasons that its quality is inferior. SPFCM passes weighted cluster centers to each subsequent PDA to be processed by WFCM. After the first few PDAs, these weighted cluster centers tend to dominate. Consider when $fPDA = 0.05$. After 10 PDAs are clustered, the weighted cluster centers represent over 50% of the dataset! A review of the diagnostic logs verified that the cluster center positions did not deviate much after the first few PDAs had been clustered. So, if the initial PDAs are not proportional to the whole dataset, the final set of cluster centers may be influenced negatively by the initial PDAs weighted cluster centers.

[6] On the MRI datasets, OFCM has a slightly lower $DQ\,R_m\%$ than SPFCM, but Table 4.10 does not have the precision to show it.

In contrast, OFCM does not cluster the combined dataset of weighted cluster centers until the final step. The results from each PDA have equal influence on the final partition produced.

4.5 Conclusions

4.5.1 Assessing Quality

While the algorithms are designed to reduce R_m, their underlying purpose is to partition the dataset. Changes to the partition are recorded in the $CC\%$ metric. In Tables 4.4 and 4.5, very small values of $DQ\,R_m\%$ correlate to large changes in cluster assignments ($CC\%$). Consequently, only using the objective function value to determine how close two partitions are can be deceiving.

To assess fidelity properly when comparing accelerated algorithms, both a metric to assess the functioning of the algorithm, such as $DQ\,R_m\%$, and a metric to assess its effects, such as $CC\%$, are needed.

The original premise of the experiment was that the FCM algorithm would serve as a reference for performance for the other algorithms. In Table 4.10, the comparison between SPFCM and OFCM, note that one of the $DQ\,R_m\%$ entries for Pendigits is negative.

The $DQ\,R_m\%$ metric was calculated using Equation 2.20, substituting the R_m value for FCM as R_{m2}. Negative values for the $DQ\,R_m\%$ indicate that the candidate algorithm had, on average, a lower R_m value than FCM. In this case, one could say the quality of OFCM is better because the objective function value being minimized is lower.

Table 4.10 lists averages over experiments. For the pre-randomized Pendigits dataset clustered by OFCM, the $DQ\,R_m\%$ values for all experiments were negative. A one-tailed Welch's t-test (Section 2.4.7.1) was employed in order to ascertain whether the difference between FCM and OFCM for the experiment with $fPDA = 0.10$ was significant. The $DQ\,R_m\%$ is only -0.1974%, but the t-test yielded $t = 1.83$ with 29 d.f. This results in $p = 0.0388$, which may be considered statistically significant at $\alpha = 0.05$.

Originally, it was assumed that the $DFV\%$ and $CC\%$ fidelity metrics could express the objective function quality loss of the accelerated variant as compared to the optimal reference algorithm, FCM. This assumption was not valid when the accelerated variant had a lower R_m than FCM,

because the R_m value might have been a more desirable extremum. When $DQ\,R_m\%$ is negative, the $DFV\%$ and $CC\%$ metrics express the quality improvement. Thus, it can be deceiving to only view a partition-based fidelity metric, such as $CC\%$, $DFV\%$, or ARI in discussing quality.

The $DFV\%$ and $CC\%$ values listed in Tables 4.3, 4.4, and 4.5 showed some variation, but were almost always the same order of magnitude for the same experiment. Deviation between the two measures occurred when the fidelity, as measured by both metrics, was poor. This makes sense because the $DFV\%$ assesses the change in cluster positions and $CC\%$ assesses the effects of that change. This fact and the experimental results suggest that the $DFV\%$ and $CC\%$ metrics are largely redundant. As the $CC\%$ metric reflects changes in the actual partition of the dataset, it is a more meaningful metric.

4.5.2 Ranking the Algorithms

The FCM algorithm and four accelerated variants were compared with respect to speed and three quality metrics. The code base and experiments were carefully constructed to ensure comparisons on as equal a basis as possible.

The algorithms listed in order of speed from slowest to fastest are: FCM, OFCM, eFFCM, SPFCM, and rseFCM. OFCM had a surprisingly small speed improvement over FCM. Analysis showed that, despite improved starting cluster centers, each PDA took many iterations to terminate. The differences between SPFCM and OFCM that influenced speed were data randomization and the use of weighted data objects for cluster initialization.

The time taken to randomize data was included in the runtime calculations for eFFCM, SPFCM, and rseFCM. This amount of time was often a significant percentage of the total runtime. If it could be assumed that the data had been provided in random order, the speedups of these three variants would improve further.

The algorithms are more difficult to rank in order of quality, because you want to consider fidelity also. Judging solely from $DQ\,R_m\%$, the eFFCM algorithm appears to have the best quality overall and rseFCM the worst. There was little consistency, however, in quality measures across datasets. Any ranking of "best algorithm" overall would be quite subjective. This study demonstrates that

tradeoffs must be made between speed and quality, and that there is variation in performance across datasets.

4.5.3 Observations

The goals of the experimentation were to discover why accelerated clustering algorithms perform like they do and how this knowledge can be leveraged to improve these algorithms.

Some accelerated algorithms produce a speedup by clustering only a sample of the dataset. The rseFCM algorithm clusters a random sample of user-defined size. The eFFCM algorithm also clusters a randomly selected sample, but it validates the sample with a statistical test. The validation step increases the runtime, but it ensures a sample representative of the whole dataset. The eFFCM algorithm, because of this sampling method, yielded higher-quality results compared to those of rseFCM. These higher-quality results, however, came at the expense of speedup.

On the MRI datasets, rseFCM and eFFCM differed little in quality. This suggests that the samples which rseFCM used were fairly representative of the whole dataset, and that little advantage was gained by using a statistical test. The MRI datasets are large relative to the Pendigits and Landsat datasets, and have a smaller number of clusters and data features. Recall that the experimental setup used $fPDA$ to determine the sample size. When the $fPDA = 0.05$, rseFCM had a sample size 1/20 of the whole dataset: 194,139 from MRI016, but only 322 from Landsat.

The SPFCM and OFCM algorithms produce a speedup by incrementally clustering all the data, one sample at a time. Representative objects hold the partition information from each sample. Comparing SPFCM and OFCM, the experiments that used pre-randomized data were faster and had better quality than those that did not. Again, the pre-randomized data is more likely to be representative of the dataset as a whole. This has the apparent effect of improving speedup as well as quality.

SPFCM was always faster than OFCM, regardless of whether or not the data had been pre-randomized. For initialization, SPFCM used weighted data objects as cluster centers, unlike OFCM, which used the cluster center positions. The existence of the weighted data objects influenced the positions of the cluster centers, which resulted in fewer iterations. In Section 2.3.2.1, the runtime

complexity of SPFCM is shown to be identical to that of FCM. SPFCM's speedup is due to improved cluster center initialization after the initial PDA. The implementation of OFCM uses the same strategy as SPFCM to initialize cluster centers. On identical datasets, the difference in speed between SPFCM and OFCM is solely due to weighted cluster center initialization.

Regarding quality, the use of weighted cluster centers had the opposite effect. These weighted data objects greatly influenced the cluster centers produced by each PDA. If the initial PDAs clustered by SPFCM were not representative of the whole dataset, the final set of cluster centers drifted to resemble the results of the initial PDAs. OFCM, however, clustered the best representatives of each PDA, which reflected the whole dataset better. Under identical conditions (dataset randomization, algorithmic parameters), OFCM had consistently better quality than SPFCM. A one-tailed Welch's t-test (Section 2.4.7.1) was employed in order to ascertain whether the differences in $DQ\,R_m\%$ between SPFCM and OFCM were significant. Over all 30 experiments conducted, the least significant test yielded $t = 1.99$ with 29 d.f. This results in $p = 0.0280$, which may be considered statistically significant at $\alpha = 0.05$. Thus one can conclude that OFCM provided statistically significantly better quality results than SPFCM for the quality metric and α value used.

To sum up, SPFCM and rseFCM worked best on datasets with small numbers of features and classes. The eFFCM algorithm had the best quality and fidelity on datasets with larger numbers of features and classes, but the speedup was modest. The OFCM algorithm had the best quality and fidelity on datasets with data objects that were already in random order with respect to class, though the speedup was small. For every dataset, choice of algorithm represented a tradeoff of speed and quality/fidelity.

Significant observations on the entire experiment are as follows:

- A smaller sample size decreases the runtime.
- A sample representative of the whole dataset results in a higher-quality partition.
- A larger sample size can make a statistical test superfluous.
- A distributed clustering solution, using representative objects, can produce high-quality results.

- An initial set of cluster centers closer to the final partition reduces runtime.
- SPFCM's final reported set of cluster centers did not deviate significantly after the first few PDAs were clustered.
- The use of weighted cluster centers for initialization reduces runtime.
- The use of weighted cluster centers can have a negative impact on quality if the sample is not representative of the whole dataset.

These observations were condensed to the following *ideas* stated in Section 1.3

1. Use of a statistically significant sample of the dataset reduces runtime while preserving quality.
2. An algorithm designed to cluster the data incrementally can produce a high-quality result when stopped before all data has been processed. This is especially true when the data is presented in random order.
3. The use of representative objects, either weighted or un-weighted, can overcome difficulties of scale, if properly utilized.
4. For a particular class of clustering algorithms, providing a "starting point" close to the optimal solution reduces runtime and can improve quality.

In the following sections, these ideas will be explored further to create new accelerated clustering algorithms.

Chapter 5: Accelerating FCM

"When you come to a fork in the road, take it." - Lawrence "Yogi" Berra [2]

The experiments in Chapter 4 investigated the ways that FCM can be accelerated by reducing n (eFFCM and rseFCM) or i (SPFCM and OFCM). The methods developed in this chapter seek to accelerate FCM by simultaneously reducing n and i.[7]

5.1 Estimating the Random Sample Size

The accelerated clustering algorithms discussed in Section 2.3.1 and Chapter 4 sample the dataset, but they typically do not use a statistical method to determine the sample size. Domingos and Hulten's technique [67] estimates the initial sample size using Hoeffding bounds for HCM clustering, but this does not directly generalize to FCM [72].

The SPFCM algorithm uses a parameter ($fPDA$) to define a static sample size [46]. The eFFCM algorithm uses a statistical test to validate a sample, but not to determine the sample size [68] [72]. The mrFCM algorithm and Altman's method also use a parameter to define the sample size for cluster center initialization [62] [63]. The size of the sample influences the performance of the algorithms [22], but the parameters in each case are determined empirically.

As suggested in [61], the sample must proportionally represent each cluster in order to provide an improved starting point for an algorithm such as FCM, that uses alternating optimization. A known difficulty in using a sample to generate starting points for a clustering algorithm occurs when the sample fails to represent all clusters sufficiently [61] [62]. This results in skewed starting

[7] Content in this chapter is an edited version of the author's previously published works [22] [23] and is re-used under terms of the copyright © 2012 and 2013 IEEE. New material and analysis has been added.

points. One solution to this problem is to ensure that the sample has proportional representation. This solution was suggested in [62] but not elaborated upon.

Gu (et al.) studied the effects of an improper starting sample size when using progressive sampling on supervised learning problems [101]. They implemented a divergence test on a sample to ensure it represented the dataset distribution. Similarly, in [68] and [73], Pal, Bezdek, and Hathaway test the sample for the proportionality to the dataset as a whole, but they use the sample for calculating the clustering solution rather than for estimating clusters for initialization. Regardless, to ensure proportionality, this sort of technique requires collection of information from the entire dataset. A larger sample of the dataset can be used for this purpose, but uncertainty remains as to the validity of the size of this larger sample.

Another approach is to select a probabilistically large enough sample to represent all clusters at a desired level of confidence. If one assumes that the clusters correspond to a set of currently unknown classes, selecting a sample to represent each cluster sufficiently is analogous to selecting a sample to estimate a multinomial proportion of classes. This is so because, if the sample provides an acceptable estimate of a proportion of classes, that sample will have proportional representation of the clusters in the data.

Thompson developed a method [102] to find the smallest sample size, λ, such that a random sample from a multinomial population would result in "class" proportions within a specified distance of the true population proportions, with probability at least 1 - α. It was shown that the minimum sample size, λ, is:

$$\lambda = \max_{\mu} z^2(1/\mu)(1 - 1/\mu)/d^2 \tag{5.1}$$

where d is the maximum absolute difference from the true proportion that will be tolerated for any class. The value z is the upper $(\alpha/2\mu) \times 100th$ percentile of the standard normal distribution.

Thompson showed that μ, an integer, is the number of classes present in the population for which the calculated value of λ is a maximum. For $\alpha \leq 0.10$, a practical value for clustering, the maximum values for λ occur when μ is between 2 and 3. As the clustering problems that interest

us have the number of classes $c \geq 3$, to accept the maximum value for λ would allow us to ignore the value of μ. For details, see [102].

Phoungphol and Zhang borrowed Thompson's definition for μ as part of a technique to estimate the sample size for HCM. They implemented a "hard" version of rseFCM where the sample size was estimated with their technique [103].

Solutions to Thompson's formula have been published in a tabular form pairing desired significance levels, α, with values for $d^2\lambda$. For example, a desired significance level of $\alpha = 0.05$ would correspond to a value of $d^2\lambda = 1.27359$. If the desired maximum absolute difference is $d = 0.02$, the minimum sample size is $\lambda = \frac{1.27359}{0.02^2} = 3,184$. Thus, a sample size of 3,184 is the minimum to ensure with a 95% probability $(1-\alpha)$ that the maximum absolute difference in class representation is 0.02.

If one uses this method to obtain samples for a clustering problem, she must consider the total number of classes present. Assume that a full dataset, X, has 5 equally distributed classes. The true proportion, π, of each class, c, equals 0.20. Using the example above, with $d = 0.02$, a sample size of 3,184 is calculated. At the desired significance level, $\alpha = 0.05$, the method predicts with a 95% probability that the sample represents all clusters at the proportion $p = 0.20 \pm 0.02$. This is a suitable proportion for many clustering problems.

If instead, in the example above, X has 100 equally distributed classes, $\pi = 0.01$. The absolute difference would still be $d = 0.02$. Thus, the tolerated difference would *exceed* the expected proportion of each class $p = 0.01 \pm 0.02$. In this case, the *average* number of data objects from each class would be 32 but would *range* from 0 to 96 (with a 95% probability). Therefore, d must be adjusted in order to ensure that each class is represented with enough data objects to be clustered.

Assuming an equal distribution, each class will have a true proportion of $\pi = \frac{1}{c}$. Thompson's formula, however, assumes an *absolute* difference, d. At the level of significance desired, the expected proportion of each class in the sample is $\frac{1}{c} \pm d$. In the examples above, the value of d was kept fixed, and the value of c was increased by a factor of 20. This caused the absolute difference allowed in the sample to be greater than the true proportion of the classes: $\pi << d$.

This problem can be repaired by tying the absolute difference to c. Let us define a value, r, as the "relative difference." Next, we set $d = \frac{r}{c}$. Now, the proportion of each class in the sample is $\frac{1}{c} \pm \frac{r}{c}$, though rewriting it as $\frac{1 \pm r}{c}$ makes it clear why r is defined as the "relative difference."

Using the assumptions above, $\frac{r}{c}$ can be substituted for d. Now the formula for the desired minimum sample size can be expressed as:

$$\begin{aligned} d^2\lambda &= v(\alpha) \\ \frac{r^2\lambda}{c^2} &= v(\alpha) \\ \lambda &= \frac{v(\alpha)c^2}{r^2} \end{aligned} \tag{5.2}$$

where $v(\alpha)$ is the calculated value (or from Thompson's published table) for a specified α value, and the other variables are defined as above.

For example, assume that the desired significance level is $\alpha = 0.05$, which corresponds to $v(\alpha) = 1.27359$; that the number of clusters, $c = 5$; and that the desired relative difference $r = 0.10$. Using Equation (5.2), the estimated sample size $\lambda = \frac{1.27359 \times 5^2}{(0.1)^2} = 3,184$. Note that this is the same result from the example above.

Another example: Keeping the desired significance level at $\alpha = 0.05$ and increasing the desired relative difference to $r = 0.20$, let us find the minimum sample size for $c = 100$. Using Equation (5.2), the estimated sample size $\lambda = \frac{1.27359 \times 100^2}{(0.2)^2} = 318,398$.

5.2 Algorithms Based on Thompson's Method

Insight on how best to leverage Thompson's method for selecting a set of examples comes from understanding how accelerated algorithms function. Research on how these algorithms function was presented in Chapter 4. In Section 4.5.3 is a list of observations significant to runtime and quality. The following observations from this list were considered:

1. A smaller sample size decreases the runtime.

2. A sample representative of the whole dataset results in a higher-quality partition.

3. An initial set of cluster centers closer to the final partition reduces runtime.

4. The use of weighted cluster centers for initialization reduces runtime.

5. SPFCM's final reported set of cluster centers did not deviate significantly after the first few PDAs were clustered.

These observations and the availability of Thompson's formula led to the creation of two algorithms, geometric progressive fuzzy c-means (GOFCM) and minimum sample estimate random fuzzy c-means (MSERFCM). Both of these algorithms use Thompson's formula to estimate an initial sample size for an expected number of clusters. These methods assume, as does clustering in general, that a dataset processed by these algorithms has the expected number of clusters reflected by the features. If the features do not provide any distinction between the clusters, the data will not have multinomial properties and Thompson's method will not be valid.

5.3 The GOFCM Algorithm

The GOFCM algorithm, designed as an improvement to SPFCM, leverages progressive sampling, Thompson's method, and a new stopping criterion. GOFCM operates like SPFCM, except as follows. The initial partial data access (PDA) size is estimated by Thompson's method. The sizes of subsequent PDAs are calculated using a geometric schedule [66]. Once the calculated size of the PDA exceeds a user-provided value, it stops growing. When this occurs, the PDA size is fixed to equal the user-provided value.

As in SPFCM, each PDA is processed by WFCM. The partition information from previous PDAs is retained and compressed by weighting the cluster centers from each step of the progressive sampling. The stopping criterion, discussed in detail below, is based on the rate of change (slope σ) of cluster center positions in successive PDAs. The algorithm terminates when the slope rises above a user-defined value.

GOFCM has the same expected runtime complexity as SPFCM (Section 2.3.2.1). Due to a faster convergence that reduces i and the new stopping criterion that reduces n, GOFCM will in practice often have a shorter runtime than SPFCM's. Algorithm 7 presents a detailed description of GOFCM.

Algorithm 7: Geometric Progressive Fuzzy c-means

Input: X, c, m, ϵ, a, σ, $fPDA$, r, α
Set $t = 1$
Calculate the initial PDA size, n_1 of dataset X using Thompson's method.
Create the initial PDA (x_1) by randomly selecting n_1 data objects from X without replacement.
Cluster x_1 with WFCM
Retain weighted clusters V_1
repeat
    $t = t + 1$
    Calculate new PDA size $n_t = a \times n_{t-1}$
    if $n_t > n \times fPDA$ **then**
        $n_t = n \times fPDA$
    end if
    Create PDA (x_t) by randomly selecting n_t data objects from X without replacement.
    Add the c weighted cluster centers V_{t-1} to x_t.
    Cluster x_t with WFCM
    Retain weighted clusters V_t
    Calculate the change of cluster centers between PDAs, $\delta(V_t, V_{t-1})$.
    Save $ln(\delta(V_t, V_{t-1}))$ in a buffer.
    if $t > 6$ **then**
        Calculate the slope σ_t
    else
        $\sigma_t = \sigma$
    end if
until $\sigma_t > \sigma$
return V_t

---

where:
X is a dataset.
$n = |X|$
c is the number of clusters.
$m > 1$ is the "fuzzifier."
ϵ is a parameter for FCM's termination criterion.
$fPDA$ is the fractional size for the maximum-sized PDA, $\hat{n} = fPDA \times |X|$.
$a \geq 1$ is the geometric schedule factor.
σ is the maximum slope.
r is the relative difference.
α is the desired level of significance for Thompson's method.

One key principle of GOFCM is based on an observation made about SPFCM. After a number of PDAs have been clustered, the cluster centers produced by SPFCM do not change in any appreciable way. This is similar to Provost's observation concerning induction algorithms [66]. Thus, GOFCM may terminate early, without needing to process all the data.

The GOFCM algorithm follows a pattern similar to those in Gu et al. [101] and Provost [66], in that the base algorithm selects and processes multiple samples. GOFCM also resembles algorithms that use estimation for a better set of starting cluster centers [62] [63] [64].

Some key differences distinguish GOFCM from these similar methods. The first difference is GOFCM's use of Thompson's method to derive the initial sample size. The second is that GOFCM reuses the information from each sample (PDA). This is so because the cluster centers obtained from a PDA are weighted, combined with the next PDA, and used as the starting cluster centers. These differences have benefits that decrease the runtime of the algorithm. The initial cluster center estimates are generated using the minimum amount of sampled data. The cluster center estimates represent, using weights, all previously processed data. This reduces the number of iterations needed by each PDA until termination [46].

In GOFCM, progressively larger samples are taken until the stopping criterion has been met. The size of the samples is controlled by a parameter $a \geq 1$, the geometric schedule factor. If $a = 1$, the sample size remains constant, and the algorithm is identical to SPFCM though with a different stopping criterion (see below). As noted in [66] [104], the actual type and rate of scheduling is a tradeoff between cost (loss of fidelity to FCM) and benefit (speedup).

The GOFCM algorithm is also similar to eFFCM and its variants because it progressively samples the dataset while retaining the data already sampled. As discussed above, its method of "retaining" the data differs from eFFCM's and mirrors SPFCM's.

As shown in the SPFCM experiments in Chapter 4, the final cluster centers did not change very much after the first few PDAs had been clustered. This suggested that stopping GOFCM before all the data was clustered would improve speedup and have little impact on quality. A difficult decision in the development of GOFCM was the stopping criterion. Provost identifies detection of

convergence in the context of induction algorithms as an important area of future research [66]. The same is true for clustering algorithms.

Unlike Provost's method for induction algorithms with labeled data, there are no objective criteria, such as model accuracy, to compare the quality of clustering algorithms. The typical alternative method of developing a stopping criterion is to identify whenever some metric associated with the algorithm fails to change more than a specified threshold.

The candidate metrics available for developing a stopping criterion are limited in number: the value of the objective function, the membership values of the data examples, the amount of data processed, the number of iterations, and the position of the cluster centers. All candidate metrics were considered in the development of GOFCM. Thought and experimentation uncovered considerable challenges with each.

Use of the reformulated objective function (R_m) was deemed infeasible. While the base FCM algorithm uses an objective function, the objective function for each sample is not comparable. One could use the reformulated objective function (Equation 2.20) for the entire dataset, but to calculate this value would be time-consuming for a large amount of data. In fact, for large datasets requiring accelerated algorithms, calculation of R_m would account for the majority of the runtime.

Use of membership values was also deemed infeasible. GOFCM samples the dataset without replacement, so the PDAs have no data objects in common. GOFCM would require some other strategy, such as comparing membership values of the initial sample of data objects across each PDA. Regardless, such alternative strategies would be time consuming and cumbersome.

The number of iterations was considered as a stopping criterion. As mentioned above, the number of iterations to process a PDA falls as the cluster centers' initial starting positions approach the final position. Assuming that GOFCM estimates cluster centers closer and closer to the final positions as time goes on, one would expect the number of iterations to drop to a steady level.

Experiments were performed using this stopping criterion. A flaw in this technique is that the number of iterations is an integer. Variation in the composition of the PDA can create minor variations in the number the iterations. The number of iterations proved to be a slightly volatile measure, resulting in different points of termination depending on initialization and random sam-

pling. The results from multiple trials had a moderate degree of variation, and the technique was abandoned.

The most promising metric was the cluster center position. This metric was studied with a large dataset, MRI017, known to cluster well with FCM and its variants (Figure 5.1). The mean distance between successive cluster centers was selected as the norm. While the difference between Vs initially reduced while the amount of data increased, it did not converge to a particular value. Instead, the algorithm reached a steady state with significant variation in cluster center position between subsamples.

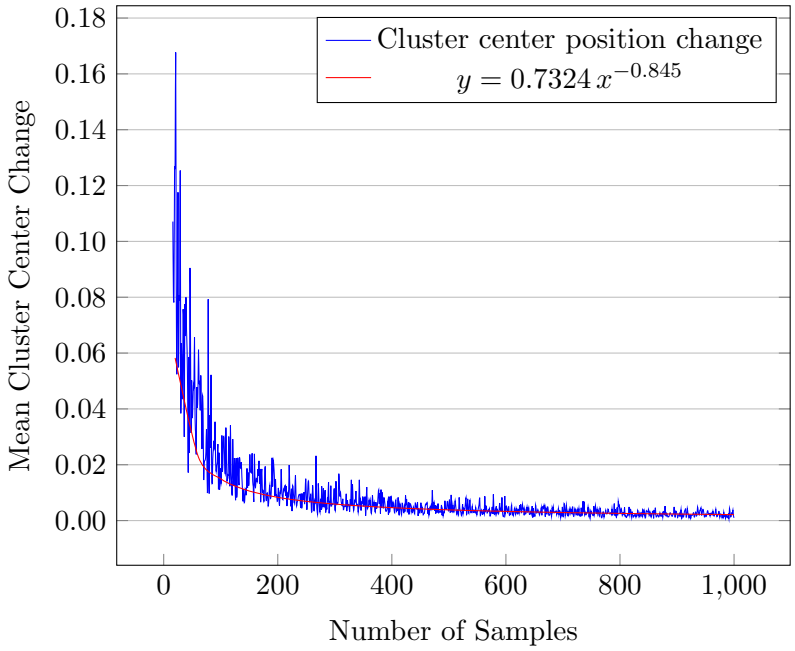

Figure 5.1: Cluster Center Position Change

A simple thought experiment reveals why this is so. Imagine that a sample produces the ideal set of cluster centers signifying an extremum for the objective function if all the data objects were present. Now, another, possibly larger sample is drawn, and the weighted cluster centers from the previous sample are added to it. This new sample is drawn from the remaining data in the dataset and is extremely likely to have a data distribution that differs from that of the former sample.

The difference in data distribution will cause the cluster centers to deviate between samples. This condition is present for every data sample clustered.

The FCM algorithm seeks to minimize the objective function from the data that is present. Because the distribution of the data in the samples will always be slightly different, the cluster centers will always experience some random variation. Let us consider this random variation as noise.

Note in Figure 5.1 that the changes in cluster centers ($\delta(V)$) between samples are asymptotic when noise is removed. The shape of this curve appears to be the inverse of the learning curves noted by Provost [66] and Meek [104], but the same challenge is present: At what point in the curve should the sampling be stopped?

If the stopping criterion is defined to be when $\delta(V)$ falls below a user-defined value, the noise present can be greater than the value of $\delta(V)$. In test experiments using this criterion, a large degree of variability was noticed in the final partitions.

Examination of the dataset and other datasets showed that this metric generally obeys the Power Law after the first few samples. In Figure 5.1, the best fit equation, $y = 0.7324x^{-0.845}$, is plotted alongside the change in cluster centers.

In Figure 5.2, the logarithms of the x and y coordinates are plotted. Here, the best fit equation is the straight line $y = -0.845x - 0.3114$. Note that $ln(0.7324) = -0.3114$.

Figure 5.2 provides a clear view of the noise generated by each subsample and suggests the stopping criterion selected for GOFCM.

After each sample has been processed, the logarithm of $\delta(V)$ is saved, and simple linear regression finds the best fit equation. The best fit equation is then converted back to the original coordinates, and the slope between the last two samples is found. The best fit line is of the form $y = ax^{-b}$, so the slope will have a range of $(-\infty, 0)$. If this slope rises above a user-defined value, σ, GOFCM will terminate.

The selection of σ is a tradeoff between speedup and quality compared to FCM clustering the full dataset. A small value for σ provides more speed but less quality, while a large value of σ provides higher quality but less speed (more iterations).

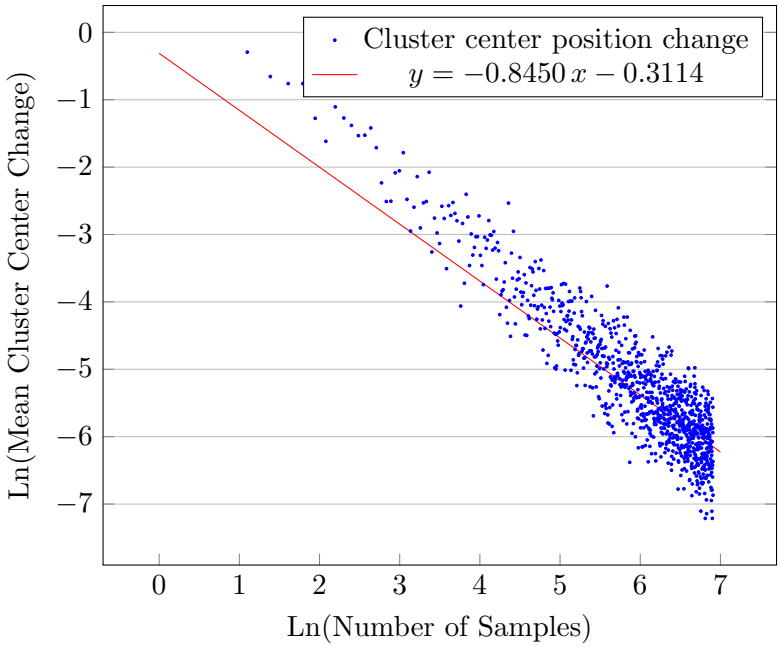

Figure 5.2: Log of Change in V for GOFCM and Dataset MRI017

For a new dataset, one could estimate a suitable value for σ by using GOFCM to cluster a small sample of the data using different values for σ and comparing the results to FCM on the same sample. As FCM scales linearly with n, the speedups obtained for different σ can be used to estimate runtimes for GOFCM on the full dataset.

Due to noise generated by the sampling, the algorithm occasionally terminated prematurely. In order to prevent this from occurring, GOFCM was not allowed to terminate until a minimum number of PDAs had been processed. This is a concept similar to linear regression with local sampling (LRLS) used by Provost [66]. The minimum number of PDAs to process before calculating the slope, a value that could have been parameterized, was set to a constant in the software implementation. For the datasets tested, the number 6 was the lowest minimum value that provided consistent results.

Hall and Goldgof proved the convergence of Weighted FCM (WFCM) to a local minimum or saddlepoint in the context of SPFCM and OFCM [105]. GOFCM differs from SPFCM in the PDA

size, however the functionality of WFCM on each PDA is unchanged. Thus, GOFCM also converges to a local minimum or saddlepoint.

GOFCM also differs from SPFCM in that its stopping criterion typically halts GOFCM before the entire dataset is clustered. Each PDA clustered by WFCM still converges, and the use of an "early" stopping criterion is analogous to a scenario in which the data clustered by GOFCM is all the data that is available.

A related issue is how well the overall stopping criterion would function if GOFCM were applied to streaming data. The GOFCM algorithm, as defined, draws random samples from the dataset. In a streaming scenario, the incoming data might not be randomly distributed, nor proportionally represent the whole dataset. In these cases, the stopping criterion might not cause the selection of subsets to cluster to cease.

To see how the stopping criterion might work in another setting, I applied it to SPFCM, also. The assumption was that it would save time at the cost of leaving some of the data unused. See Section 5.5 for details.

5.4 The MSERFCM Algorithm

Minimum Sample Estimate Random Fuzzy C-Means (MSERFCM) was designed as an improvement to rseFCM. It is similar to, but much simpler than, methods that try to find a better set of starting cluster centers [62] [63] [64]. Algorithm 8 presents a detailed description of MSERFCM.

The rseFCM algorithm uses c randomly selected data objects as initial cluster centers. In contrast, MSERFCM processes a sample of the dataset to estimate initial cluster centers. This is the only major difference between rseFCM and MSERFCM, unless one of the assumptions (see below) is violated.

For a dataset, X of size n, the minimum size of a sample, n_1, is estimated using Thompson's method. A sample, x_1 of size n_1, is drawn without replacement from the dataset and clustered by FCM. The positions of the cluster centers, V_1, produced by FCM are saved. Then a second sample, x_2, is drawn from X. This second sample size is user-specified. The amount of available random access memory (RAM) in the computing environment or some other practical concern may

influence the choice of the second sample size. In the software implementation of MSERFCM, the user-specified sample size, $n_2 = |x_2|$, is defined as $fPDA \times n$, which happens to be the same sample size used by rseFCM. The previously saved cluster center positions, V_1, are used to initialize FCM to cluster x_2.

The MSERFCM algorithm assumes that the estimated sample size, n_1, is less than both the specified sample size, n_2, and the total dataset size, n: $n_1 < n_2 < n$. This assumption may not be correct when Thompson's method estimates a large value for n_1. If this occurs, MSERFCM will be less efficient than rseFCM. To correct this, the following adjustments were made.

When $n_2 < n_1 < n$, the estimated sample size exceeds the user-specified sample size and MSERFCM degenerates to rseFCM with a sample of size n_1. When $n_2 < n < n_1$, the estimated sample size exceeds the available data, and MSERFCM degenerates to FCM, processing the entire dataset. In both of the latter cases, the sample can exceed the available RAM which would provide the actual limit.

5.4.1 Runtime Complexity

MSERFCM has an expected runtime complexity of $O(n_2 i_2 sc + n_1 i_1 sc)$, due to two successive applications of FCM (Section 2.2.2.1). The rseFCM algorithm has an expected runtime complexity of $O(n_2 isc)$. In practice, MSERFCM usually has a shorter runtime than rseFCM, because of the improved set of starting clusters which reduce i_2 to compensate more than enough for the additional $O(n_1 i_1 sc)$ time.

5.5 The MODSPFCM Algorithm

Modified Single Pass Fuzzy c-means (MODSPFCM) is identical to SPFCM except for the stopping criterion. If the conditions for the stopping criterion designed for GOFCM (Section 5.3) are met, MODSPFCM will terminate immediately. MODSPFCM converges to a local minimum or saddlepoint in the same manner as GOFCM [105]. MODSPFCM is formally described as follows:

Algorithm 8: Minimum Sample Estimate Fuzzy c-means

1: **Input:** X, c, m, ϵ, $fPDA$
2: Calculate the estimated sample size, n_1 of dataset X using Thompson's method.
3: Calculate the user-defined sample size, n_2 of dataset X where $n_2 = fPDA \times n$.
4: **if** $n_1 < n_2$ **then**
5: Create a data sample, x_1, by randomly selecting n_1 data objects from X without replacement.
6: Cluster x_1 with FCM using random initialization. FCM returns clusters centers, V_1.
7: Create a data sample, x_2, by randomly selecting n_2 data objects from X without replacement.
8: Cluster x_2 with FCM using V_1 as initialization. FCM returns clusters centers, V_2.
9: **else if** $n_1 > n$ **then**
10: Cluster X with FCM using random initialization. FCM returns cluster centers, V_2.
11: **else**
12: Create a data sample, x_2, by randomly selecting n_2 data objects from X without replacement.
13: Cluster x_2 with FCM using random initialization. FCM returns clusters centers, V_2.
14: **end if**
15: **return** V_2

where:
X is a dataset.
$n = |X|$
c is the number of clusters.
$m > 1$ is the "fuzzifier."
ϵ is a parameter for FCM's termination criterion.
$fPDA$ is the fractional size of the user-defined sample size, $n_2 = fPDA \times n$.

5.6 Experiments

GOFCM, MSERFCM, and MODSPFCM were compared in terms of speedup and quality to the algorithms used in the "simple experiment" in Chapter 4. The experiments applied FCM and seven accelerated variants to four large real-world datasets and two artificial datasets.

Earlier work by Havens, et al. used three of the same datasets as well as four of the same algorithms used in my research. Additional experiments, with identical parameters to those used in [16], were done to compare results directly.

Algorithm 9: Modified Single Pass Fuzzy c-means

1: **Input:** X, c, m, ϵ, σ, $fPDA$
2: Set $t = 1$
3: Calculate the PDA size, $\hat{n} = n \times fPDA$
4: Create the initial PDA (x_1) by randomly selecting $\hat{n}$ data objects from X without replacement.
5: Cluster x_1 with WFCM
6: Retain weighted clusters V_1
7: **repeat**
8: $t = t + 1$
9: Create PDA (x_t) by randomly selecting $\hat{n}$ data objects from X without replacement.
10: Add the c weighted cluster centers V_{t-1} to x_t.
11: Cluster x_t with WFCM
12: Retain weighted clusters V_t
13: Calculate the change of cluster centers between PDAs, $\delta(V_t, V_{t-1})$.
14: Save $ln(\delta(V_t, V_{t-1}))$ in a buffer.
15: **if** $t > 6$ **then**
16: Calculate the slope σ_t
17: **else**
18: $\sigma_t = \sigma$
19: **end if**
20: **until** $\sigma_t > \sigma$
21: **return** V_t

where:
X is a dataset.
$n = |X|$.
c is the number of clusters.
$m > 1$ is the "fuzzifier."
ϵ is a parameter for FCM's termination criterion.
$fPDA$ is the fractional size for the maximum-sized PDA, $\hat{n} = fPDA \times |X|$.
σ is the maximum slope.

5.6.1 Experimental Procedures

Three sets of experiments were performed. The main experiment compared GOFCM and MSERFCM to algorithms previously compared in Chapter 4. A second experiment mirrored work performed by Havens [16]. A third, smaller experiment, compared MODSPFCM to related algorithms.

The experimental procedures, except where noted, were identical to those described in Chapter 4. To recount, the cluster centers predicted by the FCM family vary based on the initial set of

cluster centers, V. Therefore, initialization for all algorithms was performed by randomly selecting c data objects in the dataset, X, as the initial values of V. Each experiment consisted of 30 trials to ensure a statistically significant sample. While the initialization for each trial of an experiment was different, the same set of 30 initializations was used for each algorithm in the experimentation. The average values over 30 trials were recorded for their runtime and quality metrics.

All algorithms except for FCM and OFCM assume that the data is in random order, or the implementation performs random sampling. In these experiments (excepting for FCM and OFCM), the entire dataset was randomized before processing each trial using the procedure described in A.2. In addition to recording the runtime of the algorithm, the software implementation separately recorded the time taken to sample the data randomly, as well as the time taken to perform I/O. Unless otherwise noted, reported times and speedup comparisons include the runtimes for both randomization and I/O. The quality and fidelity metrics $DQ\,R_m\%$, $CC\%$, and ARI were recorded.

The main experiment compared the algorithms FCM, SPFCM, OFCM, eFFCM, rseFCM, GOFCM, and MSERFCM. Different datasets were used than those in Chapter 4. The Pendigits and Landsat datasets were not used because of their small size. The main experiment used the MRI datasets, MRI016, MRI017, and MRI018, a challenging real-world dataset of plankton images, PLK01, and two artificial datasets, D6C5 and D10C7. Details about these datasets are in Chapter 3.

The second experiment was modeled on an experiment in Havens's work, "Fuzzy c-Means Algorithms for Very Large Data" [16]. Conveniently, his experiments clustered rseFCM, SPFCM, and OFCM using the same MRI datasets as in my research. His experiments differed in several ways. Only 21 trials were performed, the fuzzifier was set to 1.7, and the termination criterion was changed to use the maximum change in V. Havens reports results for SU and ARI; these were rounded to nearest whole number and two decimal digits respectively.

His algorithm implementation was done in MATLAB rather than in a Linux/C implementation. Havens pre-randomized the files and did not count that step in the algorithm execution time, but he did consider sampling and I/O time [106]. As noted in Chapter 4, the experiments and software implementation reported the time spent to randomize the files and to perform I/O in the algorithm

execution time. It was not possible to make the runtime results perfectly comparable, since my reported results included more overhead. As a consideration to make the experimentation as close as possible, the software implementation was modified to pre-randomize the datasets clustered by OFCM. Results from both Havens's experiments and mine are presented in a format as identical as possible to that presented by Havens [16].

The third experiment consisted of comparing MODSPFCM to FCM, SPFCM, and GOFCM.

As described in Chapters 2 and 4, these algorithms have multiple parameters. The experiments were intended to explore accelerating algorithms. Thus, for any given dataset, only the parameter affecting the sample size ($fPDA$) was varied, whereas the other parameters were kept fixed. Experimental parameters are summarized in Table 5.1. The series of experiments using MODSPFCM added two additional settings for the $fPDA$ parameter. These settings, which are not listed in Table 5.1, are $fPDA$ in {0.02,0.06}.

The value for the fuzzifier, m, is not consistent across the datasets. Initial experiments on the MRI datasets with $m = 2.0$ provided acceptable results, but this was not the case for the other datasets. Some tuning of m was necessary; setting it to a value of 1.7 vastly improved results with respect to runtime and improved fidelity to the cluster centers of the artificial and plankton datasets when using FCM and all the data.

Table 5.1: Experiment Parameter Settings

Parameter	Value
trials	30 (21)
m	2.0 (1.7) (MRI) 1.7 (PLK01,D6C5,D10C7)
termination criterion	max change in U (max change in V)
ϵ	0.001
$fPDA$	0.1, 0.0333333, 0.01, 0.00333333, 0.001
α (eFFCM)	0.200
δPDA (eFFCM)	20% of the value of $fPDA$
σ (GOFCM)	-0.01
α (GOFCM)	0.05
a (GOFCM)	2.0
r (GOFCM)	0.1

Parameter values modified to match [16] are in parentheses.
MRI, D6C5, D10C7, and PLK01 refer to particular datasets.

5.6.2 Results

The algorithms' speedup results are presented in tables, and the quality and fidelity results in graphs. As the sample size ($fPDA$) changes, the graphs make it easy to compare relative quality and fidelity between algorithms and trends.

The results for all MRI datasets were similar. I report the average results from the three MRI datasets, as was done for the "simple experiment" (Chapter 4). These results are reported in Tables 5.2 and 5.3, and Figures 5.3 and 5.4. Complete results for the MRI datasets are in Tables B.3, B.4, and B.5 in Appendix B.

While no ground truth exists for the MRI images, the differences in cluster assignment by all methods studied never exceeded 1%. This difference was measured by $CC\%$, from the average FCM partition obtained from 30 experimental trials. This is more consistent than human experts (radiologists), whose assignments have been observed to differ by 16% or more [107] on MRI images of the brain.

For the MRI datasets, MSERFCM typically had the highest speedup, rseFCM often the second-highest, and GOFCM consistently the third-highest speedup. Assuming that the data has been pre-randomized increases the speedup considerably. Compare Tables 5.2 and 5.3, and note the speedup difference between these options.

The SPFCM algorithm had the lowest (and therefore the best) $DQ\,R_m\%$ in all experiments that used the MRI datasets, and it also had the lowest $CC\%$ in 80% of the experiments. GOFCM and eFFCM had either the second or third-best quality metric in 80% of the experiments.

Table 5.2: MRI Speedup

$fPDA$	0.100	0.033	0.010	0.003	0.001
OFCM	1.39	1.55	1.32	1.04	1.05
SPFCM	3.01	3.70	4.12	4.16	4.17
eFFCM	2.08	2.12	1.93	1.55	2.51
GOFCM	4.46	6.56	8.60	9.11	9.51
MSERFCM	**6.59**	**8.27**	**9.54**	**9.39**	9.53
rseFCM	4.79	7.25	9.14	9.36	**9.61**

Bold type indicates fastest speedup for each $fPDA$

Table 5.3: MRI Speedup (Ignoring Randomization and I/O)

$fPDA$	0.100	0.033	0.010	0.003	0.001
OFCM	1.40	1.56	1.32	1.04	1.05
SPFCM	4.43	6.25	7.36	7.74	7.86
eFFCM	3.36	4.22	5.65	9.25	227.98
GOFCM	8.42	20.63	53.55	122.97	301.24
MSERFCM	**19.15**	**50.94**	**119.70**	**313.54**	**599.68**
rseFCM	9.13	28.24	85.79	241.59	575.05

Bold type indicates fastest speedup for each $fPDA$

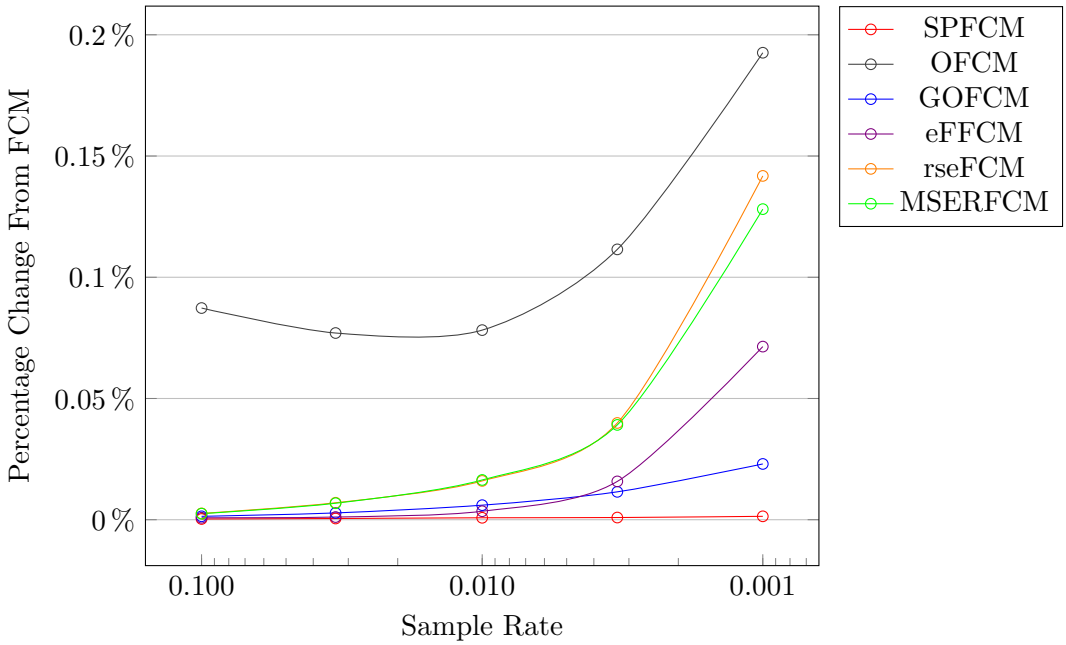

Figure 5.3: $DQ\,R_m\%$ (MRI)

The results for the artificial datasets are shown in Tables 5.4 and 5.5, and Figures 5.5, 5.6, 5.7, and 5.8. The speedups for D6C5 and D10C7, for identically configured experiments, were of the same order of magnitude; however, the D10C7 datasets had consistently higher speedups. The quality and fidelity metric results are quite different. The D6C5 dataset had lower $DQ\,R_m\%$ values, but higher $CC\%$ values, than D10C7. The relative quality of all algorithms' performances were not consistent across the two artificial datasets.

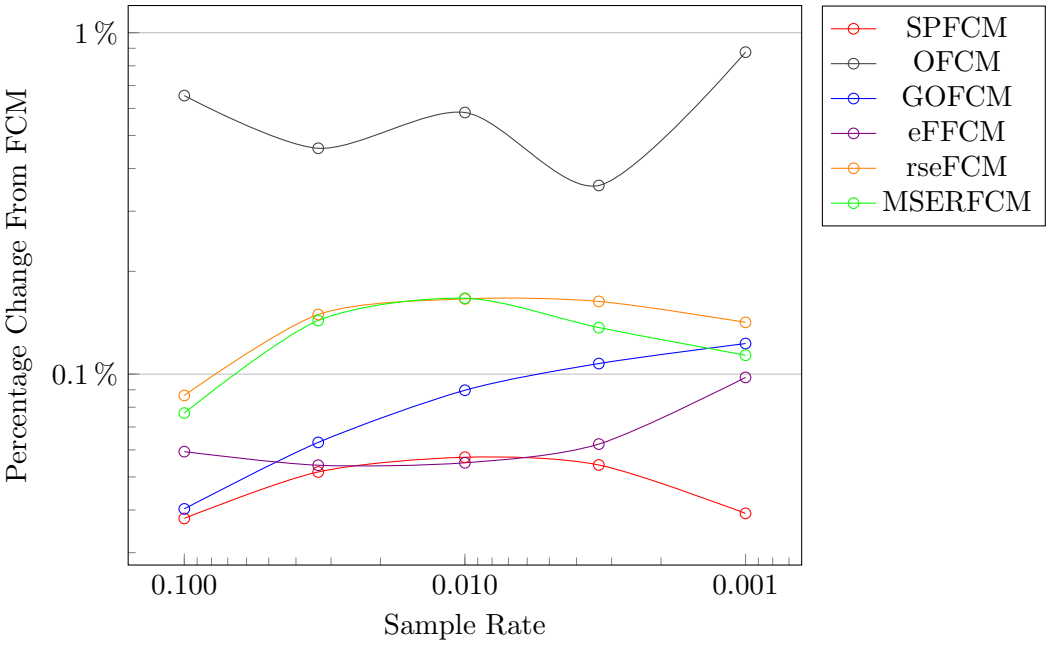

Figure 5.4: Cluster Center Change % (MRI)

Table 5.4: D6C5 Speedup

$fPDA$	0.100	0.033	0.010	0.003	0.001
OFCM	2.76	2.85	2.74	2.46	2.23
SPFCM	3.61	5.00	5.74	5.94	5.91
eFFCM	3.91	5.52	7.08	7.65	12.46
GOFCM	9.83	15.63	21.26	24.00	26.78
MSERFCM	**12.50**	**20.21**	**25.02**	25.32	26.16
rseFCM	6.87	14.88	23.35	**26.07**	**27.64**

Bold type indicates fastest speedup for each $fPDA$

Table 5.5: D10C7 Speedup

$fPDA$	0.100	0.033	0.010	0.003	0.001
OFCM	3.43	3.98	3.86	3.62	3.32
SPFCM	3.89	5.56	6.41	6.89	6.87
eFFCM	4.82	6.99	7.49	7.93	6.16
GOFCM	10.27	16.63	23.89	32.64	36.78
MSERFCM	**17.11**	**25.25**	**29.30**	32.66	31.62
rseFCM	7.05	16.11	28.30	**35.45**	**37.76**

Bold type indicates fastest speedup for each $fPDA$

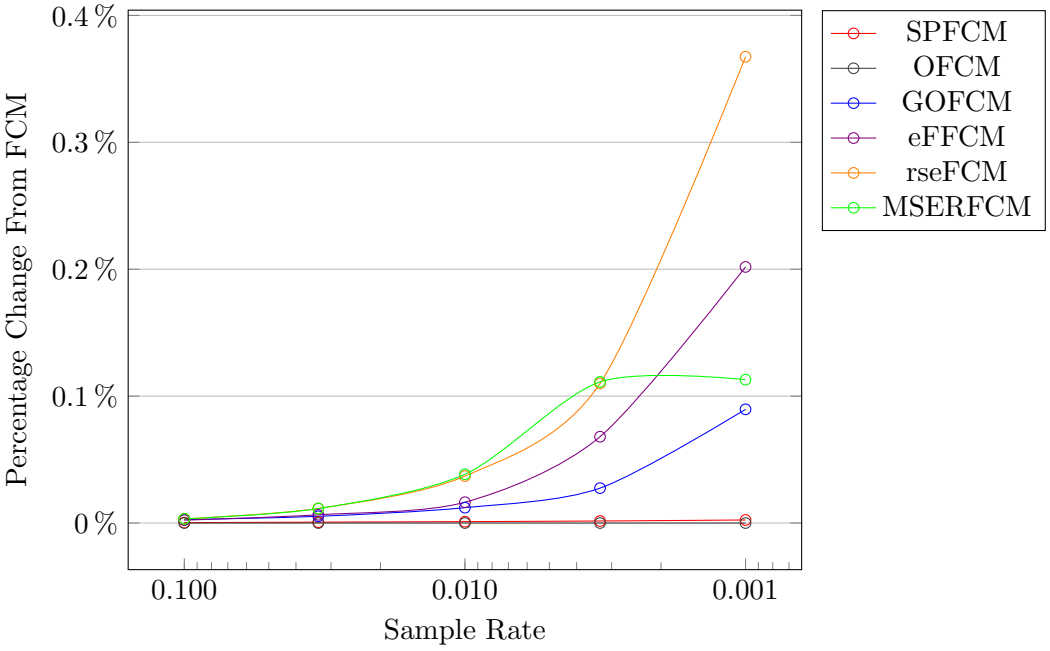

Figure 5.5: $DQ\,R_m\%$ (D6C5)

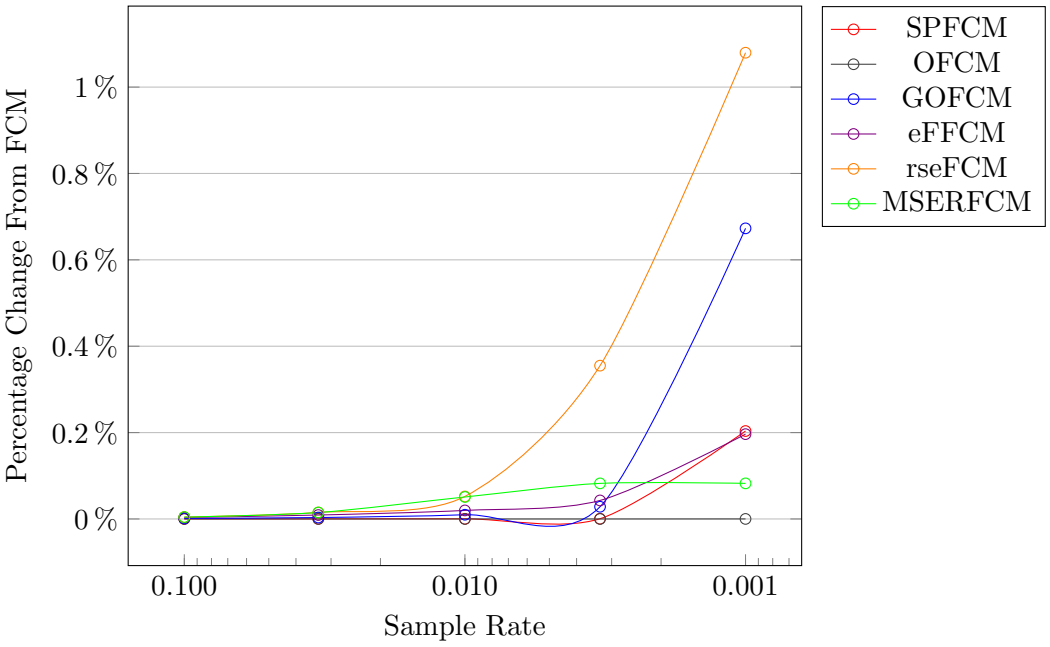

Figure 5.6: $DQ\,R_m\%$ (D10C7)

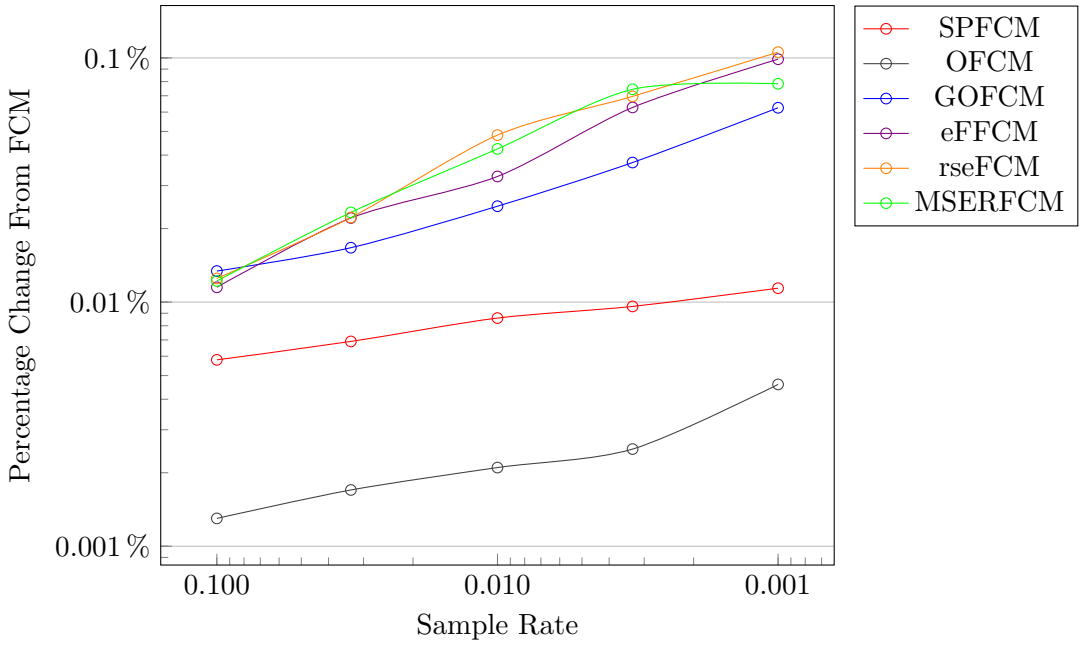

Figure 5.7: Cluster Center Change % (D6C5)

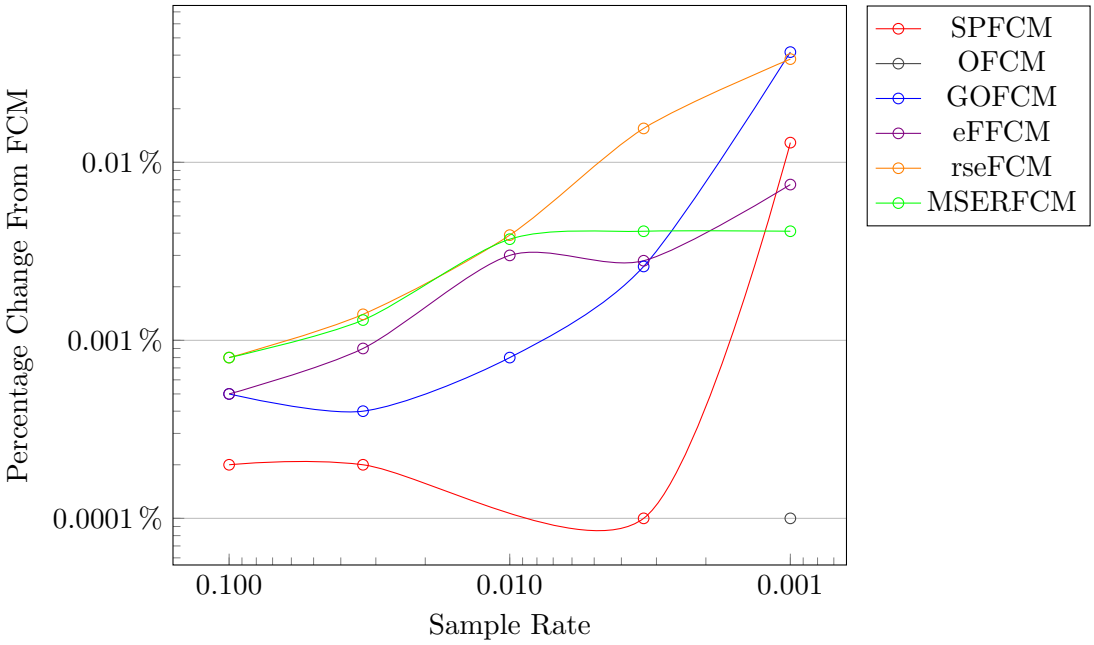

Figure 5.8: Cluster Center Change % (D10C7)

Note: OFCM has CC%=0 for all but the highest sample rate

The results for PLK01 are shown in Table 5.6, and Figures 5.9 and 5.10. The speedup of rseFCM was highest, followed by GOFCM's. Except for MSERFCM, all algorithms had poorer quality metrics for PLK01. Surprisingly, MSERFCM consistently had the best quality on the PLK01 dataset.

Table 5.6: PLK01 Speedup

$fPDA$	0.100	0.033	0.010	0.003	0.001
OFCM	2.84	2.75	1.75	1.47	1.11
SPFCM	6.93	13.58	18.77	21.73	22.83
eFFCM	2.74	4.08	5.45	7.29	6.28
GOFCM	8.19	18.29	33.04	41.12	47.95
MSERFCM	4.00	4.03	4.04	4.04	4.04
rseFCM	**8.52**	**21.55**	**38.39**	**46.48**	**49.57**

Bold type indicates fastest speedup for each $fPDA$

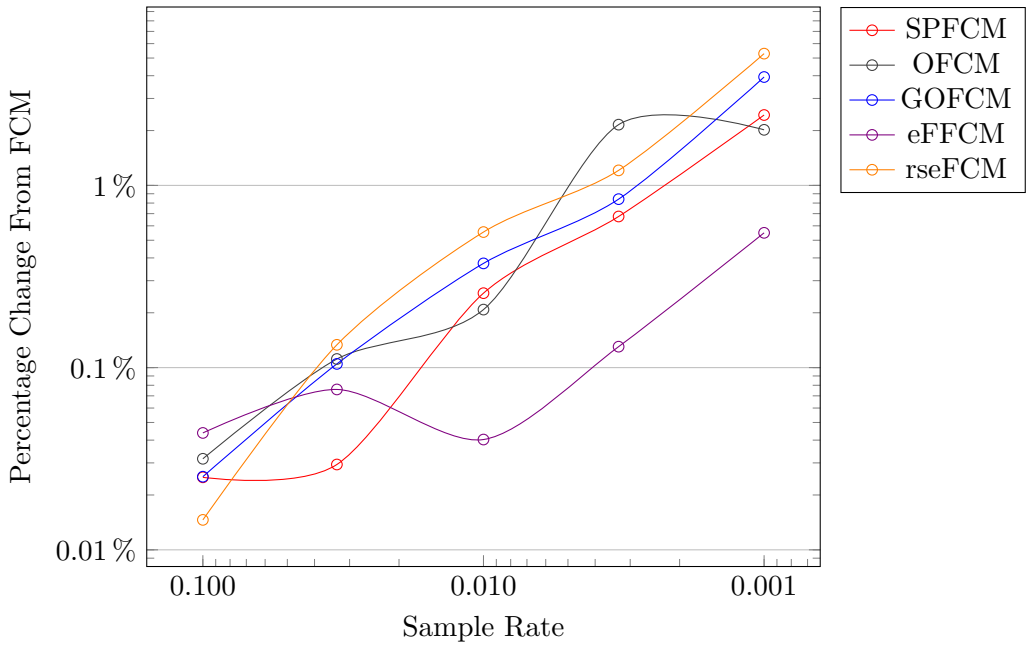

Figure 5.9: $DQ\,R_m\%$ (PLK01)

Note: MSERFCM not shown as $DQ\,R_m\% = -0.0078$ for all sample rates

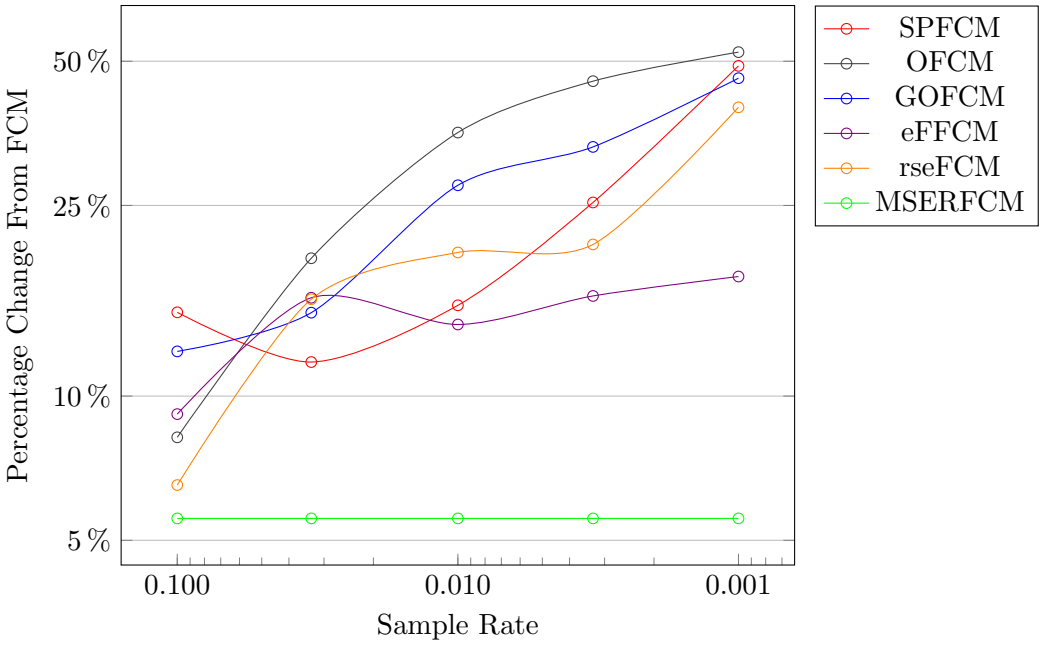

Figure 5.10: Cluster Center Change % (PLK01)

The GOFCM algorithm provides a consistent speedup over the reference FCM algorithm. Depending on the size of the PDA and dataset, the speedup of GOFCM ranged from roughly 4 to 48 times. Designed as an improvement to SPFCM, GOFCM provides a more consistent speedup. On the MRI datasets, the speedup was on average 2 times faster than SPFCM's. On D6C5 and D10C7, the speedup ranged from 3 to 5 times faster than SPFCM's. GOFCM was also consistently faster than SPFCM on PLK01.

If the time taken for randomization and I/O were ignored, GOFCM would provide an even greater speedup. The speedup on the MRI datasets would range from 8 to 300 times faster than FCM, and the speedup would range from 2 to 40 times faster than SPFCM (Table 5.3). Speedups on the D6C5, D10C7, and PLK01 datasets would be even greater, ranging from 10 to over 700 times faster than FCM.

The price of GOFCM's speedup is a loss in fidelity when compared to FCM.

GOFCM's quality was consistently worse than SPFCM's on the MRI datasets. GOFCM's $DQ\,R_m\%$ ranged from 0.0013% to 0.0230%, while SPFCM's ranged from 0.0002% to 0.0014%. Fidelity to FCM, as judged by the $CC\%$ metric was closer. GOFCM's fidelity loss ranged from

0.040% to 0.123% on the MRI datasets, while SPFCM's fidelity loss over the same datasets ranged from 0.038% to 0.057%.

On the artificial datasets, the results were similar to those for the MRI datasets, in that GOFCM consistently had quality inferior to SPFCM's. The corresponding values for these metrics were much closer on these artificial datasets than on the MRI datasets.

PLK01 was a difficult dataset for most of the algorithms tested. The quality metrics for GOFCM and SPFCM were very close on this dataset, with GOFCM actually having better quality than SPFCM on some experiments. GOFCM's $DQ\,R_m\%$ ranged from 0.025% to 3.937%, while SPFCM's ranged from 0.025% to 2.434%. GOFCM and SPFCM had very similar $CC\%$ losses in fidelity to FCM: GOFCM's ranged from 12% to 46%, while SPFCM's ranged from 11% to 48%.

MSERFCM, designed as an improvement to rseFCM, has performance slightly superior with respect to speed and quality, on the MRI datasets. MSERFCM was faster than rseFCM in 80% of the experiments. MSERFCM's quality as measured by $DQ\,R_m\%$ was either equal to or better than rseFCM's on 80% of the experiments. Its fidelity to FCM, as measured by the $CC\%$ metric, was either equal or better than rseFCM's on 64% of the experiments. The fidelity comparison was impacted by relatively poorer results by MSERFCM on a single dataset (MRI016); otherwise it would have been equal or better 75% of the time. For all differences of speed and quality, both algorithms were very close – on a few occasions differing by only 0.0001% or less.

For the artificial datasets, MSERFCM was faster than rseFCM on 60% of the experiments. MSERFCM's quality, measured by both the $DQ\,R_m\%$ and $CC\%$ metrics, was equal to or better than rseFCM's on 78% of the experiments. Again, the results were extremely close in all experiments. Despite D6C5's and D10C7's differences with respect to number of clusters and dimensions, the differences between them with respect to quality were very small, except at the low sample rates ($fPDA = 0.001$ or 0.00333333).

If the time taken for randomization and I/O were ignored, MSERFCM was faster than rseFCM on 73% of the MRI experiments and on 80% of the experiments with artificial data. Usually, when rseFCM was faster than MSERFCM, the sample rate was low. When this occurred, the difference in speed was not trivial, and rseFCM suffered a noticeable loss in quality.

Results were different for the plankton dataset. Here, rseFCM consistently outperformed MSERFCM in terms of speed, while MSERFCM consistently outperformed rseFCM in terms of quality and fidelity. In fact, out of all six FCM variants, MSERFCM had the best quality metrics. Also, MSERFCM had a consistent speedup of 4 times FCM in all experiments. The eFFCM algorithm was the only consistent competitor to MSERFCM in terms of quality; it had a speedup ranging from 2.7 to 7.3 times FCM. Section 5.8.2 explains the very different performance of the algorithms on the plankton dataset, compared to the other datasets.

The MODSPFCM algorithm was tested against FCM, SPFCM, and GOFCM on all datasets. Results are listed in Tables 5.7, 5.8, 5.9, and 5.10, and shown in Figures 5.11, 5.12, 5.13, 5.14, 5.15, 5.16, 5.17, and 5.18. In addition to five experiments using the $fPDA$ values listed in Table 5.1, two additional experiments were run with $fPDA = 0.02$ and $fPDA = 0.06$ to add evidence to the observed trends.

Table 5.7: MODSPFCM MRI Speedup

$fPDA$	0.100	0.060	0.033	0.020	0.010	0.003	0.001
SPFCM	3.01	3.38	3.70	3.85	4.12	4.24	4.13
MODSPFCM	3.40	4.51	5.88	6.84	8.26	9.41	9.41
GOFCM	**4.40**	**5.44**	**6.65**	**7.32**	**8.58**	**9.52**	**9.44**

Bold type indicates fastest speedup for each $fPDA$

Table 5.8: MODSPFCM D6C5 Speedup

$fPDA$	0.100	0.060	0.033	0.020	0.010	0.003	0.001
SPFCM	3.70	4.49	5.01	5.36	5.77	6.03	6.15
MODSPFCM	4.43	6.62	9.68	13.38	18.54	24.93	**28.71**
GOFCM	**10.72**	**12.77**	**15.56**	**18.00**	**21.32**	**25.07**	**28.71**

Bold type indicates fastest speedup for each $fPDA$

Table 5.9: MODSPFCM D10C7 Speedup

$fPDA$	0.100	0.060	0.033	0.020	0.010	0.003	0.001
SPFCM	3.88	4.81	5.56	6.09	6.66	6.91	7.00
MODSPFCM	4.33	6.65	10.99	15.53	22.19	**32.58**	**37.84**
GOFCM	**10.23**	**12.88**	**16.62**	**19.90**	**24.83**	**32.58**	**37.84**

Bold type indicates fastest speedup for each $fPDA$

Table 5.10: MODSPFCM PLK01 Speedup

$fPDA$	0.100	0.060	0.033	0.020	0.010	0.003	0.001
SPFCM	6.98	9.86	13.88	16.63	18.80	22.15	23.75
MODSPFCM	8.31	**11.60**	18.77	**25.13**	**33.46**	**42.92**	51.27
GOFCM	**8.31**	11.58	**18.80**	25.09	33.45	**42.92**	**51.28**

Bold type indicates fastest speedup for each $fPDA$

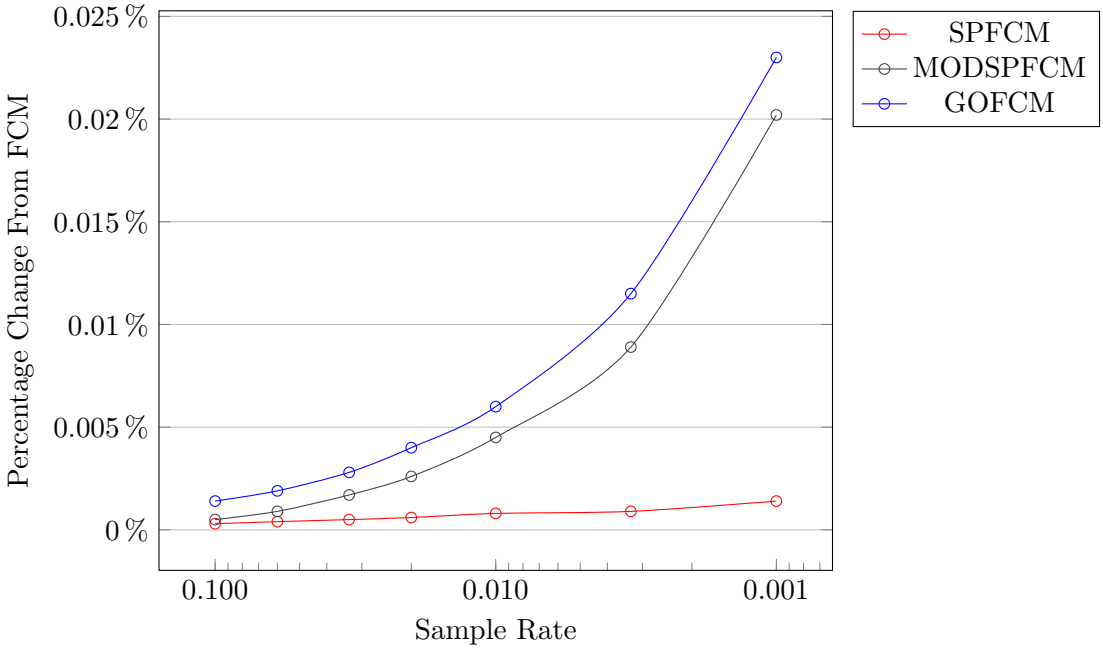

Figure 5.11: $DQ\,R_m$% (MRI)

The speedup of MODSPFCM generally fell between those of SPFCM and GOFCM. On three occasions, MODSPFCM was slightly faster than GOFCM on PLK01 by a very narrow margin. Statistical significance was tested for, on the largest of these speed differences, using a one-tailed Welch's t-test. The t-test returned $t = 0.025$ with 58 d.f. This corresponds to $p = 0.4901$, which is not considered statistically significant.

The quality of MODSPFCM, as measured by $DQ\,R_m$% also falls between that of the other two algorithms. In the smallest two sample rates for D10C7 and all sample rates for PLK01, the $DQ\,R_m$% values for MODSPFCM and GOFCM were identical. In these cases, the estimated sample size exceeded the limits set by $fPDA$, and GOFCM "degenerated" to MODSPFCM.

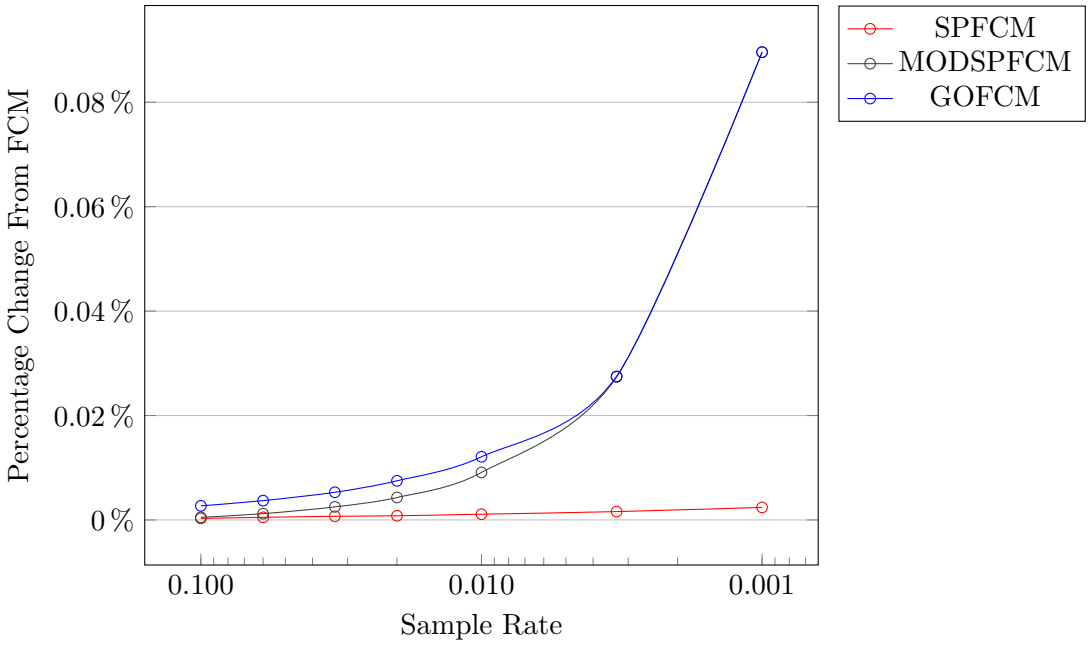

Figure 5.12: $DQ\, R_m\%$ (C6D5)

MODSPFCM's fidelity to FCM, as measured by $CC\%$, was always worse than SPFCM's and similar to that for GOFCM. On the MRI datasets, MODSPFCM's fidelity to FCM was worse than GOFCM, but the opposite was true for D6C5. For these algorithms, fidelity has some variation depending on the dataset. This supports the idea of using multiple metrics to measure quality and fidelity.

The results for the experiments modeled on Havens's research are shown in Table 5.11. With the same parameters, the results of my experiments and those of Havens are fairly similar for OFCM and rseFCM. The speedup reported by Havens for SPFCM, however, suggests a significant difference between our software implementations. The most likely reason for this is additional time taken in my implementation to perform randomization. Regardless, the algorithms have the same order according to speedup: OFCM, SPFCM, rseFCM. This suggests that if GOFCM and MSERFCM were to be implemented in MATLAB in a similar way to Havens's OFCM and rseFCM implementations [16], the order according to speedups would be the same for both his implementations and mine.

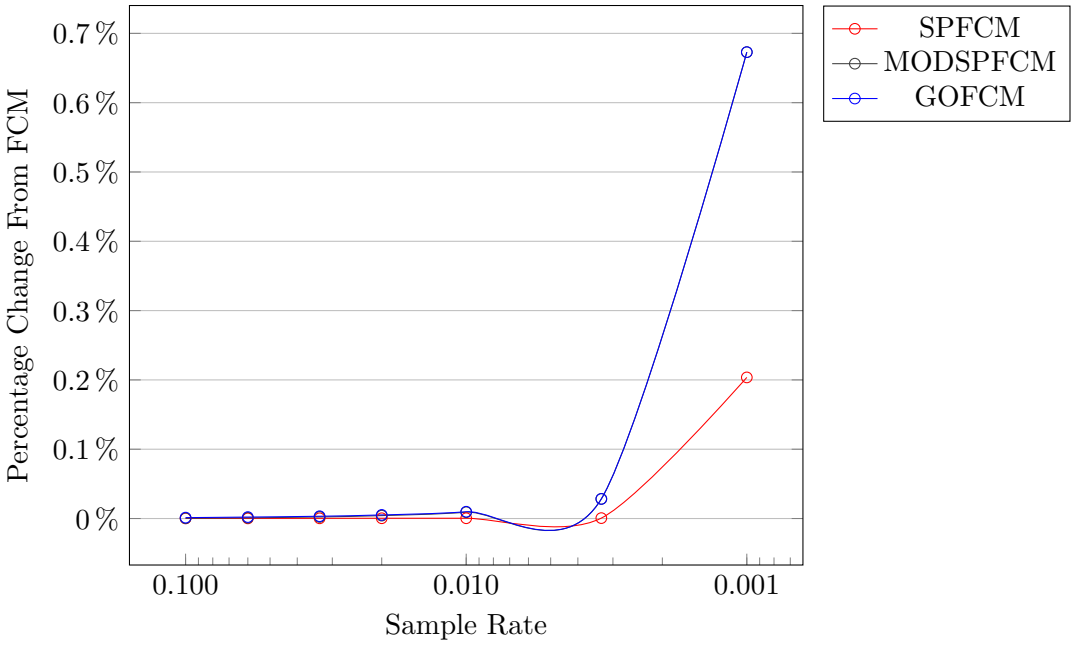

Figure 5.13: $DQ\,R_m\%$ (C10D7)

The *ARI* metric was recorded solely to compare Havens's work to mine. GOFCM had a consistent, but small loss in fidelity to FCM as measured by *ARI* when compared to SPFCM. This difference in fidelity is so slight that, in Table 5.11, the *ARI*s for SPFCM and GOFCM differ only twice at the listed level of precision.

Even with the dissimilar implementations, GOFCM and MSERFCM have consistently higher speedups and commensurate quality to what Havens reported for SPFCM and rseFCM.

5.7 GOFCM vs. Related Methods

Why is GOFCM faster than SPFCM and other related methods? There are two main reasons: the estimated sample size and the stopping criterion. The runtime complexity of GOFCM is linear with respect to n, i, s, and c. If we compare the performances of two algorithms on the same dataset, assuming s and c to be constant will make the comparative runtime complexity $O(ni)$. At the beginning of GOFCM, n is the (presumably small) estimated sample size, but initialization of the cluster centers is random. Thus, the number of iterations, i, is usually large. Recall that

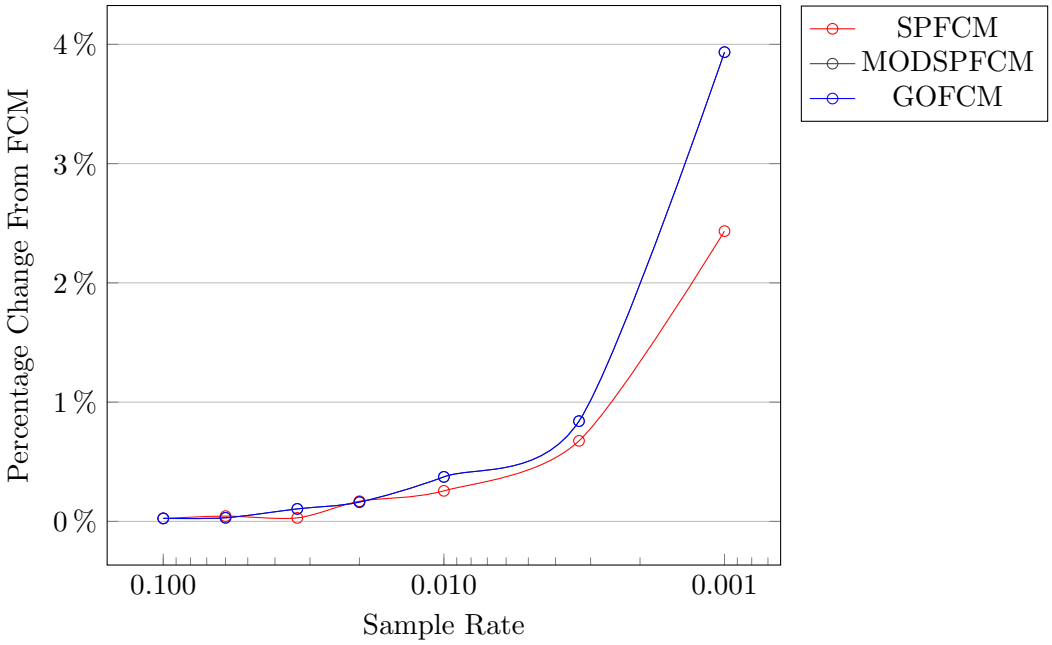

Figure 5.14: $DQ\,R_m\%$ (PLK01)

GOFCM uses a geometric schedule for sampling, so the second sample will be larger than the first by some multiplicative factor. Hence, in the second sample, there are more data objects, but the cluster center initialization is improved, requiring fewer iterations. The GOFCM algorithm achieves an accelerated performance because when n is small, i is large, and as n increases, i decreases. This keeps the runtime more consistent across samples processed, demonstrating how sample size and cluster center initialization impact speed.

The second reason why GOFCM is faster is its stopping criterion. It stops processing data when the predicted cluster centers do not show a high degree of change. Related methods process all available data.

There is a tradeoff between speed and quality. The effect of this tradeoff is evident when one compares GOFCM and eFFCM. On the datasets tested, eFFCM often had better quality, but much lower speedups than GOFCM. This is clearly shown in Table 5.2, and Figures 5.3 and 5.4 for the MRI datasets. The GOFCM algorithm selects a starting sample aiming to have the number of data objects for each cluster within the specified range. This does not guarantee that the range of *feature values* in each cluster is proportionally represented in the sample. This is one difference

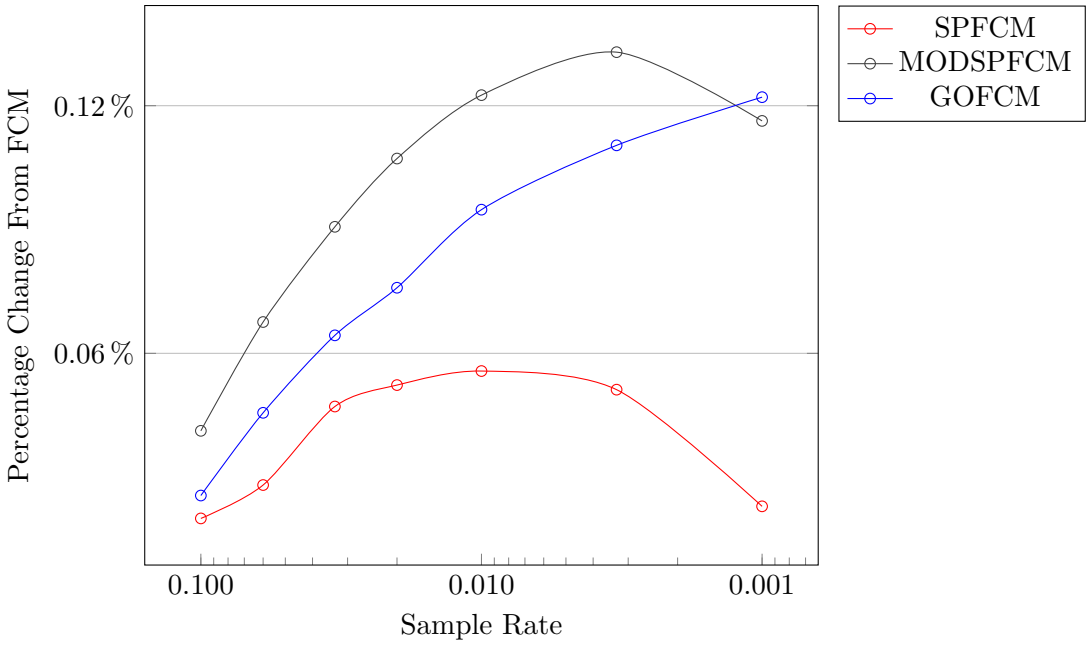

Figure 5.15: Cluster Center Change % (MRI)

between GOFCM and techniques that perform a divergence test on samples against the sample distribution [68] [69].

The process of performing a divergence test on a sample is time-consuming. The entire sample must be analyzed for ranges of values, bins must be selected, and the sample's values must be assigned to bins. This technique is also subjective, as there is no optimal way to select the bins or parameters. Analysis of an implementation of eFFCM found that 5%-42% of the dataset had been sampled before a Chi-squared test was passed; these tests were performed on relatively simple datasets [68]. Analysis of my own implementation found that 0.2%-34.6% of the test datasets had been sampled before the Chi-squared test was passed.

In contrast, the GOFCM implementation determines a starting sample size via a lookup table and a simple equation. This step, though less precise, is much faster.

GOFCM's quality is controlled by the stopping criterion parameter, σ. A fixed setting for σ in the experiments provided a consistent speedup of GOFCM over SPFCM and the resulting consistent loss in quality. It is reasonable to assume that a stricter setting for σ should result in a smaller speedup and higher quality. The converse should also apply.

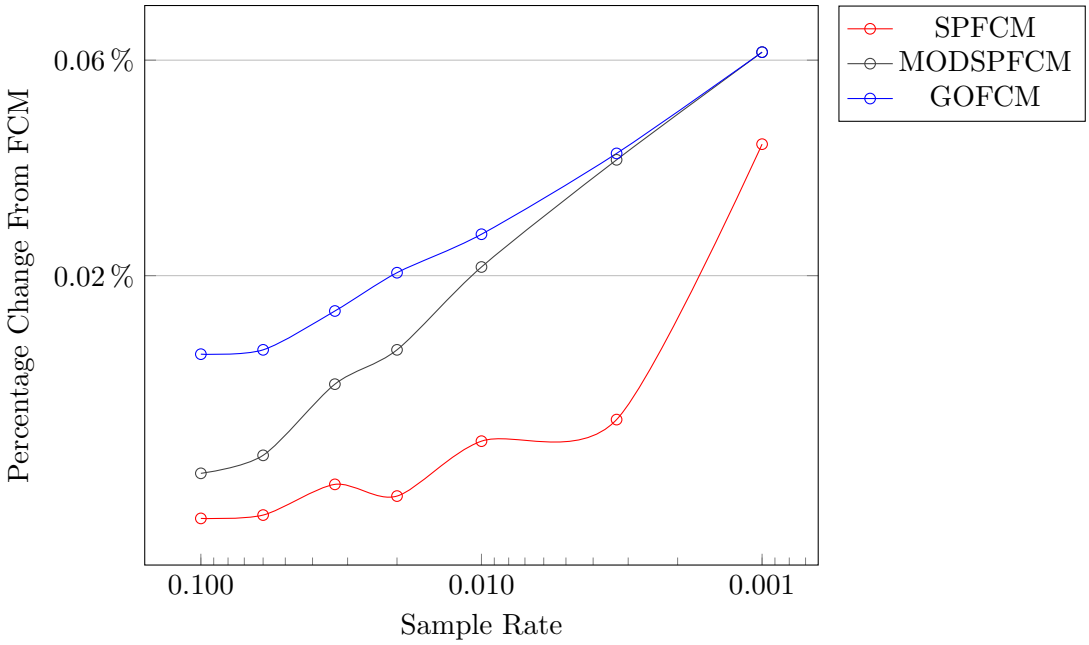

Figure 5.16: Cluster Center Change % (D6C5)

A small experiment was performed to demonstrate this. MODSPFCM and GOFCM clustered the MRI016 dataset over a range of different settings for σ. All other parameters were set as listed in Table 5.1 with $fPDA = 0.01$. The results are shown in Table 5.12 and Figures 5.19 and 5.20.

The results match the original assumptions. Recall that SPFCM does not use σ as a parameter, so its results did not change. The speedup for both algorithms decreased as the setting for σ increased in strictness (i.e. was reduced) (Table 5.12). The quality, as measured by $DQ\,R_m\%$, improved as the setting for σ increased in strictness (Figure 5.19).

The expected relationship between σ and fidelity with FCM, as measured by $CC\%$, was also observed. For this dataset, the $CC\%$ for MODSPFCM and GOFCM indicated more fidelity to FCM than SPFCM when $\sigma = -0.001$. This type of deviation is not entirely unexpected. Figure 5.1 in Section 5.3 shows how cluster center positions normally deviate for this class of algorithms. For the case of MRI016, the dataset apparently provides some long period of stable cluster center positions that are close to those of FCM's.

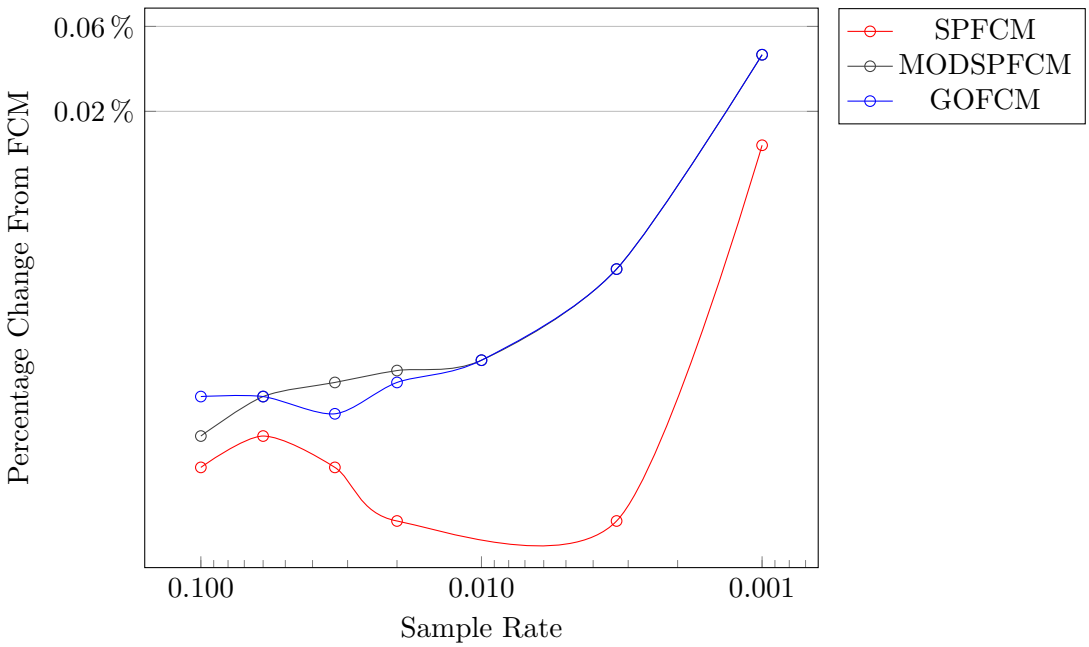

Figure 5.17: Cluster Center Change % (D10C7)

Another limitation on GOFCM's quality is when the dataset requires a larger sample than that allowed by the maximum sample size ($fPDA \times n$). In these cases, GOFCM is forced to predict cluster centers with a suboptimal sample. This is fully discussed in Section 5.8.2.

The experiments with MODSPFCM revealed the role that the stopping criterion plays in GOFCM's speedup. MODSPFCM is equivalent to either SPFCM with GOFCM's stopping criterion, or GOFCM without progressive sampling. Table 5.7 shows how MODSPFCM's speedup falls between those of SPFCM and GOFCM. When the $fPDA$ is a comparatively large number (0.1, 0.06, 0.033333), the advantage of GOFCM's sampling method is clearly shown. As the $fPDA$ becomes smaller, the speedups of GOFCM and MODSPFCM approach the same value. The example below explains why this is so.

Imagine an experiment with GOFCM and MODSPFCM, where $fPDA = 0.001$. On the MRI datasets, using Equation 5.2 with the parameters from Table 5.1, the initial sample size for GOFCM is about 1,100 data objects. The MRI datasets have roughly 4×10^6 data objects each. When $fPDA = 0.001$, the initial sample size for MODSPFCM is about 4,000 data objects. Recall that

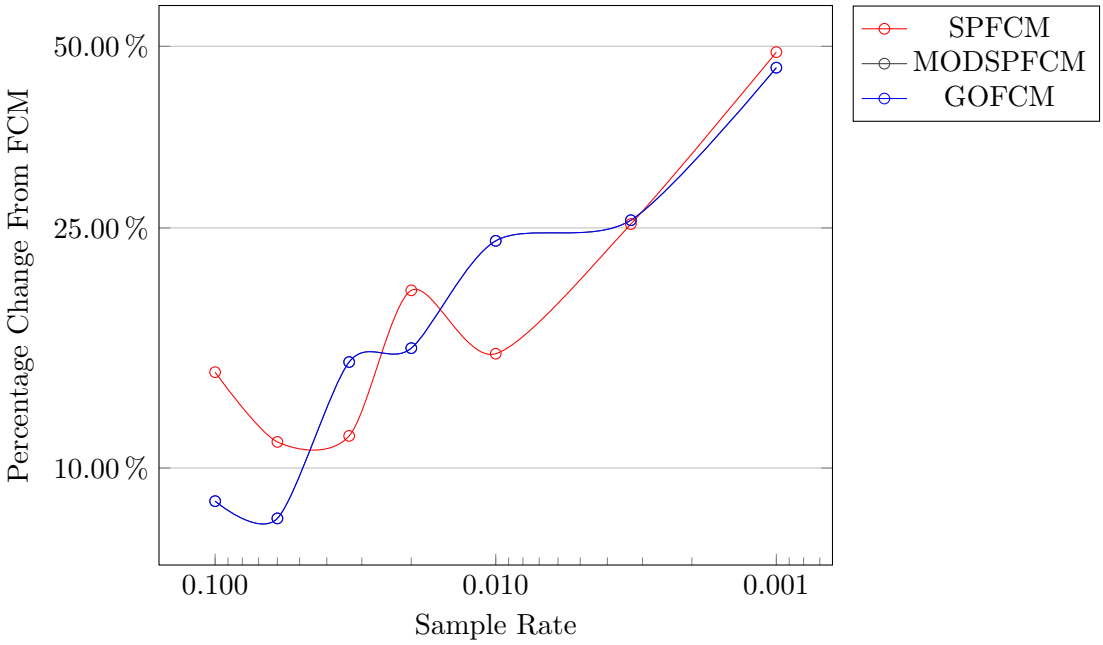

Figure 5.18: Cluster Center Change % (PLK01)

the geometric scheduling parameter for GOFCM is set to 2.0, and that in our experiments the maximum sample size was set by $fPDA$. Thus, by the third PDA, the scheduled sample size exceeds the maximum, and the PDA sizes for both algorithms are the same. In this example, GOFCM only has an advantage in using a smaller n for the first two PDAs, after which both algorithms process the same amount of data and use the same stopping criterion. If the initial sample size is below that calculated by Equation 5.2, GOFCM "degenerates" to MODSPFCM.

5.8 Artificial Datasets and OFCM

Experiments for the artificial datasets D6C5 and D10C7 had very similar results. The results of GOFCM and MSERFCM for these datasets were not radically different from those for the MRI datasets. The only surprise here was the performance of OFCM.

The speedup of OFCM on D6C5 and D10C7 (Tables 5.4 and 5.5) was consistently the lowest. This was also the case on the MRI datasets (Table 5.2). The quality of OFCM as measured by $DQ\,R_m$% and fidelity to FCM as measured by CC% for the artificial datasets (Figures 5.5, 5.6, 5.7,

Table 5.11: Comparison with Havens' Results

(a) $fPDA = 0.001$

Dataset	MRI016				MRI017				MRI018			
Researcher	Havens		Parker		Havens		Parker		Havens		Parker	
Metric	SU	ARI	SU	ARI	SU	ARI	SU	ARI	SU	ARI	SU	ARI
OFCM	2	0.78	2	1.00	2	0.78	1	1.00	2	0.85	2	1.00
SPFCM	16	0.96	8	1.00	14	0.97	7	1.00	12	1.00	7	1.00
GOFCM			25	1.00			20	1.00			21	0.99
rseFCM	29	0.97	26	0.99	25	0.97	21	0.99	22	0.97	22	0.99
MSERFCM			26	0.99			21	0.99			23	1.00

(b) $fPDA = 0.01$

Dataset	MRI016				MRI017				MRI018			
Researcher	Havens		Parker		Havens		Parker		Havens		Parker	
Metric	SU	ARI	SU	ARI	SU	ARI	SU	ARI	SU	ARI	SU	ARI
OFCM	2	0.93	2	1.00	2	0.78	2	1.00	2	1.00	2	1.00
SPFCM	13	0.96	7	1.00	11	0.98	6	1.00	10	1.00	6	1.00
GOFCM			18	1.00			15	1.00			16	0.99
rseFCM	24	1.00	22	1.00	21	0.99	18	1.00	18	1.00	19	0.99
MSERFCM			24	1.00			20	1.00			20	0.99

(c) $fPDA = 0.1$

Dataset	MRI016				MRI017				MRI018			
Researcher	Havens		Parker		Havens		Parker		Havens		Parker	
Metric	SU	ARI	SU	ARI	SU	ARI	SU	ARI	SU	ARI	SU	ARI
OFCM	3	1.00	2	1.00	2	1.00	2	1.00	2	1.00	2	1.00
SPFCM	7	0.96	4	1.00	6	0.97	3	1.00	5	1.00	4	1.00
GOFCM			6	1.00			5	1.00			5	1.00
rseFCM	8	1.00	8	1.00	8	1.00	7	1.00	6	1.00	7	0.99
MSERFCM			10	1.00			9	1.00			9	0.99

and 5.8) was greatly improved compared to its quality and fidelity for the MRI datasets (Figure 5.3 and 5.4). In fact, OFCM had better quality and fidelity metrics than any other algorithm for the artificial datasets at all sample rates.

Recall that OFCM processes data in order; the algorithm does not randomly sample the data. In my experiments, the difference in quality was due to the fact that the artificial datasets were

Table 5.12: Speedup over Range of σ (MRI016)

σ	-0.100	-0.033	-0.010	-0.003	-0.001
SPFCM	4.76	4.76	4.76	4.76	4.76
MODSPFCM	9.62	9.50	9.28	8.70	7.66
GOFCM	10.71	10.16	9.66	8.96	7.72

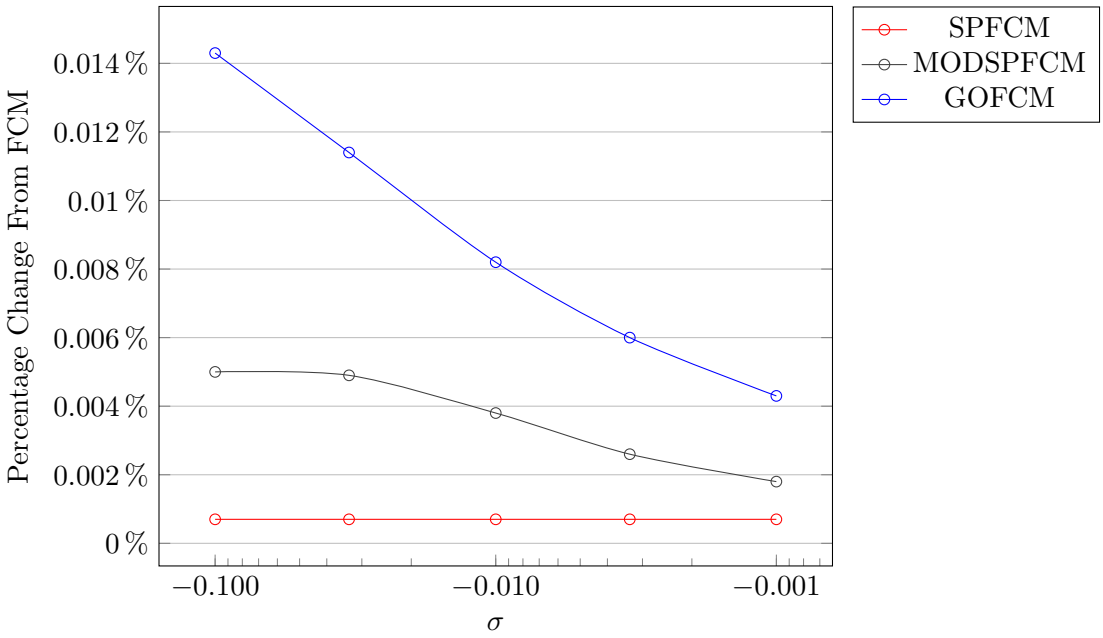

Figure 5.19: $DQ\,R_m$% over Range of σ (MRI016)

randomized before the experimentation. Some naturally occurring datasets, such as an MRI scan, do not have random ordering with respect to clusters.

Pre-randomizing the artificial data made it more likely that each sample processed by OFCM was proportional. In the worst case, with $fPDA = 0.001$, the sample size for D6C5 was 1,000. Using the formula from [102], a sample size of 1,000 corresponded to a maximum absolute difference of 0.03 when $\alpha = 0.05$. It so happened that the 5 true clusters in D6C5 each accounted for 20% of the total. Thus, a sample size of 1,000 would result in each true cluster consisting of 17-23% of the total (with a 95% probability).

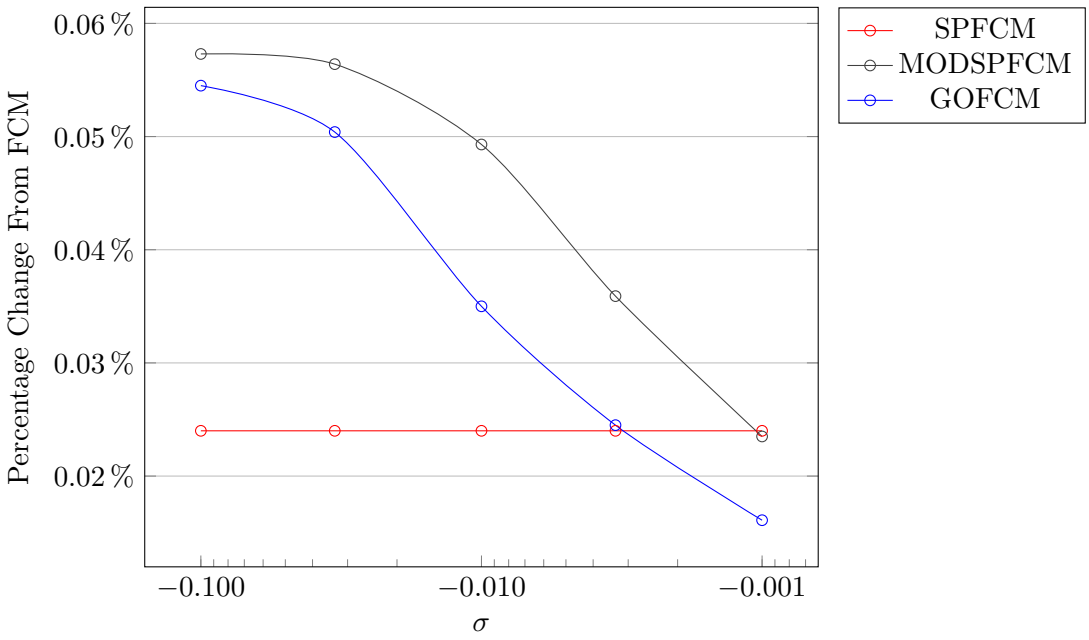

Figure 5.20: Cluster Center Change % over Range of σ (MRI016)

The 5 cluster centers calculated from each PDA did a fairly reliable job of representing the 1,000 data objects, with very little skewing due to the "uniform effect" [90]. In the last step of OFCM, WFCM processed the combined set of weighted cluster centers from each PDA. The resultant, final cluster centers had the best fidelity to the full FCM algorithm, as measured by $DQ\,R_m\%$ and $CC\%$.

The difference in speedup of OFCM using non-randomized vs. pre-randomized data was studied in Chapter 4 [22]. The speedup of OFCM for MRI datasets was reported as improving from 49% to 77% of SPFCM's speedup, when the dataset had been pre-randomized.

This observation suggests that an efficient method of randomly sampling the data can improve both speed and quality of OFCM.

5.8.1 MSERFCM

MSERFCM, designed as an improvement to rseFCM, was usually the fastest algorithm in all experiments for the MRI and artificial datasets (Tables 5.2, 5.3, 5.4, and 5.5).

Whenever MSERFCM's speedup was less than rseFCM's, the sample size was small. This occurred for the MRI datasets for $fPDA = 0.001$. MSERFCM initially used a sample size of

1,147 (Equation 5.2 with c=3) to calculate the starting cluster centers for FCM with a subsequent sample size of about 4,000 objects. So, in these cases, MSERFCM processed over 5,000 objects, while rseFCM processed about 4,000 objects. The speedup gained from a better set of starting cluster centers was not enough to compensate for the time taken to process the increased amount of data.

When D6C5 ($n = 10^6$) was clustered with the parameter $fPDA = 0.001$, the estimated sample size to predict cluster centers was 3,184. In this case, the estimated sample size exceeded the user-specified sample size ($n \times fPDA$), and the MSERFCM algorithm degenerated to rseFCM with a sample size of 3,184. This explains the faster performance of rseFCM, which used the user-specified sample size of 1,000.

With respect to quality, MSERFCM was a better choice than rseFCM the majority of the time. This is expected in situations where MSERFCM processed a larger sample size than rseFCM. In the example above, MSERFCM processed a random sample three times larger, making it likely that MSERFCM would have more fidelity to FCM.

The situation where the estimated sample size exceeded the user-specified sample size occurred in 6 out of the 25 experiments using the MRI and artificial datasets. By design, MSERFCM draws a separate sample to calculate the set of starting cluster centers to improve speedup. Both MSERFCM and rseFCM use the same-size samples to cluster the dataset, so one would *expect* no difference in *quality* between MSERFCM and rseFCM in the remaining 19 experiments.

This, however, was not the case. Of the remaining 12 MRI experiments, MSERFCM had (ignoring ties) average quality and fidelity better than rseFCM's: 67% of the time for the $DQ\,R_m$% metric, and 72% of the time for the CC% metric. Of the remaining 7 artificial dataset experiments, MSERFCM had (ignoring ties) average fidelity better than rseFCM's: 67% of the time for both the $DQ\,R_m$% and the CC% metrics.

FCM is guaranteed to converge to a local (or global) minimum or saddlepoint [91]. One possibility is that the calculated starting cluster centers for MSERFCM allow for better discovery of local minima than do the randomly determined starting cluster centers for rseFCM. Research using the HCM algorithm supports this observation. A comprehensive study of different initialization

methods for HCM, showed variation in quality by initialization method, as measured by final objective function value [108]. The runtime also varied by initialization method. Bradley and Fayyad's seminal paper on initialization methods also reported that a refined starting point for HCM could improve runtime and quality [61]. Research using the FCM algorithm, discussed in Section 2.3.1, also reports how an improved starting point for FCM improves runtime.

5.8.2 Plankton Dataset Challenges

Clustering the full plankton dataset, PLK01, showed the limitations and capabilities of the algorithms.

The speedup for all algorithms on PLK01 (Table 5.6) is greater than the corresponding speedup for the MRI datasets (Table 5.2) except MSERFCM. The MSERFCM algorithm has a consistent but small speedup, just barely greater than that of OFCM.

This is so because of the sample size rules for MSERFCM. Thompson's method (Equation 5.2) estimates a minimum sample size of 50,944 for PLK01. Thus, in all experiments, MSERFCM degenerates to rseFCM, with a sample size of 50,944. In contrast, the largest sample size for the other algorithms is 20,328, when $fPDA = 0.1$.

Note that MSERFCM had the best quality (Figure 5.10). It was also the only one to have consistent quality across all experiments, but this was to be expected, since the algorithm used the same data samples in each experiment. MSERFCM's $CC\%$ metric for PLK01 was 5.56%, and its $DQ\,R_m\%$ was -0.0078%, suggesting that MSERFCM returned quality results superior to those of FCM.

Statistical significance for the small difference in R_m between FCM and MSERFCM was tested for, using a one-tailed Welch's t-test. The t-test returned $t = 0.43$ with 50 d.f. This corresponds to $p = 0.3345$, which is not considered statistically significant.

The eFFCM algorithm had fairly consistent, good-quality results on PLK01, but eFFCM has a mechanism to increase its sample size dynamically if statistical measures are not met. The average sample sizes of eFFCM for PLK01 ranged from 10.7% to 34.6%. All other algorithms suffered a degradation of quality as the sample size was reduced. This was attributable to suboptimal

sample sizes. The fidelity to FCM, as measured by $CC\%$, made these results unusable for many applications of clustering.

The quality of the results from MSERFCM and eFFCM demonstrated the utility of using a statistical method for determining sample size.

The PLK01 dataset also provided a nice demonstration of GOFCM's operation. As with MSERFCM, the estimated minimum sample size was greater than the user-defined sample size ($fPDA \times n$). What happened here was that GOFCM degenerated to use the same, consistent sample rate as SPFCM.

When this occurred, the only difference between SPFCM and GOFCM was the stopping criterion. SPFCM always processed 100% of the data, but GOFCM stopped short of that if the stopping criterion were met. An examination of Table 5.6 shows that SPFCM and GOFCM had a similar speedup when the $fPDA$ (sample rate) was 0.1, and GOFCM's speedup increased compared to SPFCM's as the $fPDA$ decreased. Figure 5.9 shows that the $DQ\,R_m\%$ for both algorithms increased as the $fPDA$ decreased, with SPFCM's $DQ\,R_m\%$ consistently lower than GOFCM's.

Observe the $CC\%$ of SPFCM, OFCM, and GOFCM when the $fPDA = 0.001$ (Figure 5.10). Note that the values are very similar. When $fPDA = 0.001$, the sample size is only 204. Experimentation was kept consistent across all datasets; in reality there is no reason for such a small sample. Recall that $c = 20$ for PLK01. The cluster representation for PLK01 is not uniform, and the sample size is small, making it unlikely that all clusters are even represented in each sample. The base FCM algorithm will still try to fit 20 clusters, likely resulting in predicted cluster centers unrepresentative of the full dataset.

Chapter 6: Accelerating FCMdd

"It's not too far, it just seems like it is." - Lawrence "Yogi" Berra [2]

6.1 Distributed FCMdd

Breaking a dataset into overlapping or disjoint subsets and then performing clustering is not a new idea. Strehl and Ghosh provided an analysis of how best to combine clustering results from different subsets of data [109]. Their work focused on solving the problem of efficiently aligning like clusters, rather than accelerating a clustering algorithm, but they do mention that speedups can occur.

Hore based his algorithms, SPFCM and OFCM, on clustering subsets of the full dataset and on combining the results from disjoint sets [46] [65] [71]. Labroche duplicated Hore's algorithms for use with relational data, substituting FCMdd for FCM [54].

The Distributed FCMdd (DFCMdd), as the name implies, is an accelerated algorithm that distributes a relational dataset into disjoint subsets. It is designed to speedup the clustering by both reducing the sample size and by decreasing the average number of iterations. Quality is preserved by exploiting the observations about OFCM's performance on pre-randomized data.

The DFCMdd algorithm has two stages. In stage one, it breaks the dataset into a user-defined number of subsets, called folds. Each data object in the dataset is randomly assigned into one of f folds. The folds are equal in size, so for a dataset with n objects, each fold has $\frac{n}{f}$ data objects.

Each fold is then clustered using FCMdd (also referred to in this chapter as the reference algorithm) to return a set of c medoids. After all folds have been clustered, a set of $f \times c$ medoids are retained. This dataset is called the "medoid dataset."

In stage two, a "linking method" is used to cluster the medoid dataset. The linking method produces a set of c medoids as a final clustering solution.

6.1.1 Linking Methods

The linking method combines the results from each fold into one solution. This is a concept similar to a "consensus function" in cluster ensembles [109], except for the fact that DFCMdd assumes that the data in each fold is disjoint and that the strength of the relation between any two data objects is known.

Four different linking methods were developed. The first linking method (LM1) reapplies FCMdd to the medoid dataset. The initial medoids used by FCMdd are randomly selected. This arrangement is nearly identical to OFCMD [54], except in that the medoid dataset is not weighted.

One necessary decision was whether or not to weight the medoids and to use a weighted version of FCMdd, which is similar to work by LaBroche [54] or Mei [110]. A consideration was that two of the linking methods use Single Linkage and weights are not meaningful to that algorithm. Thus, a weighting strategy was not implemented.

The second linking method (LM2) applies Single Linkage to the medoid dataset. As described in Section 2.1.1, the last $c-1$ links are removed to separate the final dendrogram into c clusters. Medoids from each cluster are defined as the data object that has the smallest total dissimilarity over all objects in its cluster. The medoid, for a cluster k, is calculated by:

$$q = argmin_{1 \leq j \leq n; x_j \in X_k} \sum_{i=1}^{n} \rho(x_i, x_j); v_k = x_q; \tag{6.1}$$

where:

X is a dataset where $n = |X|$, and X_k is the subset assigned to the k^{th} cluster.

x_i is the i^{th} data object.

V is the set of cluster centers; v_k is the k^{th} cluster center.

$\rho(x_i, x_j)$ is the dissimilarity between the i^{th} and j^{th} data objects.

Table 6.1: Linking Methods

Linking Method	Clustering Method	Initialization
LM1	FCMdd	Random
LM2	SL	N/A
LM3	FCMdd	Medoids predicted by SL
LM4	FCMdd	Medoids from first fold

The quality and speed of a partition clustering algorithm can be improved when the initial set of cluster medoids are accurately estimated rather than randomly selected. This approach was discussed at length in Section 2.3.1 in the context of HCM and FCM. Here, I explore if this approach will have the same effect on FCMdd. The last two linking methods use FCMdd to cluster the medoid dataset with the initial set of medoids estimated in two different ways.

The third linking method (LM3) combines SL and FCMdd. This method uses the clustering solution calculated by LM2 as the initial set of medoids for a reapplication of FCMdd on the medoid dataset. The c medoids returned by FCMdd are used as a final clustering solution.

The fourth linking method (LM4) resembles the first. The only difference is that, instead of randomly selecting the initial medoids, it uses the set of medoids calculated by the first fold of FCMdd. I chose the first fold as the source of starting medoids for simplicity. Randomly choosing a fold would also have been equally acceptable.

Table 6.1 summarizes the four approaches to linking.

6.1.2 Discussion

One of the inspirations for DFCMdd was OFCM's improvement in quality when clustering randomized as opposed to non-randomized datasets (Section 4.4.4). In DFCMdd, each data object is randomly assigned to one of many folds, which are then clustered independently. In theory, clustering the data one fold at a time would provide a speedup with only a small loss of quality.

That left the decision of how to cluster the medoids produced by each fold. The simplest linking method, LM1, or just clustering the medoids, was chosen as the baseline to which other methods would be compared. LM1, except for the absence of weighting medoids, is an identical concept to that of OFCM and OFCMD.

Clustering algorithms impose an assumed structure on the data [28] [4]. The FCMdd algorithm seeks to reduce an objective function, finding for each cluster a centrally located representative. Single Linkage is a relational algorithm that imposes a different structure on the data. To explore the benefits of a different assumed structure, Single Linkage was selected for the basis of LM2.

Initial experiments with LM1 revealed the potential to improve speedup and fidelity. For the remaining linking methods, the well-known strategy of using an improved starting position for clustering was employed (Section 2.3.1). LM3 continues the exploration of a different assumed structure by using the medoids predicted by SL as a starting point for FCMdd.

LM4 uses the set of medoids produced by the first fold as the starting medoids to cluster the "medoid dataset." This linking method employs an idea similar to SPFCM's passing along the clustering solution of the previous PDA as a starting point for the next PDA. It is also similar to the algorithms that use a sample of the data to predict an improved initialization point.

6.1.3 Runtime Complexity

The FCMdd algorithm has a runtime complexity of $O(n^2ci)$. As the FCMdd algorithm has a quadratic runtime complexity with respect to n, reducing n over f folds will provide a speedup proportional to f.

In stage one, each fold is clustered using FCMdd.

$$\begin{aligned} T_1 &= f \times O((\frac{n}{f})^2 ci) \\ &= f \times O(\frac{n^2}{f^2} ci) \\ &= \frac{1}{f} O(n^2 ci) \\ &= O(n^2 ci) \end{aligned}$$

The value $\frac{1}{f}$ is a constant and is not considered as part of the runtime complexity. For practical purposes, it should produce a speedup roughly f times the reference algorithm.

One must also consider the time taken by the linking method in stage two. Both SL and FCMdd have a quadratic runtime complexity with respect to n. In this case, though, the number of data objects equals $f \times c$. If one assumes that $fc << n$, the amount of time taken by the linking method is negligible.

6.2 Experiments

FCMdd and DFCMdd were compared in terms of speedup and quality on five real-world and four artificial datasets: the real-world datasets were MRI016R, MRI017R, MRI018R, PLK02, and Pendigits; the artificial datasets were D3C6-1, D3C6-2, D4C5, and D7C10. See Chapter 3 for dataset details.

I performed additional preprocessing for the MRI datasets. There were 12,000 data objects randomly selected from each original MRI dataset to serve as experimental datasets. The data features were linearly scaled to fall in the range [0-1], based on the maximum and minimum values in the original dataset.

The dataset sizes were kept relatively small compared to the experimentation using FCM and its variants. FCMdd has a runtime complexity that is quadratic with respect to the number of data objects. The size of datasets were balanced to ensure that enough data was present for a realistic test, but small enough so that experimentation could be completed in a timely fashion.

The number of data objects was set to 12,000 in order to ensure that the sample proportionally represented each class. As in Equation 5.2, Thompson's formula estimates that a minimum sample size of 1,178 is required in order to ensure a proportional sample when $r = 0.10$ at the 95% confidence level given that $c = 3$. When one of the MRI datasets is broken into 10 folds, each fold will have a proportional sample.

To verify that selection of 12,000 data objects was not merely an anomaly resulting in good (or bad) performance, I created an additional MRI dataset containing 20,000 data objects. This

dataset, MRI017R-2, was created from MRI017 and was processed in a manner otherwise identical to the other MRI datasets.

The artificial datasets consisted of either 12,000 or 16,000 data objects. Each data feature was scaled so that the values fell in the range $[0 - 1]$.

6.2.1 Experimental Procedures

The FCMdd and Single Linkage algorithms are designed to cluster relational data. The data objects in the datasets used for experimentation are vectors of numeric features. The numeric data was converted to relational data by defining the dissimilarity function, $\rho(x_i, x_j)$, as the Euclidean distance.

All experiments consisted of 30 trials. Each dataset was clustered by the reference algorithm (FCMdd). DFCMdd was used to cluster each dataset twice, once using 5 folds and the other time using 10 folds. Each DFCMdd experiment resulted in a "medoid dataset" that contained the medoids from each fold. Each of the four linking methods was applied to each medoid dataset. Thus, there were four final sets of medoids from each experiment.

The runtime for each algorithm was recorded as the number of clock ticks that elapsed while the algorithm was executing. Time taken to pre-process the data was not included in this time.

Equation 2.11 and the final set of medoids for each trial were used to calculate the cluster membership for each data object. This calculated cluster membership was in turn used to calculate J_m for each trial.

The intra $CC\%$ was calculated for each experiment. The inter $CC\%$ was calculated between the reference algorithm clustering solution and each DFCMdd experiment that used the same dataset. Before calculating $CC\%$, cluster membership was "hardened," i.e., each data object was assigned solely to the cluster for which it had the highest membership. Details on intra and inter $CC\%$ are in Section 2.4.3.

Accuracy was calculated for datasets for which the class identities were known.

6.2.2 Parameters

A few parameters needed to be set for FCMdd and DFCMdd. The number of clusters, c, was set to the number of known classes in each dataset. Experiments were run for $f = 5$ and $f = 10$ folds. The fuzzifier, m, was set to 1.5 for all experiments. This is a lower setting than in my FCM experiments, but Krishnapuram advises setting m at 1.5 or lower for FCMdd.

This is because m controls how fuzzy each cluster will be. The cluster centers, however, are medoids and have a fuzzy membership in their cluster equal to one. Because m is an exponent, it has no effect on the medoid's fuzzy membership. However, a high setting of m will make the fuzzy cluster memberships of all other data objects less distinct. This makes it less likely that the medoid for each cluster will change [52].

The Single Linkage algorithm is deterministic and only requires the parameter c.

6.2.3 Results

The results for 10 datasets, 2 fold settings, and 4 linking methods created a large volume of data. Complete results are available in Tables B.1 and B.2 in Appendix B. Representative subsets of the results are presented here.

DFCMdd provides a speedup of about 6.5 times when there are 5 folds, and a speedup of about 14 times when there are 10 folds, regardless of linking method.

No linking method was consistently the fastest in all datasets. For the 20 experiments with different combinations of datasets and fold settings, LM2 was fastest over seven experiments. For any particular dataset and fold setting, the linking methods' speedups did not differ much.

Table 6.2 illustrates the lack of variation in speedup of MRI016R, and Table 6.3 lists the average speedup and standard deviation for each fold setting and linking method.

There was some variation in speedup across datasets, suggesting that some datasets were "easier" for DFCMdd to cluster than others. The speedup on dataset D3C6-1 was much higher than those of the other datasets. If D3C6-1's values are omitted, the speedup values in Table 6.3 fall slightly, and the standard deviation is tightened. This is shown in Table 6.4.

Table 6.2: Speedups for MRI016R

Folds	Linking Method	Speedup
5	LM1	6.66
5	LM2	6.91
5	LM3	6.86
5	LM4	6.82
10	LM1	15.18
10	LM2	14.82
10	LM3	15.08
10	LM4	14.17

Table 6.3: DFCMdd Speedup by Linking Methods

Folds	Linking Method	SU	Std. Dev. SU
5	LM1	6.79	1.28
5	LM2	6.84	1.36
5	LM3	6.80	1.30
5	LM4	6.79	1.26
10	LM1	14.88	3.44
10	LM2	15.18	3.89
10	LM3	15.07	4.03
10	LM4	15.04	3.93

Speedup averaged over all datasets by number of folds and linking method.

Three quality metrics were calculated for all datasets: $DQ\,J_m\%$, intra $CC\%$, and inter $CC\%$. $DQ\,J_m\%$ was calculated in a manner similar to $DQ\,R_m\%$ for the FCM variants, but it uses the objective function for FCMdd extended to the full dataset. Intra $CC\%$ is a measure of how much the cluster assignments vary over multiple trials of a single clustering algorithm. Inter $CC\%$ is a measure of how much the cluster assignments vary between two clustering algorithms over multiple trials. These metrics are discussed in detail in sections 2.4.2 and 2.4.3.

Intra $CC\%$ was calculated for FCMdd for each full dataset; this is the reference intra $CC\%$. The reference intra $CC\%$ indicates how much partitions created by FCMdd naturally vary over multiple, randomly initialized trials. Intra $CC\%$ was also calculated for DFCMdd, for each linking method, for each dataset. The inter $CC\%$ was calculated between FCMdd and DFCMdd for each experiment.

Table 6.4: DFCMdd Speedup Omitting D3C6-1

Folds	Linking Method	SU	Std. Dev. SU
5	LM1	6.45	0.60
5	LM2	6.46	0.72
5	LM3	6.44	0.66
5	LM4	6.44	0.65
10	LM1	13.93	1.82
10	LM2	14.03	1.50
10	LM3	13.91	1.80
10	LM4	13.89	1.61

Speedup averaged over all datasets by number of folds and linking method.

The rationale for calculating these $CC\%$ values is that a high-fidelity solution should not vary more than FCMdd does over the same number of trials. Two derived metrics were calculated from intra $CC\%$ and inter $CC\%$.

The intra $CC\%$ diff is the difference between the DFCMdd intra $CC\%$ and the reference intra $CC\%$ for a given experiment. The intra $CC\%$ diff signifies how much more DFCMdd's partitions vary than FCMdd's. Occasionally, the intra $CC\%$ diff was negative, signifying that DFCMdd's partitions varied less than FCMdd's.

The inter $CC\%$ diff is the difference between the inter $CC\%$ and the reference intra $CC\%$ for a given experiment. The inter $CC\%$ diff signifies how much more the variation in cluster assignment between DFCMdd and FCMdd is compared to the expected variation in cluster assignment for FCMdd across multiple trials. Occasionally, the inter $CC\%$ diff was negative, signifying that there was less variation between DFCMdd and FCMdd that what is expected over multiple trials of FCMdd.

Not surprisingly, over all experiments, the linking method with the lowest intra $CC\%$ diff also had the lowest inter $CC\%$ diff 80% of the time.

Occasionally, the differences in $CC\%$ were statistically significant. The z statistic was also calculated for each $CC\%$ diff (see Section 2.4.7.2). The null hypothesis in these cases was that the intra $CC\%$ for FCMdd would be no different from the intra $CC\%$ for FCMdd or the inter $CC\%$ for the experiment. The competing hypothesis was that the intra $CC\%$ for FCMdd would be different

from the other metric. The null hypothesis must be rejected when $z > 1.96$ or when $z < -1.96$ at the 95% level of confidence. Therefore, a statistically significant result in this context would indicate that DFCMdd had more or less variation than FCMdd, as measured by $CC\%$, depending on the sign of z. The z-values for all experiments are in Tables B.1 and B.2 in Appendix B.

There was a dichotomy regarding quality.

On artificial datasets, there was no clear superior linking method. LM1 and LM2 both had the best quality metrics over 37.5% of the experiments, with LM3 and LM4 the remaining 25%. LM4 consistently had the worst quality metrics for intra $CC\%$ diff and inter $CC\%$ diff.

On real-world datasets, LM4 had the best overall metrics. Using real-world data, LM4 had the lowest values for $DQ\,J_m\%$, intra $CC\%$ diff, and inter $CC\%$ diff, 92%, 58%, and 83% of the experiments respectively.

Tables 6.5 and 6.6 show the difference in quality between the artificial and real-world datasets.

Table 6.5: DFCMdd Artificial Dataset Results

Folds	Linking Method	Speedup	$DQ\,Jm\%$	Intra CC% diff	Inter CC% diff
5	LM1	7.59	0.91%	3.93%	2.68%
5	LM2	7.80	0.51%	0.07%	0.37%
5	LM3	7.75	0.50%	0.01%	0.34%
5	LM4	7.63	1.37%	8.07%	4.63%
10	LM1	16.76	0.69%	3.33%	2.31%
10	LM2	17.30	0.65%	2.04%	1.49%
10	LM3	17.04	0.50%	1.34%	1.09%
10	LM4	17.15	1.21%	7.80%	4.65%

Metrics averaged over all datasets by number of folds and linking method.

6.3 Discussion

6.3.1 The Artificial Datasets

The artificial datasets were intended to be moderately challenging, but proved to be especially challenging for FCMdd. Details on how artificial datasets were constructed are covered in Chapter 3.

Table 6.6: DFCMdd Real-World Dataset Results

Folds	Linking Method	Speedup	$DQ\,Jm\%$	Intra CC% diff	Inter CC% diff
5	LM1	6.26	3.82%	0.11%	4.13%
5	LM2	6.20	1.18%	-6.24%	0.75%
5	LM3	6.16	1.18%	-6.24%	0.76%
5	LM4	6.22	0.11%	-3.10%	-0.11%
10	LM1	13.62	3.38%	-2.08%	2.49%
10	LM2	13.77	5.90%	2.70%	6.68%
10	LM3	13.75	4.18%	-0.68%	3.76%
10	LM4	13.63	-0.10%	-6.99%	-1.15%

Metrics averaged over all datasets by number of folds and linking method.

One observation was that the intra $CC\%$ values for the datasets, when clustered by FCMdd, were high. The D3C6-1 dataset was constructed so that the average distance between the cluster centers was roughly uniform and 3.5 to 5 times that of the data features' standard deviations. This resulted in a larger-than-expected degree of overlap between clusters, reflected in the intra $CC\%$.

The datasets D4C5 and D7C10 were similarly constructed and had similar issues.

Each cluster in the artificial datasets was defined by a cluster center in R^s and a variance for each data dimension (feature). Each data object was assigned to a class corresponding to its cluster center. After being clustered by FCMdd, the resultant clusters were aligned to classes, and the accuracy was calculated. This helped provide insight into how FCMdd was clustering the datasets. Results are listed in Table 6.7.

Table 6.7: FCMdd Clustering Results for Artificial Datasets

Dataset	Intra CC%	Accuracy
D3C6-1	9.79%	85.09%
D4C5	20.72%	79.66%
D7C10	15.69%	90.07%
D3C6-2	0.09%	99.33%

Concurrently viewing intra $CC\%$ and accuracy (for all datasets except for D3C6-2) suggests that 10% to 20% of the data objects have significantly high membership in 2 or more clusters. These "border" data objects swapped cluster assignments every trial, making the partitions vary.

An additional dataset, D3C6-2, was constructed for subsequent experiments. Its cluster center positions were the same as D3C6-1's, but the variances were slightly reduced. This had the effect of reducing intra $CC\%$ and increasing accuracy.

6.3.2 Speedup

The speedup achieved by DFCMdd was roughly proportional to the number of folds, f. This was suggested in Section 6.1.3 and observed in Section 6.2.3. The speedup reported was 6.5 times with 5 folds, and about 14 times with 10 folds.

In order to provide further evidence of the predicted and observed trends with respect to speedup, additional experiments with 8 and 12 folds were performed for the Plankton dataset PLK02. The speedups for 8 and 12 folds were consistent with what had already been predicted. The speedup for 8 folds fell between those for 5 and 10 folds, and the speedup for 12 folds was greater than that for 10 folds. Results are listed in Table 6.8.

The speedup appeared to be largely independent of the linking method. Averages of speedup are listed by linking method in Table 6.3. There were only a few small effects attributable to the linking method.

LM2, an application of Single Linkage on the medoid dataset, was on average faster than LM3. This makes sense, because LM3 requires the medoids predicted by SL in order to initialize FCMdd for clustering the medoid dataset.

The LM4 linking method was, on average, faster than LM1. Both linking methods cluster medoid datasets with FCMdd, but LM4 uses as an initialization the medoids from the first fold of DFCMdd. This improved initialization leads to a slightly faster runtime. This was true for 65% of the experiments.

Initially, the fact that speedups were slightly faster than $\frac{1}{f}$ was surprising. This likely occurred because DFCMdd had a much lower utilization of system memory. The implementation of FCMdd loaded the dissimilarity matrix into RAM, which requires $O(n^2)$ memory. DFCMdd clustered each fold sequentially, so when $f = 10$, only $\frac{1}{100}$ of the RAM was needed. The faster loading of the dissimilarity matrix as well as the faster lookups most likely provided a speedup of their own. The

software implementation was in C#, which manages its own memory, so breaking out memory management as a runtime category was not feasible.

The speedups of D3C6-1 were much higher than those of the other datasets. An average speedup of 10 times with 5 folds, and of 25 times with 10 folds was obtained on D3C6-1 – disproportionate compared to the averages of 6.5 and 14 with the other datasets. To get an idea of why this is so, the runtimes of D3C6-1 and D3C6-2 were examined when clustered by FCMdd and DFCMdd with LM1.

Table 6.9 clearly shows how the difference in speedup occurred. The accelerated algorithm, DFCMdd (LM1), had roughly the same runtime on both datasets. The runtime of the reference algorithm, FCMdd, was longer on D3C6-1 than on D3C6-2, resulting in the speedup calculation for DFCMdd to be higher on D3C6-1. The difference had nothing at all to do with DFCMdd or the linking method.

FCMdd has a runtime complexity of $O(n^2ci)$. Both datasets have the same values for n and c, so the difference must be attributable to the number of iterations, i. The geometry of D3C6-1 consists of a set of points in three dimensions. Each point is assigned to one of six clusters, but deviates from its cluster center by a random amount in each dimension. The amount of deviation is high, so the clusters are overlapping.

When the dataset is transformed into a dissimilarity matrix, the overlapping structure of the clusters results in a higher percentage of data objects with a more uniform "dissimilarity vector." As described in [111], the dissimilarly vector for a data object is the row (or column) in the dissimilarity matrix [8] for a data object. It shows the degree to which that data object is dissimilar to every other data object in the dataset. An overlapping structure leads to data objects having dissimilarity vectors that resemble the dissimilarity vectors of a large number of other data objects in the dataset.

Having more data objects that "look similar" increases the number of iterations needed to minimize J_m. Hathaway observed this in a study of a relational version of FCM [48]. Avoiding

[8] Use of the dissimilarity matrix is not required for FCMdd or SL. The concept is the same if the dissimilarities are calculated dynamically.

this situation when sampling a relational dataset, was the rationale for the DF algorithm used by Bezdek in the development of eNERF [70].

Table 6.8: Speedups for Plankton

Folds	Linking Method	Speedup
5	LM1	6.31
5	LM2	5.61
5	LM3	5.81
5	LM4	6.22
8	LM1	10.98
8	LM2	11.00
8	LM3	11.00
8	LM4	10.94
10	LM1	13.75
10	LM2	14.34
10	LM3	14.42
10	LM4	14.51
12	LM1	18.14
12	LM2	18.49
12	LM3	18.23
12	LM4	18.18

Table 6.9: Runtimes for D3C6 Datasets

Algorithm	D3C6-1	D3C6-2
FCMdd	13,445	8,289
DFCMdd (LM1)	1,364	1,189

Runtimes listed in millions of clock ticks (M)

6.3.3 Quality Issues

The $DQ\,J_m\%$, intra $CC\%$, and inter $CC\%$ metrics assessed the quality and fidelity of results. As noted in the Section 6.2.3, there was a huge difference between the observed quality metrics from the artificial datasets and those from the real-world datasets.

The $DQ\,J_m\%$ values for artificial datasets were on average lower than those for the real-world datasets. All the linking methods, except for LM4, had similar $DQ\,J_m\%$ values.

This fourth linking method's performance for the real-world datasets was very different from its performance for the artificial datasets. LM4 was the best linking method in eleven out of twelve experiments on real-world datasets (91.7% of the time). LM4 was the best linking method in only one out of eight experiments for artificial datasets, and it was the worst linking method in five out of eight experiments.

In experiments using real world data, LM4's $DQ\,J_m\%$ values were negative five out of twelve times. This suggested that the medoids produced by LM4 in these five experiments were an improvement over FCMdd's clustering of the full dataset. No linking method returned a negative $DQ\,J_m\%$ value for any of the artificial datasets.

The intra $CC\%$ diff and inter $CC\%$ diff were not consistent for any of the linking methods over all the artificial datasets. LM4, however, usually had the highest $CC\%$.

LM4, however, for the real-world datasets, had $CC\%$ differences that 58% of the time were both better and statistically significant compared to FCMdd's. When five folds were used, LM2 and LM3 had more consistent results, as judged by $CC\%$, than FCMdd did on the real-world datasets, with $DQ\,J_m\%$ values that ranged from -0.14% to 3.24%.

Radical difference in quality metrics was observed between the artificial datasets and the real-world datasets. The complete listing of quality metrics for all DFCMdd experiments is in Appendix B, Tables B.1 and B.2.

One of the reasons for the differences in quality between artificial and real-world datasets is the same as the reason for differences in speedup, identified in Section 6.3.2. The artificial dataset construction created a significant percentage of data objects with a uniform dissimilarity vector. The high values for intra $CC\%$ suggest that this situation created many local extrema in which FCMdd could terminate. The exception was D3C6-2, which had an intra $CC\%$ of only 0.0915%; on average, only 11 data objects changed cluster assignments per trial.

Note that LM2 and LM3 had better relative quality on the artificial datasets than on the real-world datasets. These linking methods are based on Single Linkage, which clusters data with a different set of assumptions than FCMdd. Single Linkage cannot become stuck in a local extremum. Table 6.5 shows than either LM2 or LM3 had the best average quality metrics over the artificial

datasets. For many experiments, LM2 and LM3 returned identical quality results. This meant that the medoids produced by Single Linkage, when used as an initialization for FCMdd, were already in a local extremum and did not deviate further.

The difference between LM1 and LM4 on the artificial datasets was surprising. The intent of LM4 was to use an initial set of medoids based on a sample (the first fold) to produce higher-quality results. Unfortunately, LM4 had clearly inferior quality results compared to LM1 for the artificial datasets. This difference in quality between LM1 and LM4 for the artificial datasets needed further investigation.

Diagnostic logs and raw results for D3C6-1's 30-trial experiments were carefully analyzed. In 20% of the trials, the final sets of medoids from LM1 and LM4 were identical. In the rest, the final set of medoids from LM4 usually had worse quality than that from LM1. Recall that LM4 uses the medoids from the first fold as an initialization to cluster the medoid dataset. In a few of the trials, the final set of medoids did not deviate from the initialization set. This is because the medoids from the first fold were therefore already in a local extremum of the medoid dataset. In many of the other trials, the final set of medoids only deviated from the initial set of medoids by one or two of the medoids. Thus, the medoids from the first fold were already very close to a local extremum. In many of these cases, the initial set of medoids were at or near a local extremum that had an inferior (high) objective function value.

The real-world datasets had markedly different quality results from the artificial datasets. As the algorithms and linking methods were the same, the cause must have been some inherent difference in the dataset structure. The intra $CC\%$ for both the artificial and real-world datasets (see Appendix B, Tables B.1 and B.2 for a full listing) range from 6% to 33% (omitting D2C6-2), suggesting a non-trivial amount of cluster overlap for both types of dataset. Thus, overlap alone is not the cause.

The artificial datasets have a uniform cluster structure with an identical variance in each dimension. The class assignments are known for two of the real-world datasets, Pendigits and Plankton. The data objects in the Plankton dataset were separated by class, and the standard deviations of each of the 21 data features were examined by class. There was no uniformity in the standard deviations of the 21 features for the Plankton dataset, and no similarity in the standard deviations

of the features across the four classes. The same analysis was performed across the 10 classes and 16 features for Pendigits, with the same results.

This analysis suggests that the feature spaces for the Plankton and Pendigits datasets do not have as large a degree of uniformity as the artificial datasets. When these datasets are clustered with DFCMdd and LM4, their initial medoids are less likely to be stuck in local extrema, and the final set of medoids are more likely to improve. As mentioned previously, LM4 had the best quality metrics out of all linking methods over real-world datasets, with no significant difference in speedup.

6.3.3.1 Estimated Sample Size

The experiments used datasets with 3 – 6, and 10 clusters. The DFCMdd algorithm breaks the dataset into f folds. Is the size of each fold a suitable sample? This issue was explored in the development of GOFCM and MSERFCM (Section 5.2).

Assuming that the desired significance level is $\alpha = 0.05$, corresponding to $v(\alpha) = 1.27359$, and that the desired relative difference is $r = 0.10$, Equation 5.2 was used to estimate the sample size for the number of clusters in the dataset. If the significance level were relaxed to $\alpha = 0.10$, then $v(\alpha) = 1.00635$. Estimates for both significance levels are listed in Table 6.10.

Table 6.10: Sample Size Estimates from Thompson's Formula

Number clusters (c)	$\alpha = 0.05$	$\alpha = 0.10$
3	1,147	906
4	2,038	1,611
5	3,184	2,516
6	4,585	3,623
10	12,736	10,064

Sample size rounded up to next highest integer

The MRI datasets have three clusters. The MRI datasets have 12,000 data objects (except MRI017R-2, which has 20,000), so an estimated sample size of 1,147 ensures that even when 10 folds are used, the sample will be proportional in each fold. Thus, for all experiments, one can be 95% confident that for any particular fold, the sample provided will be proportional.

The PLK02 dataset has 12,000 data objects in four clusters. When ten folds are used, the estimated sample size exceeds the number selected for each fold (1,200). When five folds are used, the estimated sample size is less than the number selected for each fold (2,400). One might expect a degradation in quality between five and ten folds.

The rest of the datasets have more than four clusters, and the estimated sample sizes exceed the number of data objects placed in either five or ten folds.

Estimating the sample size will work well for that single sample, but this is not enough to guarantee quality in a multi-stage accelerated algorithm like DFCMdd. Each fold may have a good estimate of the proportion and may return a valid set of medoids, but the linking method or some factor inherent in the dataset itself may preclude good results. Table 6.11 lists the quality results for MRI017R. The sample sizes with five and ten folds both exceed the minimum predicted by Thompson's formula (at the 95% confidence level), but note that the quality varies by linking method.

Table 6.11: Quality Results for MRI017R

Folds	Linking Method	$DQ\,Jm\%$	Intra $CC\%$ diff	Inter $CC\%$ diff
5	LM1	10.3543%	12.1760%	8.1210%
5	LM2	-0.0483%	-4.8308%	-2.1072%
5	LM3	-0.0483%	-4.8308%	-2.1072%
5	LM4	0.3597%	1.5470%	0.8078%
10	LM1	4.1855%	3.5316%	2.2805%
10	LM2	5.3558%	7.8504%	4.9081%
10	LM3	4.5124%	6.0560%	3.7351%
10	LM4	0.2557%	-3.5524%	-1.3865%

Also recall that the linking methods recluster the medoids. For many of the datasets, a linking method used with ten folds will, with respect to quality, outperform [those using] five folds. These issues were explored by examining the results from the MRI017R and PLK02 datasets (Table 6.12).

As mentioned above, one might expect a degradation in quality between five and ten folds. This is true for LM2 and LM3 over both MRI017R and PL02. The $DQ\,J_m\%$ and $CC\%$ metric values are worse for ten folds than for five folds, over both datasets.

The opposite is true for LM1 and LM4. Increasing the number of folds from five to ten improved the values of the quality metrics. How can reducing the sample size improve quality?

The sample size in the context of LM1 and LM4 is not the same as that in the context of algorithms like rseFCM or eFFCM. DFCMdd distributes the data into folds, so 100% of the data is still clustered. The medoids from each fold represent the best solution for that subset of the data. When combined into the medoid dataset, they are clustered a second time with FCMdd.

FCMdd, unlike HCM and FCM, returns as a clustering solution a set of data objects (medoids), as opposed to a set of cluster centers. When DFCMdd has more folds, there are more data objects in the medoid dataset from which to choose for the final set of medoids. It is also important to note that the data objects in the medoid dataset were previously chosen as medoids by one of the folds. These medoids will be more likely than some random data object in the dataset to be good choice for a final medoid.

So in the case of MRI017R and PLK02, increasing the number of folds to ten gives the linking methods 30 vs. 15, or 40 vs. 20, medoids from which to choose the final set of medoids.

As mentioned previously, LM2 and LM3 have improved quality with five folds. This makes sense, considering how Single Linkage functions. If the medoid dataset only has a few data objects to cluster, it will be less likely to experience any chaining. This increases the odds that Single Linkage will generate a good partition of the dataset. Once the dataset has been partitioned, the data object least dissimilar to all other objects in its cluster is chosen as medoid. Assuming the number of objects in each cluster is equal, with five folds, the best choice out of five medoids is selected.

One might expect improved results with ten folds, but increasing the number of folds increases the size of the medoids dataset, thereby increasing the possibility that chaining will occur. Over 30 trials, if only a few trials experience chaining, then this will significantly affect the results.

This was observed in the raw results for MRI017R. With LM2 and five folds, the value for J_m over 30 trials was in a narrow range (761-766). When the folds were increased to ten, the value for J_m stayed in this narrow range in 25 of the trials. In the remaining 5 trials, the value for J_m jumped about 33%.

The J_m changing by 33% in 5 of the trials created a noticeable change in $DQ\,J_m\%$. For MRI017R with LM2 and five folds, $DQ\,J_m\% = -0.0483\%$. With ten folds, $DQ\,J_m\% = 5.3558\%$.

Table 6.12: Quality Results for PLK02

Folds	Linking Method	$DQ\,Jm\%$	Intra $CC\%$ diff	Inter $CC\%$ diff
5	LM1	2.6307%	10.7865%	10.2732%
5	LM2	-0.1431%	1.9762%	5.5162%
5	LM3	-0.1569%	1.9774%	5.5248%
5	LM4	-0.5432%	-0.1530%	2.3465%
10	LM1	0.6410%	3.3536%	4.4723%
10	LM2	4.3229%	11.2393%	14.4288%
10	LM3	0.2100%	3.6822%	5.6107%
10	LM4	-1.6169%	-7.1887%	0.9390%

Chapter 7: Accelerating FN-DBSCAN

"If the world were perfect, it wouldn't be." - Lawrence "Yogi" Berra [2]

7.1 Accelerating a Density-Based Algorithm

The strategy of breaking a dataset into subsets can also be used to accelerate FN-DBSCAN. The Accelerated FN-DBSCAN algorithm (AFN-DBSCAN) borrows from OFCM, DBDC, and SDBDC [65] [74] [75]. In the OFCM algorithm, the fuzzy centroids retained from clustering each subset represent the density of the dataset up to that point of the processing. The DBDC and SDBDC algorithms do not fully leverage this idea, instead choosing the discrete values for "covering points" and "covering radius" as a proxy for density.[9]

One clever idea from DBDC is the retention of a set of data objects not within ε distance of each other, in order to sample the data evenly. This is a powerful idea, which is used in AFN-DBSCAN.

The AFN-DBSCAN algorithm combines these two ideas by breaking the dataset into subsets, and by retaining weighted data objects to represent samples of the density in each subset. The representative data objects from each subset are combined, and a weighted version of FN-DBSCAN (WFN-DBSCAN) clusters that set of representative data objects. A final extension step assigns all data objects from the original dataset to clusters. AFN-DBSCAN is formally presented as Algorithm 10.

A significant departure from previous work in accelerating DBSCAN [74] [75] is that $MinCard$ is not defined as an integer, but as a real number. There is no reason for the minimum cardinality

[9]Some of the material in this chapter has been previously published by me [21] and is re-used under terms of the copyright © 2010 IEEE. The name of the algorithm was changed to conform with the rest of this work. New material and analysis has been added.

of a fuzzy set to be restricted to an integer, and it was found in the course of experimentation that for low density clusters, a real value for $MinCard$ improved performance.

Algorithm 10: Accelerated FN-DBSCAN

Input: X, ε, $MinCard$, μ, f
Break X into f equal sized subsets, $X[k] : 1 \leq k \leq f$. Randomly assign each $x_i \in X$ to a subset.
$MaxRetained = \frac{n}{f^2}$
for all $X[k] \subset X$ **do**
    Calculate $FSCard(x_i)$ (Equation 2.13) $\forall i \in X[k]$
    Add tuple $(x_i, FSCard(x_i))$ to $RetainedList_k$ where $FSCard(x_i)$ is the maximum in $X[k]$
    while $|RetainedList_k| < MaxRetained$ **do**
        Add tuple $(x_i, FSCard(x_i))$ to $RetainedList_k$ where $FSCard(x_i)$ is the maximum in $X[k]$ not within ε distance of $x_j \in RetainedList_k$
    end while
end for
Combine all tuples from $RetainedList_k : 1 \leq k \leq f$ into the combined weighted dataset, W. Each $FSCard(x_i)$ value in a tuple serves as the weight, w_i.
Cluster W with WFN-DBSCAN using ε and $MinCard$.
Obtain set of "core points" from WFN-DBSCAN.
Assign clusters to all data objects $x_i \in X$ using the set of "core points".

where:
X is a dataset consisting of n data objects.
ε is a distance.
$MinCard$ is a real number.
μ is the fuzzy neighborhood function.
f is the number of subsets.
$FSCard(x_i)$ is the local density at a data object.

The WFN-DBSCAN algorithm is identical to FN-DBSCAN except for one detail. Instead of $FSCard(x_i)$, the density at each data object is calculated with $wFSCard(x_i)$:

$$wFSCard(x_i) = \sum_{j=1}^{n} w_i \, \mu(x_i, x_j) \tag{7.1}$$

where:

X is a dataset consisting of n data objects.

w_i is the weight of x_i.

μ is the fuzzy neighborhood function.

The average runtime complexity for DBSCAN and FN-DBSCAN is $O(n^2)$ with respect to the number of data objects [24]. As the strategy to accelerate the algorithm is equivalent to that used for DFCMdd, the runtime complexity analysis is the same (Section 6.1.3). Intuitively, the speedup should be proportional to the number of subsets.

7.2 Experiments

The AFN-DBSCAN algorithm's speed and performance were tested against FN-DBSCAN's on six real world datasets from the UCI repository (Chapter 3). The FN-DBSCAN algorithm is deterministic, if the order of the data objects does not change. AFN-DBSCAN produces different results, depending on how the dataset is divided into subsets. Each experiment consisted of 30 trials of AFN-DBSCAN, each with a different subset composition.

To calculate the speedup (SU), AFN-DBSCAN's runtime was averaged over 30 trials and compared to the runtime of FN-DBSCAN. AFN-DBSCAN's fidelity to FN-DBSCAN was measured by the average $CC\%$ from the results of FN-DBSCAN for the same dataset. The clusters were aligned visually.

Wherever feasible, each dataset was broken into 6 subsets for clustering. For small datasets, this was unrealistic. I set a minimum threshold of 70 data objects per subset, and that resulted in two datasets having fewer than 6 subsets.

One difficulty in comparing AFN-DBSCAN and FN-DBSCAN is the setting of the parameter $MinCard$. Using the same setting for $MinCard$ for both algorithms caused AFN-DBSCAN to have relatively inferior performance. While the representative data objects used by AFN-DBSCAN were weighted, the actual spatial orientation of the representative data objects was lost. The need to compensate for the loss of spatial orientation was discussed in the development of DBDC and

SDBDC [74] [75]. The strategy used in experimentation was to select $MinCard$ for FN-DBSCAN and to use a reduced value, $rMinCard$, for AFN-DBSCAN. This issue is fully discussed in Section 7.4.1.

Proper setting of parameters was challenging. The parameters were tuned by hand for FN-DBSCAN to ensure that clusters were created when using the entire dataset. As a result, each dataset had a different set of parameters. These are listed in Table 7.1. The linear membership function was used for all experiments.

Table 7.1: AFN-DBSCAN Parameters

Dataset	ε	$MinCard$	$rMinCard$
Breast Cancer-W	0.16	6	2.15
Heart-Statlog	0.30	8	2.60
Iris	0.20	6	2.15
Pendigits-015	0.1666	4	1.68
Letters-AY	0.15	28	6.46
Vote	0.45	6	2.15

7.3 Results

Results are shown in Table 7.2. Speedup varied from 2.91 to 4.70. The $CC\%$ varied from 0.37% to 21.56%. The largest dataset, Pendigits015, was used to study how speedup and $CC\%$ varied as the number of subsets changed. An additional series of experiments clustered the Pendigits015 dataset with 6, 8, 10, 12, and 16 subsets. Table 7.3 shows how the speedup and $CC\%$ increased with the number of subsets.

The fidelity of the clustering to FN-DBSCAN, as measured by $CC\%$, varied between 0.75% to 21.56%. The cause of this large degree of difference is discussed in Sections 7.4.1 and 7.4.2.

7.4 Discussion

This algorithm had unique challenges due to its dependance on density. Many of the datasets clustered by AFN-DBSCAN had very "sparse" density, i.e., a relatively low ratio of data objects to features. When a sparse dataset is broken into subsets, the distances between data objects are so

Table 7.2: AFN-DBSCAN Results

Dataset	Subsets	SU	$CC\%$
Breast Cancer-W	6	4.70	1.36%
Heart Statlog	3	2.91	21.56%
Iris	2	4.60	0.37%
Pendigits-015	6	3.79	0.75%
Letters-AY	6	4.03	5.25%
Vote	6	4.15	15.40%

Speedup and CC% compared to FN-DBSCAN over full dataset.

Table 7.3: AFN-DBSCAN Pendigits Results

Dataset	Subsets	SU	$CC\%$
Pendigits-015	6	3.79	0.75%
Pendigits-015	8	4.20	0.62%
Pendigits-015	10	5.09	3.60%
Pendigits-015	12	6.03	14.88%
Pendigits-015	16	7.92	27.15%

Speedup and CC% compared to FN-DBSCAN over full dataset.

great on average that, for many initial settings of ε, the fuzzy set cardinalities of all data objects equal unity. This was observed during experimentation.

"Core points" are defined by specifying a minimum density with the parameters $MinCard$ and ε. Each fold of AFN-DBSCAN selects representative data objects for a final clustering, but does not actually cluster each fold. AFN-DBSCAN's selection of representative objects distinguishes it from earlier accelerated algorithms such as DBDC [74], and is a similarity between it and SDBDC [75].

A difference between SDBDC and AFN-DBSCAN is the fact that SDBDC is not built on a fuzzy clustering algorithm and could not fully capitalize on its use of a fuzzy measure for data object weights. Additionally, SDBSCAN's use of the "crisp" DBSCAN algorithm would require any density relaxation technique based on $MinPts$ to use a whole number density threshold, and to have thereby a very coarse measure of precision. This fact forced the use of a density relaxation technique based on extending the real-valued ε and a subsequently heavier burden of calculation and accounting.

AFN-DBSCAN samples the search space to the greatest extent possible. Only the least dense portions of the search space are not represented. This was verified during implementation; in some subsets, it was not possible to add $MaxRetained$ tuples to $RetainedList$. Fewer data objects were capable of covering all the data objects in the subset.

7.4.1 Reducing $MinCard$

The parameters $MinCard$ and ε must be tuned for each dataset. There is a technique described in [24] that works well on the crisp version of DBSCAN, but no similar technique has been developed for FN-DBSCAN. As a result, the parameters were set via trial and error using FN-DBSCAN. It was discovered that using the same measure for $MinCard$ with both FN-DBSCAN and AFN-DBSCAN resulted in dissimilar clusters. I solved this problem by reducing the setting for $MinCard$ with AFN-DBSCAN.

Reduction of $MinCard$ was found to improve the concurrence of cluster assignments between AFN-DBSCAN and FN-DBSCAN. This is a concept similar to extending ε in DBDC and SDBDC [74] [75]. Both increasing ε and reducing $MinCard$ have the effect of lowering the density requirements for cluster formation.

While this issue has nothing to do with either FN-DBSCAN or AFN-DBSCAN, it must addressed in order to compare the two algorithms experimentally.

Density requirements must be relaxed for the accelerated algorithms that use weighted representative objects. These data objects represent many others through their weights, but the actual locations of the represented data objects are lost. This loss of data makes the model cruder and requires compensation.

The location of the original data objects is helpful to link representative objects together and to create larger clusters. Loss of this spatial orientation makes cluster discovery less likely. The strategy of increasing ε makes it more likely that a representative object will discover an adjacent representative object. The disadvantage is the assumption that the adjacent representative object actually will represent any data objects within the original ε distance. For datasets where clusters have a small buffer between them, to increase ε may result in improperly combined clusters.

For the purpose of comparing AFN-DBSCAN with FN-DBSCAN, the other route was taken: to reduce $MinCard$.

The amount of reduction to $MinCard$ must compensate for the spatial orientation lost from the data objects which are covered by the much smaller set of representative objects. The dataset is broken into f subsets, so the average amount of spatial information lost in each subset is $\frac{f-1}{f}$. The density estimates at each representative object, however, are accurate for that subset and a small chance exists that this estimate is accurate for the whole dataset. It is also possible that a particular representative object will play no role in cluster formation.

This suggests that, for each representative data object, the amount of spatial information that needs to be compensated for will be somewhere between 0 and some constant divided by the number of subsets. The best solution for a particular application is to tailor the setting of $rMinCard$ to the individual dataset. For experimentation, consistency was preferred, so the following formula was used:

$$rMinCard = \frac{MinCard}{ln(f) + 1} \tag{7.2}$$

Equation 7.2 was hard-coded in software and worked well on many of the datasets tested. On the ones it did not work well on, the results were revealing (see Section 7.4.2).

A disadvantage in reducing $MinCard$ is the fact that this technique depends on a uniform distribution of representative objects across subsets. This is not a serious issue, however, because reducing $MinCard$ is only necessary to compare AFN-DBSCAN to the reference algorithm, FN-DBSCAN.

7.4.2 Cluster Splitting and Aggregation

Splitting of clusters occurred for all datasets. AFN-DBSCAN occasionally split into two or more clusters those clusters consisting of mostly one class that were found successfully by FN-DBSCAN. This is likely an effect of the assignment of data objects to subsets. If an irregularly shaped cluster were connected by a single data object, the omission of that data object in *RetainedList* would split the cluster into two.

Splitting is most likely to occur for datasets with very sparse density; i.e., datasets with a low number of data objects and a large number of features. In the case of Pendigits-015 and Letters-AY, the data described handwritten characters. Here, the splitting into multiple clusters might be an inadvertent differentiation between slightly different styles of writing the same character.

Splitting occurred in a small percentage ($< 15\%$) of trials in the experiments. When splitting occurred, only the largest split cluster was counted when calculating $CC\%$. The smaller clusters were considered noise. It would have been possible to recombine sub-clusters manually for the experimental results, but this was not done. Had this step been performed, $CC\%$ would have fallen for all datasets.

The percentage of trials where splitting occurred was not uniform across the datasets. The Heart-Statlog dataset had splitting occur in 60% of its trials. The splitting affected the results profoundly; its $CC\% = 21.56\%$ which was the highest any dataset. Note that Heart-Statlog has 13 features, but only 270 data objects.

Aggregation of clusters, i.e., multiple clusters in FN-DBSCAN combined into one by AFN-DBSCAN, happened less frequently than splitting. Only the Heart Statlog, Letters-AY, and Vote datasets had aggregated clusters. Aggregation appeared to be caused by the density relaxation, i.e., the reduction of $MinCard$. When $MinCard$ was not adjusted, aggregation did not occur.

The Vote dataset was the most impacted by aggregation; it occurred in 17% of its trials. As a result of aggregation, Vote's $CC\% = 15.40\%$. If trials where aggregation occurred were omitted from the results, the $CC\%$ would have been 7.29%. This dataset was impacted by splitting as well, which occurred in (a different) 17% of its trials.

7.4.3 Selecting the Number of Subsets

One decision that was made before using AFN-DBSCAN for experiments was the selection of the number of subsets. For a real-world application where the data is geographically distributed, this decision can be implicit, but it is still useful to demonstrate how speed and fidelity vary with the number of subsets.

A small experiment was conducted using the Pendigits-015 dataset and five different subset settings. The results are shown in Table 7.3. As expected from the runtime complexity, the speedup improved as the number of subsets increased.

However, the fidelity to FN-DBSCAN, as measured by $CC\%$, quickly degraded as the number of subsets increased. While increasing from 6 to 8 subsets, slightly improved the fidelity, it degraded when the number of subsets were 10 or greater.

The causes were splitting and noise. As explained in Section 7.4.2, as the number of subsets increased, the spatial locations of data objects needed to join clusters were lost. This resulted in increased splitting. When the number of subsets were set to 10, 13% of the trials experienced splitting. When the number of subsets increased to 12, 77% of the trials experienced splitting and when the number of subsets equalled 16, 100% of the clusters were split.

As explained above, a harsh criterion was used for calculating $CC\%$. Only the largest cluster was counted. Had all majority clusters for a class been counted, the reported fidelity to FN-DBSCAN would have improved.

Changing the calculation of CC% would not have helped the second issue: noise. The loss of spatial information when the subsets were 10 or greater also increased the amount of noise in each trial. When the number of subsets was set to 10, 1.45% of the CC% of 3.60% was attributable to noise. When the number of subsets increased to 12, 2.37% of the CC% of 14.88% was attributable to noise, and when the number of subsets was set to 16, 3.95% of the CC% of 27.15% was attributable to noise.

For this particular dataset, noise % did increase with the number of subsets, but cluster splitting had a much greater effect.

7.4.4 Conclusions

The application of representative objects to accelerate a density-based algorithm has challenges that do not exist for algorithms that reduce an objective function. Spatial information is lost when representative objects are chosen and the location of the missing objects is often critical for proper clustering.

In the case of the DBSCAN family of algorithms, the density is defined by the parameters ε and $MinCard$. A difficulty was identified when a strategy was developed to compare the partitions of FN-DBSCAN and AFN-DBSCAN. Recall that the parameters were originally tuned to FN-DBSCAN, but using the same value for $MinCard$ (assuming ε is kept constant) for FN-DBSCAN and AFN-DBSCAN resulted in dissimilar partitions.

Clearly, different tuning measures are needed for AFN-DBSCAN than FN-DBSCAN. $MinCard$, of course could have been hand-tuned for each dataset. Instead, a simple formula that generated $rMinCard$ from $MinCard$ was consistently used in order to study this difficulty.

This formula worked well for many of the datasets, but not for others. The Heart-Statlog and Vote datasets showed poor fidelity to FN-DBSCAN when clustered by AFN-DBSCAN, when the simple formula was used to generate $rMinCard$. This led to the discovery that improper selection of $rMincard$ for AFN-DBSCAN can lead to splitting or aggregation. If all other factors are kept equal, the intrinsic structure of a dataset plays a factor in fidelity to FN-DBSCAN as measured by $CC\%$.

Datasets often have sparse density, and breaking the dataset into subsets exacerbates the sparseness. Additional experiments with Pendigits015, demonstrated the effects of increased sparseness as the number of subsets was increased. There were increased instances of cluster splitting and an increase in data objects improperly assigned the "noise" label.

This suggests that compensating for the loss of spatial information cannot be achieved by the use of representative objects alone. A high-fidelity accelerated density-based algorithm must capture key elements of cluster structure beyond that which is inferred by the representative objects. This is an area for future research.

Chapter 8: Summary and Conclusions

"It ain't over 'til it's over." - - Lawrence "Yogi" Berra [2]

8.1 Summary

In this dissertation, I explored the key algorithm design principles that accelerate fuzzy clustering algorithms while preserving quality and fidelity to the original algorithm. My research led to the following contributions:

- Identification of a statistical method never before used with accelerated fuzzy clustering algorithms. This method estimates the minimum sample size required to represent each cluster proportionally. I modified the statistical formula to make it compatible with clustering algorithms.

  The issue of how to estimate the sample size has rarely been addressed in relevant literature. Thompson's method estimates the minimum sample size to proportionally represent a population within an absolute range of values. I demonstrated that in the context of clustering algorithms, the use of an absolute value is cumbersome. I adjusted the equation to use a relative difference in proportion.

- Creation of an early stopping criterion for incremental or "single pass" algorithms. This criterion determines the point at which processing additional data will have little added benefit. This allows the clustering algorithm to terminate early, providing a greater speedup with little loss in quality.

  In the domain of classification models, the idea of incrementally processing a dataset is well-known. The accuracy of the classification model is the obvious stopping criterion, allowing a

model to be created in a shorter amount of time. A similar method for incremental clustering was not possible, as no analogous stopping criterion existed. I explored a large set of viable alternative stopping criteria and discovered that one based on the change in cluster center position worked best.

- Different methods of combining representative objects were explored using fuzzy clustering algorithms which produce partitions by minimizing an objective function. I discovered that the best method used information inherent from the intermediate results to improve quality and speedup.

  Four different methods to combine representative objects for FCMdd clustering were explored. The method that had the best performance on real-world datasets used the medoids from one of the subsets as an initialization for a subsequent clustering by FCMdd.

- I developed a new method to combine representative objects in the context of density-based fuzzy clustering algorithms. The criteria to join representative objects is a user-defined, real-valued minimum fuzzy cardinality.

  Density-based clustering algorithms, have difficulty clustering subsets because the threshold density will differ between the subsets and full dataset. In the context of accelerated fuzzy neighborhood density-based clustering, I avoid the entire issue by retaining the densest set of representative objects that minimize overlap. Experimentation led to the discovery that the intrinsic structure of the dataset played a large factor in the accelerated algorithm's fidelity to the base algorithm.

- I created five original algorithms that apply these contributions and the four main ideas listed above.

  Thompson's method estimates the minimum sample size for GOFCM and MSERFCM. Both algorithms reduce runtime and minimize quality loss in comparison to the algorithms on which they were based. GOFCM and MODSPFCM use the early stopping criterion to reduce runtime while minimizing loss of quality. GOFCM, MODSPFCM, DFCMdd, and AFN-

DBSCAN all use representative objects to reduce runtime. This technique minimizes quality loss, and occasionally improves the quality of results. AFN-DBSCAN implements a new method to combine representative objects from a density-based clustering algorithm.

My original research on these subjects was published in two conference papers and two journal papers [21] [22] [55] [23]. A disk with the source code developed for all research is included in Appendix A.

8.2 Conclusions

This research is important, because clustering is a primary technique used in data analysis. The vast amounts of Big Data available contain valuable information and insights. Such a huge quantity of data cannot be clustered with traditional, basic methods. Accelerated clustering methods are therefore needed. Fuzzy clustering is a valuable tool to the data analyst and should be incorporated into clustering solutions.

The first step of the research was to study how existing accelerated fuzzy clustering methods work. In addition to reviewing existing published research, I conducted a series of experiments where I compared four accelerated fuzzy clustering algorithms to FCM. The experiments identified the following principles:

1. Use of a statistically significant sample of the dataset reduces runtime while preserving quality.

2. An algorithm designed to cluster the data incrementally can produce a high-quality result when stopped before all data has been processed. This is especially true when the data is presented in random order.

3. The use of representative objects, either weighted or un-weighted, can overcome difficulties of scale, if properly utilized.

4. For a particular class of clustering algorithms, providing a "starting point" close to the optimal solution reduces runtime and can improve quality.

These design principles, present in existing algorithms, were already well-known. The significance of my experiments and the published results [22] was that such a comparative analysis of FCM-based accelerated methods had not been previously published.[10] Most published work is limited to a single accelerated clustering method. Surveys on clustering methods typically do not focus on accelerated methods [3] [112] [113], making it infrequent, if not unlikely, that all of these principles were discussed in print simultaneously.

These design principles served as a nucleus for the study of how existing accelerated fuzzy clustering algorithms could be improved further. In the course of my research, most of the algorithms encountered used only one of these aforementioned principles. There is power in using multiple design principles in tandem.

Thompson's method of estimating a minimum sample size was useful in the context of GOFCM, MSERFCM, and MODSPFCM where a single sample is relevant. The sample size must at least proportionally represent the data to yield useful results. This is true if an estimate is needed either for initialization or the final results.

These algorithms combined the use of a minimum, estimated sample size as well as some combination of weighted representative objects, improved starting positions, and early termination criterion. It was clearly shown that a combined approach outperformed related algorithms.

For algorithms such as OFCM and DFCMdd, the proportionality of the sample is less relevant because the information inherent in the results from each PDA (or fold) is reused in order to obtain a final clustering solution. Paradoxically, DFCMdd's results showed that, on real-world data, a smaller sample size for folds yielded faster clustering and higher quality.

Representative objects must be used in an intelligent fashion. With OFCM, I demonstrated that using representative objects as an initialization can result in poorer performance, if the sample from which they were derived does not proportionally represent the whole dataset. I used this concept to implement acceleration strategies successfully for FCMdd.

The need to accelerate fuzzy clustering algorithms for Big Data motivated the identification of these design principles and my contributions. In truth, I only scratched the surface of the potential

[10]Formal publication of my comparative analysis [22] preceded Havens' [16] by six months, though the research was performed independently, at roughly the same time.

of these principles and contributions. The research presented in this dissertation can be continued in a number of ways.

Reducing the fold size for DFCMdd was shown to improve speedup and quality for two of the linking methods. I strongly suspect that this is only true over some range of fold sizes and other factors. This is clearly an area for future study for ways to intelligently use representative objects in DFCMdd, OFCM, and AFN-DBSCAN.

Weights were used for representative objects in GOFCM, MSERFCM, MODSPFCM and AFN-DBSCAN, but not DFCMdd. A version of DFCMdd can be created with weighted medoids and the performance between the two versions can be compared. Weights were shown to have advantages, but also disadvantages in that they can skew results and not account for spatial information. This was especially true for AFN-DBSCAN. An alternative means of compensating for loss of spatial information is a future area of study.

The early stopping criterion can be applied to other clustering algorithms. Development of a stopping criterion for relational data would make possible relational versions of GOFCM and MODSPFCM. A relational version of MSERFCM could also be created with the contributions in this dissertation.

This dissertation shows that the intelligent use of multiple design principles can accelerate fuzzy clustering algorithms with minimal quality loss. With the principles identified and my original contributions, I see the potential for the creation of many more useful clustering methods.

References

[1] Y. Berra, *You Can Observe a Lot by Watching.* John Wiley and Sons, 2008.

[2] ——, *The Yogi Book:" I Really Didn't Say Everything I Said".* Workman Publishing, 1998.

[3] A. K. Jain, "Data clustering: A review," *ACM Computing Surveys (CSUR)*, vol. 31, no. 3, pp. 264–323, September 1999.

[4] V. Estivill-Castro, "Why so many clustering algorithms: a position paper," *ACM SIGKDD Explorations Newsletter*, vol. 4, no. 1, pp. 65–75, 2002.

[5] A. K. Jain, "Data clustering: 50 years beyond k-means," *Pattern Recognition Letters*, vol. 31, no. 8, pp. 651–666, June 2010.

[6] A. S. Das, M. Datar, A. Garg, and S. Rajaram, "Google news personalization: scalable online collaborative filtering," in *Proceedings of the 16th international conference on World Wide Web.* ACM, 2007, pp. 271–280.

[7] J. C. Russ, *The image processing handbook.* CRC press, 2011.

[8] R. N. Kostoff, M. B. Briggs, J. L. Solka, and R. L. Rushenberg, "Literature-related discovery (lrd): Methodology," *Technological Forecasting and Social Change*, vol. 75, no. 2, pp. 186–202, 2008.

[9] G. Punj and D. W. Stewart, "Cluster analysis in marketing research: review and suggestions for application," *Journal of marketing research*, pp. 134–148, 1983.

[10] M. B. Eisen, P. T. Spellman, P. O. Brown, and D. Botstein, "Cluster analysis and display of genome-wide expression patterns," *Proceedings of the National Academy of Sciences*, vol. 95, no. 25, pp. 14 863–14 868, 1998.

[11] P. Hore, L. O. Hall, D. B. Goldgof, Y. Gu, A. A. Maudsley, and A. Darkazanli, "A scalable framework for segmenting magnetic resonance images," *Journal of signal processing systems*, vol. 54, no. 1-3, pp. 183–203, 2009.

[12] M. Benigni and R. Furrer, "Periodic spatio-temporal improvised explosive device attack pattern analysis," Technical report, Golden, CO, Tech. Rep., 2008.

[13] M. Nikravesh, "Soft computing for reservoir characterization and management," in *Granular Computing, 2005 IEEE International Conference on*, vol. 2. IEEE, 2005, pp. 593–598.

[14] D. B. Henry, P. H. Tolan, and D. Gorman-Smith, "Cluster analysis in family psychology research." *Journal of Family Psychology*, vol. 19, no. 1, p. 121, 2005.

[15] P. Huber, "Massive data sets workshop: The morning after."

[16] T. C. Havens, J. C. Bezdek, C. Leckie, L. O. Hall, and M. Palaniswami, "Fuzzy c-means algorithms for very large data," *IEEE Trans. Fuzzy Systems*, vol. 20, no. 6, pp. 1130–1146, December 2012.

[17] S. Lohr, "The age of big data," *New York Times*, vol. 11, 2012.

[18] S. Madden, "From databases to big data," *Internet Computing, IEEE*, vol. 16, no. 3, pp. 4–6, 2012.

[19] A. Jacobs, "The pathologies of big data," *Communications of the ACM*, vol. 52, no. 8, pp. 36–44, 2009.

[20] B. Ratner, *Statistical and machine-learning data mining: techniques for better predictive modeling and analysis of big data*. CRC Press, 2011.

[21] J. K. Parker, L. O. Hall, and A. Kandel, "Scalable fuzzy neighborhood dbscan," in *Fuzzy Systems (FUZZ-IEEE), 2010 IEEE International Conference on*. IEEE, 2010, pp. 1–8.

[22] J. K. Parker, L. O. Hall, and J. C. Bezdek, "Comparison of scalable fuzzy clustering methods," in *Fuzzy Systems (FUZZ-IEEE), 2012 IEEE International Conference on*. IEEE, 2012, pp. 1–9.

[23] J. K. Parker and L. O. Hall, "Accelerating fuzzy c means using an estimated subsample size," *Fuzzy Systems, IEEE Transactions on*, 2013.

[24] M. Ester, H.-P. Kriegel, J. Sander, and X. Xu, "A density-based algorithm for discovering clusters in large spatial databases with noise." Kdd, 1996.

[25] R. Sibson, "Slink: an optimally efficient algorithm for the single-link cluster method," *The Computer Journal*, vol. 16, no. 1, pp. 30–34, 1973.

[26] N. Jardine and R. Sibson, "The construction of hierarchic and non-hierarchic classifications," *The Computer Journal*, vol. 11, no. 2, pp. 177–184, 1968.

[27] C. D. Manning, P. Raghavan, and H. Schütze, *Introduction to information retrieval*. Cambridge University Press Cambridge, 2008, vol. 1.

[28] L. Kaufman and P. J. Rousseeuw, *Finding Groups in Data: An Introduction to Cluster Analysis*. Wiley-Interscience, 1990.

[29] Y. Loewenstein, E. Portugaly, M. Fromer, and M. Linial, "Efficient algorithms for accurate hierarchical clustering of huge datasets: tackling the entire protein space," *Bioinformatics*, vol. 24, no. 13, pp. i41–i49, 2008.

[30] J. MacQueen *et al.*, "Some methods for classification and analysis of multivariate observations," in *Proceedings of the fifth Berkeley symposium on mathematical statistics and probability*, vol. 1, no. 281-297. California, USA, 1967, p. 14.

[31] S. Lloyd, "Least squares quantization in pcm," *Information Theory, IEEE Transactions on*, vol. 28, no. 2, pp. 129–137, 1982.

[32] J. C. Bezdek, R. Ehrlich, and W. Full, "Fcm: The fuzzy c-means clustering algorithm," *Computers & Geosciences*, vol. 10, no. 2, pp. 191–203, 1984.

[33] R. O. Duda, P. E. Hart, and D. G. Stork, *Pattern classification*. John Wiley & Sons, 2001.

[34] D. Aloise, A. Deshpande, P. Hansen, and P. Popat, "Np-hardness of euclidean sum-of-squares clustering," *Machine Learning*, vol. 75, no. 2, pp. 245–248, 2009.

[35] J. C. Bezdek and R. J. Hathaway, "Some notes on alternating optimization," in *Advances in Soft ComputingAFSS 2002*. Springer, 2002, pp. 288–300.

[36] M. Matteucci, "A tutorial on clustering algorithms, clustering k-means demo," http://home.deib.polimi.it/matteucc/Clustering/tutorial_html/AppletKM.html, accessed: 2013-07-06.

[37] R. A. Jarvis and E. A. Patrick, "Clustering using a similarity measure based on shared near neighbors," *Computers, IEEE Transactions on*, vol. 100, no. 11, pp. 1025–1034, 1973.

[38] E. Parzen, "On estimation of a probability density function and mode," *The annals of mathematical statistics*, vol. 33, no. 3, pp. 1065–1076, 1962.

[39] N. Beckmann, H.-P. Kriegel, R. Schneider, and B. Seeger, "The r*-tree: an efficient and robust access method for points and rectangles," in *INTERNATIONAL CONFERENCE ON MANAGEMENT OF DATA*. Citeseer, 1990.

[40] A. Kandel and W. Byatt, "Fuzzy sets, fuzzy algebra, and fuzzy statistics," *Proceedings of the IEEE*, vol. 66, no. 12, pp. 1619–1639, 1978.

[41] J. C. Bezdek, *Pattern Recognition with Fuzzy Objective Function Algorithms*. Plenum Press, 1981.

[42] I. Gath and A. B. Geva, "Unsupervised optimal fuzzy clustering," *Pattern Analysis and Machine Intelligence, IEEE Transactions on*, vol. 11, no. 7, pp. 773–780, 1989.

[43] Z. Huang and M. K. Ng, "A fuzzy k-modes algorithm for clustering categorical data," *Fuzzy Systems, IEEE Transactions on*, vol. 7, no. 4, pp. 446–452, 1999.

[44] R. Krishnapuram, A. Joshi, and L. Yi, "A fuzzy relative of the k-medoids algorithm with application to web document and snippet clustering," in *Fuzzy Systems Conference Proceedings, 1999. FUZZ-IEEE'99. 1999 IEEE International*, vol. 3. IEEE, 1999, pp. 1281–1286.

[45] E. N. Nasibov and G. Ulutagay, "Robustness of density-based clustering methods with various neighborhood relations," *Fuzzy Sets and Systems*, vol. 160, no. 24, pp. 3601–3615, 2009.

[46] P. Hore, L. O. Hall, and D. B. Goldgof, "Single pass fuzzy c means," in *IEEE International Conference on Fuzzy Systems*. FUZZ-IEEE, July 2007, pp. 1–7.

[47] J. Kolen and T. Hutcheson, "Reducing the time complexity of the fuzzy c-means algorithm," *Fuzzy Systems, IEEE Transactions on*, vol. 10, no. 2, pp. 263 –267, apr 2002.

[48] R. J. Hathaway, J. W. Davenport, and J. C. Bezdek, "Relational duals of the c-means clustering algorithms," *Pattern recognition*, vol. 22, no. 2, pp. 205–212, 1989.

[49] R. J. Hathaway and J. C. Bezdek, "Nerf c-means: Non-euclidean relational fuzzy clustering," *Pattern recognition*, vol. 27, no. 3, pp. 429–437, 1994.

[50] V. V. Vazirani, *Approximation algorithms*. springer, 2001.

[51] J. Han, M. Kamber, and J. Pei, *Data mining: concepts and techniques*. Morgan kaufmann, 2006.

[52] R. Krishnapuram, A. Joshi, O. Nasraoui, and L. Yi, "Low-complexity fuzzy relational clustering algorithms for web mining," *Fuzzy Systems, IEEE Transactions on*, vol. 9, no. 4, pp. 595–607, 2001.

[53] K. S. Fu and J. E. Albus, *Syntactic pattern recognition and applications*. Prentice-Hall Englewood Cliffs, NJ, 1982, vol. 4.

[54] N. Labroche, "New incremental fuzzy c medoids clustering algorithms," in *Fuzzy Information Processing Society (NAFIPS), 2010 Annual Meeting of the North American*. IEEE, 2010, pp. 1–6.

[55] J. K. Parker and J. A. Downs, "Footprint generation using fuzzy-neighborhood clustering," *GeoInformatica*, pp. 1–15, 2013.

[56] E. N. Nasibov and G. Ulutagay, "On cluster analysis based on fuzzy relations between spatial data." in *EUSFLAT Conf.(2)*. Citeseer, 2007, pp. 59–62.

[57] I. Guyon and A. Elisseeff, "An introduction to variable and feature selection," *The Journal of Machine Learning Research*, vol. 3, pp. 1157–1182, 2003.

[58] H. Liu and L. Yu, "Toward integrating feature selection algorithms for classification and clustering," *Knowledge and Data Engineering, IEEE Transactions on*, vol. 17, no. 4, pp. 491–502, 2005.

[59] L. Parsons, E. Haque, and H. Liu, "Subspace clustering for high dimensional data: a review," *ACM SIGKDD Explorations Newsletter*, vol. 6, no. 1, pp. 90–105, 2004.

[60] R. Agrawal, J. Gehrke, D. Gunopulos, and P. Raghavan, "Automatic subspace clustering of high dimensional data," *Data Mining and Knowledge Discovery*, vol. 11, no. 1, pp. 5–33, 2005.

[61] P. S. Bradley and U. M. Fayyad, "Refining initial points for k-means clustering," Microsoft Research, Tech. Rep. MSR-TR-98-36, May 1998.

[62] T. W. Cheng, D. B. Goldgof, and L. O. Hall, "Fast fuzzy clustering," *Fuzzy sets and systems*, vol. 93, no. 1, pp. 49–56, 1998.

[63] D. Altman, "Efficient fuzzy clustering of multi-spectral images," in *Geoscience and Remote Sensing Symposium, 1999. IGARSS'99 Proceedings. IEEE 1999 International*, vol. 3. IEEE, 1999, pp. 1594–1596.

[64] M.-C. Hung and D.-L. Yang, "An efficient fuzzy c-means clustering algorithm," in *Data Mining, 2001. ICDM 2001, Proceedings IEEE International Conference on.* IEEE, 2001, pp. 225–232.

[65] P. Hore, L. Hall, D. Goldgof, and W. Cheng, "Online fuzzy c means," in *Fuzzy Information Processing Society, 2008. NAFIPS 2008. Annual Meeting of the North American.* IEEE, 2008, pp. 1–5.

[66] F. Provost, D. Jensen, and T. Oates, "Efficient progressive sampling," in *Proceedings of the fifth ACM SIGKDD international conference on Knowledge discovery and data mining.* ACM, 1999, pp. 23–32.

[67] P. Domingos, G. Hulten, P. Edu, and C. Edu, "A general method for scaling up machine learning algorithms and its application to clustering," in *In Proceedings of the Eighteenth International Conference on Machine Learning*, 2001.

[68] N. R. Pal and J. C. Bezdek, "Complexity reduction for large image processing," *Systems, Man, and Cybernetics, Part B: Cybernetics, IEEE Transactions on*, vol. 32, no. 5, pp. 598–611, 2002.

[69] L. Wang, J. C. Bezdek, C. Leckie, and R. Kotagiri, "Selective sampling for approximate clustering of very large data sets," *International Journal of Intelligent Systems*, vol. 23, no. 3, pp. 313–331, 2008.

[70] J. C. Bezdek, R. J. Hathaway, J. M. Huband, C. Leckie, and R. Kotagiri, "Approximate clustering in very large relational data," *International journal of intelligent systems*, vol. 21, no. 8, pp. 817–841, 2006.

[71] P. Hore, "Scalable frameworks and algorithms for cluster ensembles and clustering data streams," Ph.D. dissertation, University of South Florida, June 2007.

[72] R. J. Hathaway and J. C. Bezdek, "Extending fuzzy and probabilistic clustering to very large data sets," *Computational Statistics & Data Analysis*, vol. 51, no. 1, pp. 215–234, 2006.

[73] J. C. Bezdek and R. J. Hathaway, "Progressive sampling schemes for approximate clustering in very large data sets," in *Fuzzy Systems, 2004. Proceedings. 2004 IEEE International Conference on*, vol. 1. IEEE, 2004, pp. 15–21.

[74] E. Januzaj, H.-P. Kriegel, and M. Pfeifle, "Dbdc: Density based distributed clustering," in *Advances in Database Technology-EDBT 2004.* Springer, 2004, pp. 88–105.

[75] ——, "Scalable density-based distributed clustering," in *Knowledge Discovery in Databases: PKDD 2004.* Springer, 2004, pp. 231–244.

[76] N. Webster and J. L. McKechnie, *Webster's new universal unabridged dictionary.* Dorset & Baber, 1983.

[77] Y. Gu, L. O. Hall, and D. B. Goldgof, "Evaluating scalable fuzzy clustering," in *Systems Man and Cybernetics (SMC), 2010 IEEE International Conference on.* IEEE, 2010, pp. 873–880.

[78] R. J. Hathaway and J. C. Bezdek, "Optimization of clustering criteria by reformulation," *Fuzzy Systems, IEEE Transactions on*, vol. 3, no. 2, pp. 241–245, 1995.

[79] H. W. Kuhn, "The hungarian method for the assignment problem," *Naval Research Logistics Quarterly*, vol. 2, no. 1-2, pp. 83–97, March 1955.

[80] W. M. Rand, "Objective criteria for the evaluation of clustering methods," *Journal of the American Statistical association*, vol. 66, no. 336, pp. 846–850, 1971.

[81] J. M. Santos and M. Embrechts, "On the use of the adjusted rand index as a metric for evaluating supervised classification," in *Artificial Neural Networks–ICANN 2009*. Springer, 2009, pp. 175–184.

[82] L. Hubert and P. Arabie, "Comparing partitions," *Journal of classification*, vol. 2, no. 1, pp. 193–218, 1985.

[83] J. L. Myers, A. D. Well, and R. F. Lorch, *Research design and statistical analysis*. Routledge, 2010.

[84] R. Walpole and R. Myers, *Probability and Statistics for Engineers and Scientists*. MacMillan Publishing Company, 1985.

[85] S. Samson, T. Hopkins, A. Remsen, L. Langebrake, T. Sutton, and J. Patten, "A system for high-resolution zooplankton imaging," *Oceanic Engineering, IEEE Journal of*, vol. 26, no. 4, pp. 671–676, 2001.

[86] A. Remsen, T. L. Hopkins, and S. Samson, "What you see is not what you catch: a comparison of concurrently collected net, optical plankton counter, and shadowed image particle profiling evaluation recorder data from the northeast gulf of mexico," *Deep Sea Research Part I: Oceanographic Research Papers*, vol. 51, no. 1, pp. 129–151, 2004.

[87] K. A. Kramer, "System for identifying plankton from the sipper instrument platform," Ph.D. dissertation, University of South Florida, 2010.

[88] M. Hall, E. Frank, G. Holmes, B. Pfahringer, P. Reutemann, and I. H. Witten, "The weka data mining software: an update," *ACM SIGKDD Explorations Newsletter*, vol. 11, no. 1, pp. 10–18, 2009.

[89] H. Liu and R. Setiono, "A probabilistic approach to feature selection-a filter solution," in *ICML*, vol. 96. Citeseer, 1996, pp. 319–327.

[90] J. Liang, L. Bai, C. Dang, and F. Cao, "The k-means-type algorithms versus imbalanced data distributions," *IEEE Transactions on Fuzzy Systems*, vol. 20, no. 4, pp. 728–745, 2012.

[91] J. C. Bezdek, R. J. Hathaway, M. J. Sabin, and W. T. Tucker, "Convergence theory for fuzzy c-means: counterexamples and repairs," *Systems, Man and Cybernetics, IEEE Transactions on*, vol. 17, no. 5, pp. 873–877, 1987.

[92] K. Bache and M. Lichman, "UCI machine learning repository," 2013. [Online]. Available: http://archive.ics.uci.edu/ml

[93] W. H. Wolberg and O. L. Mangasarian, "Multisurface method of pattern separation for medical diagnosis applied to breast cytology." *Proceedings of the national academy of sciences*, vol. 87, no. 23, pp. 9193–9196, 1990.

[94] C. Feng, A. Sutherland, R. King, S. Muggleton, and R. Henery, "Comparison of machine learning classifiers to statistics and neural networks," *AI&Statistics-93*, vol. 6, p. 41, 1993.

[95] R. A. Fisher, "The use of multiple measurements in taxonomic problems," *Annals of eugenics*, vol. 7, no. 2, pp. 179–188, 1936.

[96] A. Srinivasan. (1993) Statlog (landsat satellite) data set. Repository. [Online]. Available: http://archive.ics.uci.edu/ml/datasets/Statlog+%28Landsat+Satellite%29

[97] P. W. Frey and D. J. Slate, "Letter recognition using holland-style adaptive classifiers," *Machine Learning*, vol. 6, no. 2, pp. 161–182, 1991.

[98] F. Alimoglu and E. Alpaydin, "Methods of combining multiple classifiers based on different representations for pen-based handwritten digit recognition," in *Proceedings of the Fifth Turkish Artificial Intelligence and Artificial Neural Networks Symposium (TAINN 96)*. Citeseer, June 1996.

[99] J. C. Schlimmer, "Concept acquisition through representational adjustment," Ph.D. dissertation, University of California, Irvine, 1987.

[100] S. Eschrich, J. Ke, L. O. Hall, and D. B. Goldgof, "Fast accurate fuzzy clustering through data reduction," *Fuzzy Systems, IEEE Transactions on*, vol. 11, no. 2, pp. 262–270, 2003.

[101] B. Gu, B. Liu, F. Hu, and H. Liu, "Efficiently determining the starting sample size for progressive sampling," in *Machine Learning: ECML 2001*. Springer, 2001, pp. 192–202.

[102] S. K. Thompson, "Sample size for estimating multinomial proportions," *The American Statistician*, vol. 41, no. 1, pp. 42–46, 1987.

[103] P. Phoungphol and Y. Zhang, "Sample size estimation with high confidence for large scale clustering," in *Proceedings of the 3rd International Conference on Intelligent Computing and Intelligent Systems*, 2011.

[104] C. Meek, B. Thiesson, and D. Heckerman, "The learning-curve sampling method applied to model-based clustering," *The Journal of Machine Learning Research*, vol. 2, pp. 397–418, 2002.

[105] L. O. Hall and D. B. Goldgof, "Convergence of the single-pass and online fuzzy c-means algorithms," *Fuzzy Systems, IEEE Transactions on*, vol. 19, no. 4, pp. 792–794, 2011.

[106] T. C. Havens, private communication, 2012.

[107] L. P. Clarke, R. P. Velthuizen, M. Clark, J. Gaviria, L. O. Hall, D. Goldgof, R. Murtagh, S. Phuphanich, and S. Brem, "Mri measurement of brain tumor response: comparison of visual metric and automatic segmentation," *Magnetic resonance imaging*, vol. 16, no. 3, pp. 271–279, 1998.

[108] M. Emre Celebi, H. A. Kingravi, and P. A. Vela, "A comparative study of efficient initialization methods for the k-means clustering algorithm," *Expert Systems with Applications*, 2012.

[109] A. Strehl and J. Ghosh, "Cluster ensembles—a knowledge reuse framework for combining multiple partitions," *The Journal of Machine Learning Research*, vol. 3, pp. 583–617, 2003.

[110] J. Mei and L. Chen, "Fuzzy clustering with weighted medoids for relational data," *Pattern Recognition*, vol. 43, no. 5, pp. 1964–1974, 2010.

[111] R. P. Duin, M. Loog, E. Pe, kalska, and D. M. Tax, "Feature-based dissimilarity space classification," in *Recognizing Patterns in Signals, Speech, Images and Videos*. Springer, 2010, pp. 46–55.

[112] R. Xu, D. Wunsch *et al.*, "Survey of clustering algorithms," *Neural Networks, IEEE Transactions on*, vol. 16, no. 3, pp. 645–678, 2005.

[113] P. Berkhin, "A survey of clustering data mining techniques," in *Grouping multidimensional data*. Springer, 2006, pp. 25–71.

[114] B. Hoyt. (2011) inih: simple .ini parser in c. Open Source Project. [Online]. Available: http://code.google.com/p/inih/

[115] I. H. Witten and E. Frank, *Data Mining: Practical machine learning tools and techniques*. Morgan Kaufmann, 2005.

[116] B. Reiter and J. Aquino. (2009) Statist 1.4.2. Open Source Project. [Online]. Available: http://wald.intevation.org/projects/statist/

Appendices

Appendix A: Algorithm Implementations

"If you can't imitate him, don't copy him." - Lawrence "Yogi" Berra [2]

A.1 Introduction

Three different codebases were developed to conduct experiments for my research. A disk is provided with this dissertation with all source code and datasets.[11]

A.2 Fuzzy c-means Codebase

The Fuzzy c-means (FCM) codebase includes the implementations of FCM and the following accelerated methods: SPFCM, OFCM, eFFCM, rseFCM, GOFCM, MSERFCM and MODSPFCM. See Chapters 2 and 5 for details on the algorithms. All algorithmic variants used the same weighted FCM implementation, written in C, and were compiled and run in a Linux environment. Original implementations of FCM by Steven Eschrich [100] and SPFCM and OFCM by Prodip Hore [71] were reviewed. Some implementation techniques were adopted, but the code was entirely rewritten. Code from [114] was used for some utility functions.

All algorithms requiring a random number, typically for initialization or randomization, used a custom function to generate a pseudo-random number in the range specified. This function used a pair of pseudo-random numbers which were bit-shifted and the OR operator was applied to obtain a 32-bit number. To provide unique randomization, each trial in an experiment was issued a different seed.

The following procedure for drawing a random sample was used for all algorithms. The dataset is first loaded into memory, and pairs of data objects were randomly selected to be swapped. The positions of data objects are swapped $n \times e$ times, where n is the number of data objects and e is the natural logarithm base. The randomized version of the dataset in memory is then written to disk. Algorithms requiring a random sample read the file sequentially to obtain the desired sample

[11] Some of the material in this chapter has been previously published by me [21] [22] [23], and is re-used under terms of the copyright © 2010, 2012 and 2013 IEEE. New material and analysis has been added.

size. For consistency, the eFFCM algorithm used the above method for sample selection, despite [68] stating that selection should be made with replacement.

If the positions of pairs of data objects are swapped $n \times e$ times, the probability of a data object not being swapped at least once is [115]:

$$\left(1 - \frac{1}{n}\right)^{2ne} = 0.00435 \tag{A.1}$$

as n approaches infinity. This ensures a probability greater than 99.5% that any given data object will have its position altered. This is a reasonably high likelihood and motivated the selection of $n \times e$ swaps.

The procedure used for random selection, while it may seem cumbersome, was intentional. The randomized datasets were written to disk. This allowed subsequent experiments to use the same samples of the data. This procedure also facilitated validation of the custom random number generator.

A.2.1 Termination Criterion

The FCM algorithm terminates when the difference between successive matrices or successive sets of cluster centers (as measured by a convenient matrix norm) falls below ϵ.

Given the goal of the research, a comparison of algorithms across multiple datasets, using a matrix norm to compare either alternative is problematic. The dataset sizes, sizes of PDA, and range of the data differ in each experiment. Fixing the parameter, ϵ, to a single value makes fair comparison difficult.

For example, imagine comparing two successive U matrices by using the summation of differences between cluster memberships as the matrix norm. This can be tuned for a single algorithm, but the same value for ϵ cannot be used as termination criterion to compare FCM and SPFCM. The dataset size is n for FCM, but $fPDA \times n$ for SPFCM. To obtain an equal value of ϵ, FCM

would require a smaller average difference in individual u values than would SPFCM, increasing its runtime.

Comparing V matrices has the same problem as described above when one wishes to compare performance across different datasets with different numbers of clusters. Using the same value for ϵ would require higher quality results from datasets with more clusters and permit lower quality results from datasets with fewer clusters. Another difficulty in using a V norm is that different datasets have different ranges of data. This makes relative quality of results dependent on the dataset. Scaling the data would correct this one issue, if one wished to compare datasets with the same number of clusters.

The solution is to use the U matrix sup norm, which is less dependent on the dataset size, scale, or number of clusters. In my research, the termination criterion used the maximum difference, $maxChange$, in the U matrix sup norm. If the maximum membership value for a data object in successive Us fell below the value for ϵ, the algorithm terminated. As this criterion tests the stability of the membership values, it is independent of dataset size and data scale. While the effects due to number of clusters are unknown, this technique provides a clear and unambiguous stopping criterion.

This leaves the question of how to initialize FCM. It is possible to initialize either the V matrix or the U matrix. The technique described in earlier accelerated fuzzy clustering work was used [62] [64]. The V matrix is initialized by randomly selecting c data objects from the input dataset. The U membership matrix was then initialized by calling the function that executed Equation (2.8) above. We then iterated V and U until termination.

As discussed above, the software implementation calculates the maximum difference in membership value ($maxChange$) for a data object in X while Equation (2.8) is executed. The stopping criterion for the FCM implementation is when $\epsilon \geq maxChange$. An alternate termination criterion using sup norm V was implemented in order to compare the accelerated algorithms directly with work by Havens [16].

A.2.2 eFFCM

The eFFCM algorithm [68] presented the greatest implementation challenge. Details were not rigid, leaving it ambiguous as to how to implement eFFCM. The first decision was to select a test for statistical significance; we selected the χ^2 statistic. Using this statistic, Equation (A.2) is used to estimate "goodness of fit" at the desired level of significance (α)[84]:

$$\chi^2 = \sum_{i=1}^{k} \frac{(o_i - e_i)^2}{e_i} \tag{A.2}$$

where:

k is the number of 'bins'

o_i is the observed number of objects in bin i

e_i is the expected number of objects in bin i

This still leaves a few decisions of high impact on the algorithm's functioning. I decided to consider each data feature of the dataset separately. The mean and standard deviation for each feature are calculated over the entire dataset. The values for each feature for every data object in the dataset are placed into bins with a width equal to the standard deviation divided by the number of clusters.

The goodness of fit equation requires a minimum of 5 objects per bin. Recall that the initial sample drawn by eFFCM has $fPDA \times n$ data objects, where n is the number of data objects and $fPDA \in [0, 1]$. To ensure that successful *sampling* is possible, any bin with fewer than $5/fPDA$ data objects is merged with an adjacent bin until all surviving bins have a minimum of $5/fPDA$ data objects from the full dataset. So, if $fPDA = 0.05$, each bin must have a minimum of 100 data objects.

The process of merging the bins begins with the lowest value bin. If the bin has fewer data objects than required, it is merged with the next higher bin and retested. The process is repeated

for each bin, until all but the last bin have been tested. When the last bin is tested, the merging changes direction until the last bin tested is valid.

A sample size of $fPDA \times n$ is then collected, and each feature is tested against Equation (A.2). If tests pass for all features, the sample is considered statistically significant. Otherwise, a sample of size $\delta PDA \times n$ is added to the initial sample, and the combined sample is retested. This process repeats until a sample passes all tests.

The χ^2 statistic was calculated with code from [116].

A.2.3 Kolen's Optimization

A direct implementation of the FCM algorithm has a runtime complexity of $O(nisc^2)$. An optimization developed by Kolen and Hutcheson reduces the runtime complexity to $O(nisc)$ [47].

The alternating optimization performed by FCM with Equations 2.8 and 2.9 are combined into a single step. The values for u_{ik} in Equation 2.8 are only used to update V. Kolen's optimization calculates the values for u_{ik} for each $x_i \in X$ and as it does so, it incrementally updates the numerator and denominator of Equation 2.9. For details, see [47].

The pseudocode provided by Kolen was implemented into the FCM codebase with very little modification. Storing the U matrix would no longer be required had this been a code implementation for production. This would have had the benefit of freeing $O(nc)$ memory. As the intent of this implementation was research, the U matrix was retained for any future study of membership values.

A.3 Fuzzy c-medoids Codebase

The Fuzzy c-medoids algorithm, and all its distributed variants, were implemented in C#. Two of the linking methods require the Single Linkage algorithm, which is also implemented in this codebase. The use of C# allowed for a very efficient, rapid implementation. C# manages its own memory, so I was unable to separately assess the effects of memory management on runtime.

The code is almost entirely original. The Hungarian algorithm, used for aligning clusters, was adapted from the C implementation used for FCM.

The dissimilarity matrix is loaded into memory in order to increase the speed of lookups. If vector data is used, the dissimilarity can be dynamically calculated, but this makes the algorithm run slower, depending on the number of data features. The use of the dissimilarity matrix, of course, limits the size of the data that can be loaded. A true scalable codebase would not be structured this way and would probably not be written in C#.

A.4 Fuzzy Neighborhood DBSCAN Codebase

The SFN-DBSCAN algorithm was implemented with Java, using the open source Weka 3 Data Mining Software as a framework [88]. An implementation of SFN-DBSCAN requires an implementation of FN-DBSCAN, however. Weka had an implementation of DBSCAN as a reference. Unfortunately, a simple extension of the DBSCAN Java class was not possible, as it would have required "fuzzy versions" of several ancillary classes.

Conveniently, one can easily modify the Weka framework. Using the DBSCAN class as a guide, FN-DBSCAN and a weighted version of FN-DBSCAN were implemented. Linear, trapezoidal, exponential, and "crisp" membership functions were created for use with these algorithms.

Appendix B: Expanded Results

This appendix contains large detailed sets of results for the curious reader.

Table B.1: Complete DFCMdd Artificial Dataset Results

Dataset	Folds	Linking Method	Speedup	$DQ\,Jm\%$	Intra CC%	Inter CC%	Intra CC% diff	Inter CC% diff	z value (intra CC% diff)	z value (inter CC% diff)	Accuracy
D3C6-1	1	N/A	1.00	0.00%	9.79%	N/A	N/A	N/A	N/A	N/A	85.09%
D3C6-1	5	LM1	9.86	0.98%	15.00%	12.67%	5.21%	2.88%	6.21	4.33	82.66%
D3C6-1	5	LM2	10.21	1.05%	14.43%	12.40%	4.64%	2.61%	6.64	4.23	83.05%
D3C6-1	5	LM3	10.05	1.03%	14.40%	12.39%	4.61%	2.60%	6.58	4.21	83.05%
D3C6-1	5	LM4	9.90	1.63%	22.70%	17.16%	12.91%	7.36%	17.37	11.55	78.86%
D3C6-1	10	LM1	23.36	1.28%	17.69%	14.54%	7.90%	4.75%	9.99	7.24	80.95%
D3C6-1	10	LM2	25.51	1.34%	16.46%	13.69%	6.67%	3.90%	8.98	6.14	81.90%
D3C6-1	10	LM3	25.45	0.97%	15.00%	12.82%	5.21%	3.03%	7.07	4.82	82.60%
D3C6-1	10	LM4	25.36	1.24%	18.15%	14.62%	8.36%	4.83%	11.05	7.56	80.88%
D3C6-2	1	N/A	1.00	0.00%	0.09%	N/A	N/A	N/A	N/A	N/A	99.33%
D3C6-2	5	LM1	6.97	0.21%	0.18%	0.15%	0.09%	0.06%	25.36	20.92	99.29%
D3C6-2	5	LM2	7.23	0.21%	0.17%	0.15%	0.08%	0.06%	24.50	20.44	99.29%
D3C6-2	5	LM3	7.12	0.21%	0.17%	0.15%	0.08%	0.06%	24.91	20.68	99.29%
D3C6-2	5	LM4	7.26	2.13%	4.86%	2.56%	4.77%	2.47%	12.71	12.53	96.92%
D3C6-2	10	LM1	15.10	0.13%	0.15%	0.14%	0.06%	0.05%	17.27	16.95	99.30%
D3C6-2	10	LM2	14.70	0.14%	0.15%	0.14%	0.06%	0.05%	17.69	17.24	99.30%
D3C6-2	10	LM3	13.83	0.14%	0.15%	0.14%	0.06%	0.05%	18.59	17.57	99.30%
D3C6-2	10	LM4	13.83	1.68%	4.55%	2.36%	4.46%	2.27%	10.12	10.11	97.11%
D4C5	1	N/A	1.00	0.00%	20.72%	N/A	N/A	N/A	N/A	N/A	79.66%
D4C5	5	LM1	7.15	0.51%	19.80%	21.19%	-0.93%	0.47%	-1.27	0.72	80.20%
D4C5	5	LM2	7.25	0.71%	22.80%	22.39%	2.08%	1.67%	2.74	2.54	79.00%
D4C5	5	LM3	7.36	0.65%	22.60%	22.29%	1.88%	1.57%	2.47	2.38	79.06%
D4C5	5	LM4	6.94	0.42%	27.50%	24.78%	6.77%	4.06%	9.59	6.40	75.82%
D4C5	10	LM1	16.18	0.10%	16.44%	19.27%	-4.28%	-1.46%	-5.91	-2.24	82.21%
D4C5	10	LM2	15.96	0.93%	26.38%	24.30%	5.66%	3.58%	7.73	5.57	76.84%
D4C5	10	LM3	16.24	0.72%	25.01%	23.57%	4.29%	2.85%	5.71	4.39	77.46%
D4C5	10	LM4	16.08	0.43%	25.87%	24.10%	5.14%	3.38%	6.91	5.17	76.32%
D7C10	1	N/A	1.00	0.00%	15.69%	N/A	N/A	N/A	N/A	N/A	90.07%
D7C10	5	LM1	6.37	1.92%	27.03%	23.01%	11.34%	7.32%	18.29	13.01	81.68%
D7C10	5	LM2	6.49	0.09%	9.16%	12.83%	-6.53%	-2.86%	-11.27	-5.18	94.26%
D7C10	5	LM3	6.45	0.09%	9.16%	12.83%	-6.53%	-2.86%	-11.27	-5.18	94.26%
D7C10	5	LM4	6.41	1.30%	23.51%	20.30%	7.82%	4.61%	13.21	8.59	83.98%
D7C10	10	LM1	12.40	1.24%	25.33%	21.58%	9.64%	5.89%	16.47	11.10	82.54%
D7C10	10	LM2	13.02	0.18%	11.48%	14.11%	-4.21%	-1.58%	-7.30	-2.87	92.61%
D7C10	10	LM3	12.63	0.18%	11.48%	14.11%	-4.21%	-1.58%	-7.30	-2.87	92.61%
D7C10	10	LM4	13.32	1.47%	28.92%	23.81%	13.23%	8.12%	23.06	15.29	80.21%

Appendix B (Continued)

Table B.2: Complete DFCMdd Real-World Dataset Results

Dataset	Folds	Linking Method	Speedup	$DQ\,Jm\%$	Intra CC%	Inter CC%	Intra CC% diff	Inter CC% diff	Z value (intra-intra)	Z value (inter-intra)	Accuracy
MRI016R	1	N/A	1.00	0.00%	12.22%	N/A	N/A	N/A	N/A	N/A	N/A
MRI016R	5	LM1	6.66	2.76%	6.98%	10.43%	-5.25%	-1.80%	-5.04	-1.88	N/A
MRI016R	5	LM2	6.91	3.24%	9.52%	11.76%	-2.70%	-0.47%	-2.39	-0.47	N/A
MRI016R	5	LM3	6.86	3.24%	9.54%	11.77%	-2.69%	-0.45%	-2.37	-0.46	N/A
MRI016R	5	LM4	6.82	0.42%	4.72%	9.04%	-7.50%	-3.19%	-8.49	-3.49	N/A
MRI016R	10	LM1	15.18	1.45%	3.84%	8.98%	-8.38%	-3.25%	-9.08	-3.47	N/A
MRI016R	10	LM2	14.82	7.76%	17.51%	17.03%	5.28%	4.80%	4.36	4.67	N/A
MRI016R	10	LM3	15.08	6.43%	15.24%	15.23%	3.02%	3.01%	2.47	2.94	N/A
MRI016R	10	LM4	14.17	0.48%	3.65%	8.69%	-8.57%	-3.53%	-10.09	-3.86	N/A
MRI017R	1	N/A	1.00	0.00%	6.32%	N/A	N/A	N/A	N/A	N/A	N/A
MRI017R	5	LM1	6.56	10.35%	18.50%	14.44%	12.18%	8.12%	10.24	9.48	N/A
MRI017R	5	LM2	6.66	-0.05%	1.49%	4.21%	-4.83%	-2.11%	-8.93	-3.45	N/A
MRI017R	5	LM3	6.73	-0.05%	1.49%	4.21%	-4.83%	-2.11%	-8.93	-3.45	N/A
MRI017R	5	LM4	6.65	0.36%	7.87%	7.13%	1.55%	0.81%	2.14	1.26	N/A
MRI017R	10	LM1	13.77	4.19%	9.85%	8.60%	3.53%	2.28%	3.44	3.05	N/A
MRI017R	10	LM2	14.37	5.36%	14.17%	11.23%	7.85%	4.91%	7.08	6.13	N/A
MRI017R	10	LM3	14.17	4.51%	12.38%	10.06%	6.06%	3.74%	5.55	4.78	N/A
MRI017R	10	LM4	13.78	0.26%	2.77%	4.93%	-3.55%	-1.39%	-5.89	-2.23	N/A
MRI017R-2	1	N/A	1.00	0.00%	16.28%	N/A	N/A	N/A	N/A	N/A	N/A
MRI017R-2	5	LM1	6.96	2.31%	7.28%	14.42%	-9.00%	-1.86%	-8.94	-2.09	N/A
MRI017R-2	5	LM2	6.92	0.65%	4.52%	13.10%	-11.76%	-3.18%	-13.25	-3.68	N/A
MRI017R-2	5	LM3	6.33	0.65%	4.54%	13.10%	-11.74%	-3.17%	-13.23	-3.67	N/A
MRI017R-2	5	LM4	6.73	-0.39%	5.92%	12.61%	-10.36%	-3.67%	-12.41	-4.41	N/A
MRI017R-2	10	LM1	15.87	5.28%	11.99%	17.04%	-4.29%	0.76%	-3.68	0.81	N/A
MRI017R-2	10	LM2	15.33	3.97%	13.21%	17.87%	-3.07%	1.59%	-2.68	1.70	N/A
MRI017R-2	10	LM3	15.79	2.20%	9.29%	15.58%	-6.99%	-0.70%	-6.48	-0.77	N/A
MRI017R-2	10	LM4	15.95	-0.30%	3.25%	12.43%	-13.03%	-3.85%	-17.52	-4.62	N/A
MRI018R	1	N/A	1.00	0.00%	13.52%	N/A	N/A	N/A	N/A	N/A	N/A
MRI018R	5	LM1	5.32	1.24%	3.97%	10.10%	-9.55%	-3.42%	-10.75	-3.93	N/A
MRI018R	5	LM2	5.35	1.41%	6.96%	11.48%	-6.56%	-2.04%	-6.37	-2.26	N/A
MRI018R	5	LM3	5.33	1.41%	6.94%	11.49%	-6.58%	-2.03%	-6.39	-2.26	N/A
MRI018R	5	LM4	5.10	0.56%	9.94%	12.20%	-3.58%	-1.32%	-4.03	-1.56	N/A
MRI018R	10	LM1	10.75	4.12%	9.28%	12.94%	-4.24%	-0.58%	-3.90	-0.64	N/A
MRI018R	10	LM2	11.14	8.34%	19.00%	19.13%	5.48%	5.61%	4.44	5.67	N/A
MRI018R	10	LM3	10.42	6.11%	14.15%	15.71%	0.63%	2.19%	0.52	2.28	N/A
MRI018R	10	LM4	10.95	-0.13%	2.33%	9.48%	-11.19%	-4.04%	-14.92	-4.81	N/A
Pendigits	1	N/A	1.00	0.00%	32.96%	N/A	N/A	N/A	N/A	N/A	55.48%
Pendigits	5	LM1	5.77	3.63%	34.45%	46.44%	1.49%	13.48%	2.62	26.22	52.23%
Pendigits	5	LM2	5.77	1.97%	19.41%	39.75%	-13.54%	6.79%	-23.51	12.68	65.27%
Pendigits	5	LM3	5.93	1.97%	19.40%	39.74%	-13.55%	6.78%	-23.52	12.66	65.27%
Pendigits	5	LM4	5.82	0.26%	34.38%	37.29%	1.42%	4.33%	2.34	7.93	61.08%
Pendigits	10	LM1	12.40	4.61%	30.53%	44.22%	-2.43%	11.26%	-4.02	21.66	55.63%
Pendigits	10	LM2	12.62	5.62%	22.40%	41.69%	-10.56%	8.73%	-17.57	16.50	58.70%
Pendigits	10	LM3	12.64	5.63%	22.49%	41.67%	-10.47%	8.71%	-17.38	16.46	58.68%
Pendigits	10	LM4	12.42	0.70%	34.54%	37.91%	1.59%	4.95%	2.59	9.03	60.20%
Plankton	1	N/A	1.00	0.00%	17.63%	N/A	N/A	N/A	N/A	N/A	67.88%
Plankton	5	LM1	6.31	2.63%	28.41%	27.90%	10.79%	10.27%	11.49	14.34	60.10%
Plankton	5	LM2	5.61	-0.14%	19.60%	23.14%	1.98%	5.52%	2.63	8.25	69.97%
Plankton	5	LM3	5.81	-0.16%	19.61%	23.15%	1.98%	5.52%	2.63	8.26	69.98%
Plankton	5	LM4	6.22	-0.54%	17.48%	19.97%	-0.15%	2.35%	-0.21	3.49	72.52%
Plankton	10	LM1	13.75	0.64%	20.98%	22.10%	3.35%	4.47%	4.31	6.57	65.76%
Plankton	10	LM2	14.34	4.32%	28.87%	32.06%	11.24%	14.43%	14.05	21.16	65.73%
Plankton	10	LM3	14.42	0.21%	21.31%	23.24%	3.68%	5.61%	4.34	8.03	69.75%
Plankton	10	LM4	14.51	-1.62%	10.44%	18.57%	-7.19%	0.94%	-10.99	1.41	75.15%

Appendix B (Continued)

Table B.3: Complete MRI016 Results

$fPDA$	Algorithm	Speedup	Speedup (less I/O & sampling)	$DQ\,Rm\%$	CC%
0.001	SPFCM	4.85	9.09	0.0023	0.0349
0.001	OFCM	1.16	1.16	0.2213	1.3944
0.001	GOFCM	11.12	334.94	0.032	0.0809
0.001	eFFCM	1.26	16.56	0.0897	0.1564
0.001	rseFCM	11.20	403.98	0.1586	0.1816
0.001	MSERFCM	11.01	255.66	0.1268	0.1898
0.003	SPFCM	4.73	8.91	0.0011	0.0403
0.003	OFCM	1.14	1.14	0.1381	0.3964
0.003	GOFCM	10.24	133.54	0.0161	0.0576
0.003	eFFCM	1.81	9.46	0.0136	0.0257
0.003	rseFCM	10.51	227.02	0.0438	0.2023
0.003	MSERFCM	10.56	200.82	0.039	0.1444
0.010	SPFCM	4.76	8.47	0.0007	0.024
0.010	OFCM	1.41	1.42	0.0585	0.5563
0.010	GOFCM	9.90	58.48	0.0082	0.035
0.010	eFFCM	2.56	7.05	0.0047	0.0293
0.010	rseFCM	10.49	90.68	0.0158	0.0814
0.010	MSERFCM	11.09	136.26	0.0156	0.1054
0.033	SPFCM	4.21	7.06	0.0004	0.0175
0.033	OFCM	1.68	1.69	0.0167	0.176
0.033	GOFCM	7.39	22.26	0.0041	0.0158
0.033	eFFCM	2.57	5.16	0.0015	0.0159
0.033	rseFCM	8.18	29.95	0.0051	0.0529
0.033	MSERFCM	9.55	58.74	0.005	0.0723
0.100	SPFCM	3.32	4.78	0.0003	0.0118
0.100	OFCM	1.52	1.53	0.0274	0.3508
0.100	GOFCM	4.94	9.02	0.0022	0.0159
0.100	eFFCM	2.09	3.15	0.0008	0.033
0.100	rseFCM	5.16	9.25	0.0023	0.0231
0.100	MSERFCM	7.32	19.61	0.0022	0.0247

Appendix B (Continued)

Table B.4: Complete MRI017 Results

$fPDA$	Algorithm	Speedup	Speedup (less I/O & sampling)	$DQ\,Rm\%$	CC%
0.001	SPFCM	3.73	7.06	0.0009	0.0127
0.001	OFCM	0.94	0.94	0.1917	0.3198
0.001	GOFCM	8.41	274.91	0.0158	0.0469
0.001	eFFCM	5.78	660.68	0.0882	0.0858
0.001	rseFCM	8.62	975.29	0.1458	0.1472
0.001	MSERFCM	8.63	1241.27	0.1490	0.0953
0.003	SPFCM	3.76	7.01	0.0008	0.0328
0.003	OFCM	0.90	0.90	0.1044	0.2409
0.003	GOFCM	8.23	113.82	0.0076	0.0578
0.003	eFFCM	2.17	14.08	0.0271	0.0719
0.003	rseFCM	8.57	225.16	0.0384	0.0383
0.003	MSERFCM	8.49	178.37	0.0386	0.0170
0.010	SPFCM	3.72	6.62	0.0007	0.0490
0.010	OFCM	1.21	1.21	0.0657	0.3208
0.010	GOFCM	7.82	50.58	0.0041	0.0635
0.010	eFFCM	2.05	6.76	0.0050	0.0662
0.010	rseFCM	8.28	82.90	0.0127	0.0938
0.010	MSERFCM	8.58	104.80	0.0137	0.0768
0.033	SPFCM	3.33	5.71	0.0005	0.0573
0.033	OFCM	1.43	1.44	0.0776	0.4552
0.033	GOFCM	5.94	19.80	0.0019	0.0470
0.033	eFFCM	2.00	4.07	0.0010	0.0740
0.033	rseFCM	6.50	26.77	0.0067	0.1543
0.033	MSERFCM	7.28	46.00	0.0066	0.1349
0.100	SPFCM	2.77	4.11	0.0003	0.0465
0.100	OFCM	1.29	1.29	0.0791	0.6309
0.100	GOFCM	4.28	8.48	0.0010	0.0259
0.100	eFFCM	2.15	3.66	0.0009	0.0704
0.100	rseFCM	4.51	8.88	0.0025	0.1065
0.100	MSERFCM	6.08	18.33	0.0024	0.0884

Appendix B (Continued)

Table B.5: Complete MRI018 Results

$fPDA$	Algorithm	Speedup	Speedup (less I/O & sampling)	$DQ\,Rm\%$	CC%
0.001	SPFCM	3.94	7.43	0.0011	0.0698
0.001	OFCM	1.05	1.05	0.1647	0.9165
0.001	GOFCM	8.99	293.85	0.0212	0.2410
0.001	eFFCM	0.48	6.69	0.0362	0.0511
0.001	rseFCM	9.01	419.79	0.1211	0.0966
0.001	MSERFCM	8.93	228.23	0.1086	0.0558
0.003	SPFCM	3.97	7.30	0.0009	0.0895
0.003	OFCM	1.07	1.07	0.0921	0.4333
0.003	GOFCM	8.88	121.54	0.0108	0.2067
0.003	eFFCM	0.68	4.22	0.0068	0.0895
0.003	rseFCM	8.99	272.60	0.0374	0.2492
0.003	MSERFCM	9.13	561.42	0.0398	0.2492
0.010	SPFCM	3.89	6.99	0.0009	0.0982
0.010	OFCM	1.34	1.34	0.1103	0.8739
0.010	GOFCM	8.09	51.58	0.0057	0.1707
0.010	eFFCM	1.18	3.13	0.0008	0.0696
0.010	rseFCM	8.65	83.80	0.0194	0.3230
0.010	MSERFCM	8.95	118.03	0.0198	0.3182
0.033	SPFCM	3.56	5.98	0.0006	0.0802
0.033	OFCM	1.54	1.55	0.1366	0.7447
0.033	GOFCM	6.36	19.82	0.0024	0.1264
0.033	eFFCM	1.78	3.43	0.0008	0.0723
0.033	rseFCM	7.09	28.01	0.0091	0.2413
0.033	MSERFCM	7.99	48.10	0.0088	0.2232
0.100	SPFCM	2.94	4.40	0.0003	0.0551
0.100	OFCM	1.37	1.37	0.1553	0.9813
0.100	GOFCM	4.15	7.75	0.0009	0.0792
0.100	eFFCM	1.99	3.26	0.0008	0.0744
0.100	rseFCM	4.71	9.27	0.0029	0.1301
0.100	MSERFCM	6.37	19.52	0.0028	0.1176